MULTI-OBJECTIVE NETWORK OPTIMIZATION: MODELS, METHODS, AND APPLICATIONS

A Dissertation

presented to

the Faculty of the Graduate School

at the University of Missouri-Columbia

In Partial Fulfillment

of the Requirements for the Degree

Doctor of Philosophy

---

by

ASHKAN GHOLAMIALAM

Professor Timothy Matisziw

December 2021

The undersigned, appointed by the dean of the Graduate School, have examined the dissertation entitled

MULTI-OBJECTIVE NETWORK OPTIMIZATION: MODELS, METHODS, AND APPLICATIONS

presented by Ashkan Gholamialam,

candidate for the degree of doctor of philosophy

and hereby certify that, in their opinion, it is worthy of acceptance.

Professor Timothy Matisziw

Professor Praveen Edara

Professor Ronald McGarvey

Professor Carlos Sun

Professor Kathleen Trauth

DEDICATION

In memory of my big-hearted dad who was always there to help me learn and grow.

ACKNOWLEDGEMENT

I wouldn't have been able to finish this journey without the help and support I received from my family, friends and colleagues. My Ph.D. studies under supervision of my academic adviser, Prof. Timothy Matisziw, was a rewarding opportunity to conduct multidisciplinary research in Civil and Environmental Engineering. I took several great courses with Prof. Matisziw, most of which had direct application in my research. I acknowledge the financial support of my research that he provided through the grants from Environmental Protection Agency, Grant No. 97763201, and National Science Foundation, Grant No. 2027891. I also would like to thank the rest of my dissertation committee members, Profs. Kathleen Trauth, Praveen Edara, Carlos Sun and Ronald McGarvey for their valuable comments and feedbacks.

Content

ACKNOWLEDGEMENT ii
LIST OF ILLUSTRATIONS v
LIST OF TABLES vii
ABSTRACT ix
CHAPTER 1 INTRODUCTION 1
1.1 Bike Routing Problem in Urban Environments 6
1.2 Probabilistic Collection and Distribution of Information 6
1.3 Habitat Connectivity Assessment using Multi-objective Optimization 7
1.4 Landscape Alteration and Impacts on Habitat Connectivity 8
CHAPTER 2 BACKGROUND 9
2.1 Least Cost Path Problems 9
2.2 Multi-objective Optimization 11
2.3 Scalarization Techniques 12
2.3.1 Weighted Sum Method 12
2.3.2 Epsilon-Constraint Method 15
2.4 Pareto Dominance Approach 16
2.4.1 Ranking Algorithms 16
2.4.2 Labeling Algorithms 17
CHAPTER 3 MODELING BIKEABILITY OF URBAN SYSTEMS 20
3.1 Introduction 20
3.2 Methods 22
3.2.1 Notation 23
3.2.2 Multi-criterion Bikeable Path Model 23
3.2.3 Bikeable Route Summary Metrics 27
3.3 Application 29
3.4 Assessing Urban Bikeability 32
3.4.1 Location of Pareto-optimal Paths 38
3.5 Summary 40
CHAPTER 4 PLACEMENT OF INFORMATION IN NETWORKS 42
4.1 Flow Capturing Location Model (FCLM) 44
4.2 Location Set Covering Problem (LSCP) 45
4.3 Probabilistic Flow Capture Problem (PFCP) 49
4.4 Empirical study 51
4.5 Discussion 56
CHAPTER 5 MULTI-OBJECTIVE HABITAT CONNECTIVITY 63
5.1 Introduction 63
5.1.1 Landscape Connectivity and Conservation of Biodiversity 63

5.1.2 Modeling Ecological Networks – Least Cost Paths 64
5.2 Multi-objective Habitat Connectivity Problem 67
5.3 Solution Methodologies 69
5.3.1 NISE for Biobjective Optimization Models 69
5.3.2 MONISE for MOHCP 70
5.3.3 Multi-Criteria Labeling Algorithm for MOHCP 74
5.4 Application to Amphibian Habitat Connectivity 77
5.4.1 Factors Affecting Amphibian Habitat Connectivity 77
5.4.2 Study Area and Experimental Design 78
5.5 Results and Discussion 85
5.5.1 Solution Characteristics 86
CHAPTER 6 VULNERBILITY ASSESSMENT OF ECOLOGICAL SYSTEMS 95
6.1 Modeling System Change 95
6.2 Connectivity Degradation Problem (CDP) 97
6.3 Simulation Framework 101
6.4 Results and Discussion 103
6.4.1 Assessment and Visualization of Connectivity Change 104
6.4.2 Distribution of Path Objective Values 113
CONCLUSION 116
7.1 Bike Routing Problem 116
7.2 Placement of Information in Networks 118
7.3 Habitat Connectivity for Biodiversity Conservation 119
7.4 Future Work 122
BIBLIOGRAPHY 123
VITA 138

LIST OF ILLUSTRATIONS

Figure 1-1 Inferior and efficient solutions for a biobjective optimization model..... 3
Figure 2-1 Geometric interpretation of NISE method. 14
Figure 3-1 Pareto-optimal paths for example OD pair. 27
Figure 3-2 Study area: (a) ODs, (b) level of traffic stress. 31
Figure 3-3 Average characteristics of Pareto-optimal paths: a) length, b) number of intersections, c) number of intersections per mile, and d) LTS. 34
Figure 3-4 Pareto-optimal paths: a) number of paths; marginal benefit with respect to b) Φ_1, c) Φ_2, and d) Φ_3. 38
Figure 3-5 Number of Pareto-optimal paths identified: a) Φ_1, b) Φ_2, c) Φ_3 and d) $f(\Phi_1, \Phi_2, \Phi_3)$ 40
Figure 4-1 Ohio, USA interstate highway network. 52
Figure 4-2 Supported efficient solutions for $\alpha = 0.78$ varying β and λ. 58
Figure 4-3 Arcs selected in supported efficient solutions for model parameterization $\alpha = 0.78$, $\lambda = 0.2$ and $\beta = 4$: a) solution A, b) solution B, and c) solution C. 59
Figure 4-4 Number of times arcs are selected over the 115 supported efficient solutions for model parameterization $\alpha = 0.78$, $\lambda = 0.2$ and $\beta = 4$. 60
Figure 5-1 NISE algorithm for the biobjective optimization model. 70
Figure 5-2 MONISE algorithm for the MOHCP. 73
Figure 5-3 Multi-criteria least cost path labeling algorithm for the MOHCP. 76
Figure 5-4 Study site. 79
Figure 5-5 Thiessen polygons and the network G created for modelling terrestrial movement. 81
Figure 5-6 Network representation of wetland system. 82
Figure 5-7 Elevation, TWI, and relative risk. 85
Figure 5-8 The Pareto frontier for paths destined to wetlands 1, 2, 3, 4, 5, and 6 from: a) wetland 7, b) wetland 8, c) wetland 9, d) wetland 10, e) wetland 11, and f) wetland 12. 90

Figure 5-9 Number of non-dominated paths using arcs in anchor solutions with respect to a) Ω_1 (probability of successful traversal), b) Ω_2 (moisture weighed distance), c) Ω_3 (elevation change). 92
Figure 5-10 Non-dominated paths: a) supported, b) unsupported, and c) all. 94
Figure 6-1 Simulation framework for assessing habitat network degradation. 103
Figure 6-2 Habitat network connectivity degradation given $\tau_0 = 35$ and using all efficient paths: a) $t = 0$, b) $t = 1$, c) $t = 2$, d) $t = 3$, e) $t = 4$, f) $t = 5$, g) $t = 6$ and h) $t = 7$. 111
Figure 6-3 Habitat network connectivity degradation given $\tau_0 = 35$ and using supported efficient paths: a) $t = 0$, b) $t = 1$, c) $t = 2$, d) $t = 3$, e) $t = 4$, f) $t = 5$, g) $t = 6$, h) $t = 7$ and i) $t = 8$. 112
Figure 6-4 Habitat network connectivity degradation given $\tau_0 = 35$ and using the shortest path: a) $t = 0$, b) $t = 1$, c) $t = 2$, d) $t = 3$, e) $t = 4$, f) $t = 5$, g) $t = 6$, h) $t = 7$, i) $t = 8$ and j) $t = 9$. 113
Figure 6-5 Box and Whisker diagram for path objective values: a) Φ_1, b) Φ_2, c) Φ_3 and d) length from Wetland 1 to Wetland 5 given $\tau_0 = 35$ and using three different set of paths. 115

LIST OF TABLES

Table 3-1 Model notation..... 23
Table 3-2 Objective values of Pareto-optimal paths for example OD pair..... 27
Table 3-3 Study site characteristics. 30
Table 3-4 Criteria for assigning LTS to transportation system components. 31
Table 3-5 Summary of identified paths. 33
Table 3-6 Comparison of Pareto-optimal paths for OD pairs. 36
Table 4-1 Number of supported efficient solutions and paths for model parameterizations 58
Table 4-2 Characteristics for solutions optimal with respect to cost minimization objective 62
Table 5-1 Relative risk associated with traversal of various types of land use/land cover 84
Table 5-2 Summary of arc attributes 84
Table 5-3 Number of supported and unsupported non-dominated paths identified for each wetland 87
Table 5-4 Summary of movement objectives for supported and unsupported non-dominated paths 88
Table 6-1 Computation time and total arcs rendered inoperable given different levels of landscape change τ_0 104
Table 6-2 Model output for each period t given $\tau_0 = 15$ and using all efficient paths .. 108
Table 6-3 Model output for each period t given $\tau_0 = 35$ and using all efficient paths .. 108
Table 6-4 Model output for each period t given $\tau_0 = 15$ and using supported efficient paths 108
Table 6-5 Model output for each period t given $\tau_0 = 35$ and using supported efficient paths 109
Table 6-6 Model output for each period t given $\tau_0 = 15$ and using the shortest path ... 109

Table 6-7 Model output for each period t given $\tau_0 = 35$ and using the shortest path ... 110

MULTI-OBJECTIVE NETWORK OPTIMIZATION: MODELS, METHODS, AND APPLICATIONS

Ashkan Gholamialam

Dr. Timothy Matisziw, Dissertation Supervisor

ABSTRACT

There can be an array of planning objectives to consider when identifying alternatives for using, modifying, or restoring natural or built environments. In this respect, multi-objective network optimization models can provide decision support to both managers and users of the system. While there can be an infinite number of feasible solutions to any multi-objective optimization problem in large networks (e.g., urban transportation systems), the efficient ones are usually more desirable in the decision-making process. However, identification of efficient solutions can be challenging in practical applications. To address this issue, this dissertation details mathematical formulations and solution algorithms for a range of real-world planning problems in the context of intelligent transportation systems, vehicle routing problem, natural conservation and landscape connectivity. While the combination of objectives being optimized is unique for each application, the underlying phenomena involves modeling movement between origins and destinations of a networked system. To demonstrate the type of insights that can be achieved using these modeling approaches, the location and number of times solutions appear in different realizations of system and given different solution approaches (e.g., exact and approximate methods) are visualized on network using a commercial geographic information system.

CHAPTER 1

INTRODUCTION

In a networked system, service providers are often faced with making complex decisions such as those related to future developments or modifications intended to lead to increases in some measures of system performance. Those making use of the system are often perceived as attempting to do so in the most efficient manner. Given that individuals may have different interpretations of cost and planning agencies may have varying goals and management criteria, there are often many options, objectives and constraints in play in any networked system. For instance, in transportation routing problems, the cheapest, shortest or safest path may not necessarily be the best path, rather a path that embodies some mixture of those criteria may be the most desirable. Therefore, multicriteria shortest path models can offer a greater appeal than single criterion models in many contemporary transportation settings. In practice though, most planning applications consider only one or two objectives given the relationship that exists between complexity and number of criteria (Shi et al. 2017).

In single objective models, either one objective is to be optimized or multiple objectives are first weighted and then combined into a single objective optimization model having a composite objective function (Lowry, Furth, and Hadden-Loh 2016). While such practical approaches yield solutions that perform best with respect to only one objective or a weighted combination of multiple objectives, they do not give insight into the tradeoffs between objectives. However, in most planning problems such as corridor location (Medrano and Church 2014; Scaparra, Church, and Medrano 2014), supply chain network (Shen and Daskin 2005; Wang, Lai, and Shi 2011), nature reserve (Matisziw and Murray 2006; Wu, Murray, and Xiao 2011) and vehicle routing

(Matisziw 2019; Gholamialam and Matisziw 2019), it is necessary to effectively generate the best alternatives for any combination of modeling objectives. Biobjective approaches have been widely applied to robust and stochastic optimization models in order to identify the best balance between expected and guaranteed performance (Chassein and Goerigk 2016; Matisziw 2019). In supply chain network design, tradeoffs between two objectives are often explored by applying biobjective optimization models in order to minimize system setup and operation cost and negative environmental effects, or maximize customer service (Shen and Daskin 2005; Wang, Lai, and Shi 2011). In the context of urban transportation planning, Ehrgott et al. (2012) develop a biobjective routing optimization model for identifying routes with minimal travel time and maximal path suitability for bike travel.

In multi-objective optimization models, one solution may be optimized with respect to one or few objectives but usually it is not with respect to all. Included within a Pareto-optimal set of efficient solutions are those that are optimal with respect to at least one criterion as well as those that optimize a mixture (or tradeoff) of criterion. Any solution that is not in the Pareto-optimal set is considered an inferior solution, dominated by at least one solution in the Pareto-optimal set (Tong and Murray 2012). Within the set of efficient solutions, some exist on the convex portion of the Pareto frontier. These solutions are termed *supported* and can be found by techniques such as the weighted sum method (Ehrgott 2006). Other efficient solutions can also exist between supported solutions along the interior of the Pareto frontier. These *unsupported* efficient solutions are more challenging to identify, but can represent sizable portions of the Pareto-optimal solution set, the number of which can increase exponentially with the size of the optimization problem (Ehrgott 2008). In Figure 1-1, inferior and efficient (supported and unsupported) solutions are illustrated for a biobjective optimization model. In this graphical example, it is assumed that both

objectives f_1 and f_2 are to be minimized. The inferior solution S_{11} is dominated by the supported efficient solution S_2 and unsupported efficient solution S_7 since its both objective values seem to be greater than those of S_2 and S_7. The other inferior solution S_{12} is dominated by the supported efficient solution S_3 and unsupported efficient solution S_8 given that both objective values seem to be greater than those of S_3 and S_8. The inferior solution S_{13} is dominated by both S_5 and S_9, and the other inferior solution S_{14} is dominated by both S_5 and S_{10}. The noninferior solution S_{15} is dominated by all other solutions but S_1, S_{11}, S_6, S_{10} and S_{14}.

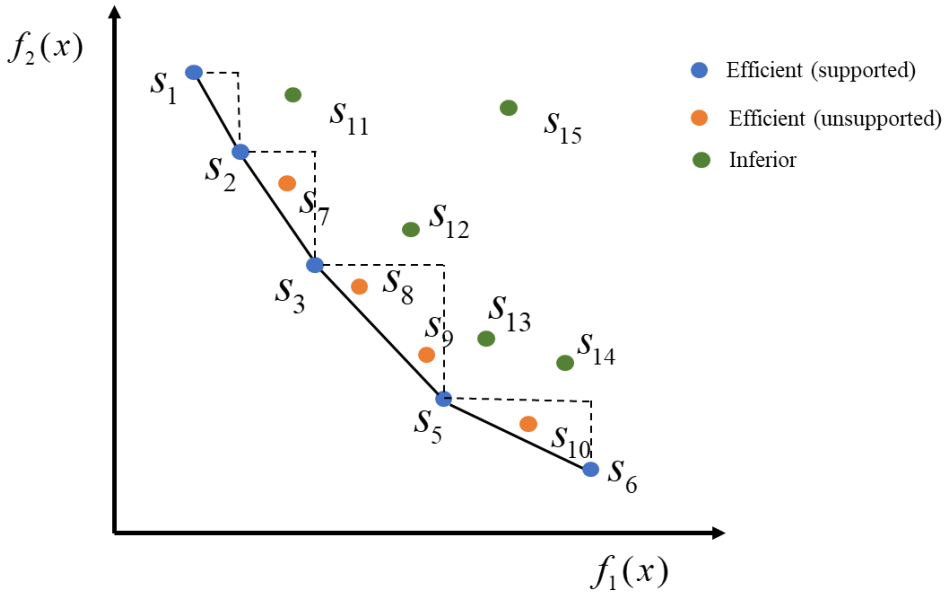

Figure 1-1 Inferior and efficient solutions for a biobjective optimization model.

A multi-objective optimization model can be solved using the *priori* approach in which one set of weights is given to the objectives based on the preferences provided for different objectives by the decision maker (Shahabi, Unnikrishnan, and Boyles 2013). Using this approach, the problem transforms into a single objective optimization model and can be solved by commercial solvers or existing heuristics, resulting one supported efficient solution (Shi et al. 2017). The most

commonly applied method is the *posteriori* approach where a set of efficient solutions are first identified and then the decision maker chooses one that best fits their preferences (Shi et al. 2017). In posteriori approaches, one way of generating the Pareto set is the *scalar* method which uses an aggregate objective function to be optimized subject to the constraints of the original problem. The most common scalarization approach is the weighted sum method which uses a linear combination of objectives to aggregate objective functions (Messac and Mattson 2004). In the basic weighting method, the problem is solved for an arbitrary, empirical, or evenly distributed set of weights which all correspond to uneven representation of Pareto-optimal set (Das and Dennis 1997; Williams 1998; Jozefowiez, Semet, and Talbi 2008). The non-inferior set estimation (NISE) method of Cohon, Church, and Sheer (1979) is one of the striking algorithms that exploits the structure of weighted sum method and can be used to solve biobjective optimization models (Balachandran and Gero 1985; Shen and Daskin 2005). The NISE method is an efficient systematic way of exploring all supported efficient solutions for a biobjective optimization model which relies on the geometric characteristics of the Pareto frontier. For three or more objectives, the extension of NISE is MONISE method which requires exploring all facets of the convex hull and weighting objectives using those facets to implement the weighted sum method in the next iteration (Huber 1980; Solanki, Appino, and Cohon 1993; Raimundo, Ferreira, and Von Zuben 2020). For both NISE and MONISE, the first step of the algorithm is to identify individual minima (anchor points) by assigning a large weight to one objective and small weights to all other objectives. Next, new supported efficient solutions are identified by new combinations of weights determined by the equation of the line (two objectives), plane (three objectives) or hyper plane (more than three objectives) traversing already found solutions in the objective space, and the resulting model is iteratively solved in order to search for other supported efficient solutions.

Given that both NISE and MONISE rely on the weighted sum method, they can only identify supported efficient solutions. While the weighted sum method suffers from the lack of capability in finding unsupported efficient solutions, it has the advantage of using a linear combination of objectives without adding any new constraints to the original problem, therefore, having the same complexity of the single objective counterpart in all recursions. Other solution procedures such as normal constraint (NC) and normal boundary intersection (NBI) are able to approximate an even representation of Pareto frontier for both convex and nonconvex regions. Unlike the NBI method, the NC method is less likely to retrieve dominated solutions and does not require the extra efforts of applying Pareto filtering techniques to remove those dominated solutions (Messac and Mattson 2004; Wang, Lai, and Shi 2011).

When applying multi-objective optimization models to routing problems in networked systems, each solution in the objective space is an efficient path on the network, connecting an origin and destination pair (OD pair). While there can be an infinite number of paths between a single OD pair in a network, only those with reasonably low traversal costs can be used in practice. As such, identification of efficient paths as means of connectivity when studying movement and travel behavior in a network is of great interest. In Chapter 2, the mathematical form of single and multi-objective optimization problems in networked systems are reviewed and different solution procedures to tackle these problems are discussed. Following this, the vehicle routing and facility location problems in urban systems are studied in Chapters 3 and 4, respectively. Next, mathematical models and solution approaches for characterizing species navigation on the landscape are presented in Chapter 5, and changes to habitat connectivity due to development projects are detailed in Chapter 6. Last, concluding remarks and future research direction are provided in Chapter 7.

1.1 Bike Routing Problem in Urban Environments

In urban transportation systems, there are characteristics of infrastructure that are thought to influence use by bicyclists given their perceived effect on safety, comfort, and efficiency. Therefore, it is important to explore the extent to which these infrastructure characteristics may affect prospects for bikeability. Prior research has primarily focused on assessing the qualities of individual road segments and analysis of one or a few routes connecting pairs of origins and destinations. To address these limitations, a multi-criterion shortest path framework is proposed in Chapter 3 for evaluating the characteristics of alternative routes and measuring their tradeoffs with respect to three routing objectives thought to be important to bicyclists – minimizing route cost, number of intersections encountered and level of traffic stress. A label correcting algorithm and dynamic programming approach is used to identify the complete set of routes optimizing the three objectives and metrics are developed to summarize variations in bikeability within an urban environment. The proposed methods are applied to a case study to illustrate a practical implementation of the framework and the types of insights that can be obtained in support of transportation planning efforts.

1.2 Probabilistic Collection and Distribution of Information

Collecting and receiving information about the state of a transportation system is essential to effective planning for intelligent transportation systems, whether it be on the part of individual users or managers of the system. However, efforts to collect or convey information about a system's status often require considerable investment in infrastructure/technology. Moreover, given variations in the development and use of transportation systems over time, uncertainties exist as to where and when demand for such services may be needed. To address these problems, a model for minimizing the cost of siting and/or collecting information while ensuring specified

levels of expected demand are served is proposed in Chapter 4. In order to demonstrate the characteristics of the proposed formulation, it is coupled with another planning objective and applied to identify optimal sites for information provision/collection in a transportation system. In order to explore how variations in the use of a transportation system can impact siting configurations, solutions are derived for multiple scenarios of system flow.

1.3 Habitat Connectivity Assessment using Multi-objective Optimization

Reasoning about the factors underlying inter-habitat movement over the Earth is essential to many areas of biological inquiry. In order to better describe and understand the ways in which the landscape may support inter-habitat movement, an increasing amount of research has focused on identification of paths or corridors that may be important in providing connectivity among habitat. The least-cost path problem has proven to be an instrumental analytical tool in this sense. A complicating aspect of such path identification methods is how to best reconcile and integrate the array of criteria or objectives that species may consider in traversal of a landscape. In cases where use of an ecological corridor is thought to be influenced or guided by multiple objectives, numerous solutions to least-cost path problems can exist, representing tradeoffs between the objectives. In practice though, identification of these solutions can be very challenging and as such, only a small proportion of them are typically found, resulting in a weak characterization of the paths important to ecological corridor. To address this computational challenge, a multi-objective optimization framework is proposed in Chapter 5. A multi-objective non-inferior set estimation (MONISE) algorithm for identifying supported efficient solutions to the multi-objective model is first detailed. A multi-criteria labeling algorithm is then described for identifying the full set of efficient solutions (supported and unsupported) to the multi-objective model. The developed framework is applied to assess different conceptualizations of amphibian movement in a wetland

system. The results highlight the range of tradeoffs in movement objectives that can exist for least-cost paths and that the number of unsupported efficient solutions (which are typically ignored) can vastly outweigh that of the supported efficient solutions.

1.4 Landscape Alteration and Impacts on Habitat Connectivity

Allocation of resources for biodiversity enhancement can be very challenging due to the dynamic and multifaced nature of the problem. Urbanization and development projects cause landscape fragmentation and are significant barriers to dispersal and survival of wildlife species. On the conservation planning side, mitigation efforts will be effective only if adequate information about location and timing of landscape changes as well as species response to those changes is available. To this end, a network optimization framework is proposed in Chapter 6 to identify the maximal damage to ecosystem connectivity given a fixed amount of resources for development projects, and next to simulate how these changes would impact species navigation in the altered landscape. This interrelationship between landscape change and ecosystem degradation is modeled over multiple periods and ends once there is no connectivity between any pair of habitats. Several global network measures for quantifying connectivity change are introduced and the proposed framework is applied to a wetland system. The results indicate that some changes to the landscape may have no or little impact to connectivity now but coupled with future changes can be enormous barriers. Also, landscape changes in the vicinity of wetlands have the highest negative impact to connectivity.

CHAPTER 2

BACKGROUND

In many transportation problems, especially those involving network flows (Hodgson 1990; Kuby and Lim 2005; Upchurch and Kuby 2010), a critical task is to identify a set of viable paths that connect origins and destinations within a network (Jozefowiez, Semet, and Talbi 2008). For example, in traffic assignment models, the traffic flow is distributed among a set of feasible paths based on stochastic dynamic traffic assignment (Basu and Maitra 2010) or user equilibrium principals (Riemann, Wang, and Busch 2015). In other applications such as communication networks (Tsaggouris and Zaroliagis 2009), logistics and supply chain network design (Wang, Lai, and Shi 2011), and corridor planning (Williams 1998; Scaparra, Church, and Medrano 2014), the routing procedure is the core part of problem setting. In general, a path may be optimized with respect to a generalized cost function of one or multiple network arc attributes (Mirchandani and Wiecek 1993; Khani and Boyles 2014).

2.1 Least Cost Path Problems

The mathematical model used for identifying paths of minimal costs in a network is known as the shortest path problem or more generally as the least-cost path problem (Pinto and Keitt 2009; Parks, Mckelvey, and Schwartz 2012; Mirchandani and Wiecek 1993; Shi et al. 2017). Methodologically, least-cost path problems involve a network G with N nodes and A arcs, $G(N, A)$ in which a path between an origin node $(o \in N)$ and a destination node $(d \in N)$ is sought. In least-cost path problems, the decisions are to identify whether or not each arc $(i, j) \in A$ should be included as part of the path. These decisions are typically modeled using binary-integer variables $x_{ij} = \{0,1\}$, where $x_{ij} = 1$ if an arc (i, j) is selected as part of the path and $x_{ij} = 0$,

otherwise. The objective (or criterion) to be optimized in least-cost path problems is usually some function of the arc decision variables (x_{ij}) and their associated costs (c_{ij}), such as the product of the arc cost and associated decision variable as in Eq. (2.1) (Dantzig 1957). Feasible solutions to a least-cost path problem are those that adhere to Constraints (2.2) and (2.3).

$$Minimize\ \Omega = \sum_{(i,j)\in A} c_{ij}x_{ij} \tag{2.1}$$

s.t.

$$\sum_{j|(i,j)\in A} x_{ij} - \sum_{j|(j,i)\in A} x_{ji} = \begin{cases} 1 & \text{if } i = o \\ 0 & \text{if } i \neq o, d\,(i = 1,...,N) \\ -1 & \text{if } i = d, \end{cases} \qquad i \neq j \tag{2.2}$$

$$x_{ij} = \{0,1\} \qquad \forall (i,j) \in \mathrm{A} \tag{2.3}$$

Constraints (2.2) are conservation of flow conditions and ensure that: a) an arc that exits the origin node is selected, b) an arc that enters the destination node is selected, and c) for all nodes other than the origin and destination, if a selected arc enters a node, an arc that exits the node must also be selected. Constraints (2.3) stipulate that all arc decision variables are binary-integer, though it is known that relaxing the binary-integer restriction $\left(0 \le x_{ij} \le 1\right)$ will also result in a binary-integer solution (Dantzig 1957). Exact solutions to many forms of least-cost path problems can be readily obtained using well-known algorithms, such as those of Dijkstra (1959) and Floyd (1962). Given that these types of algorithms are not computationally burdensome and are very accessible, they have been widely implemented in open-source and commercial software products (Landguth et al. 2012; Ribeiro et al. 2017).

2.2 Multi-objective Optimization

Multi-objective approaches work to integrate a broader set of criteria into analysis/planning problems. Unlike with single objective optimization models (e.g., the least-cost path problem), in multi-objective models, there can be many solutions, each optimal with respect to some mix of the objectives considered (termed Pareto-optimal solutions). Eq. (2.4) is a generic multi-objective least-cost path problem in which there are a set of $l \in L$ objectives. Each of objectives l represents some function of the arc decision variables and their associated cost components $\left(c_{ij}^{l}\right)$. The multiple objectives are subject to Constraints (2.2) and (2.3) as in the single objective version.

$$Minimize \left(\left(f_1(c_{ij}^{1} x_{ij}) \,|\, (i,j) \in A\right), ..., \left(f_{|L|}(c_{ij}^{|L|} x_{ij}) \,|\, (i,j) \in A\right)\right) \tag{2.4}$$

Unlike the single objective least-cost path problem, the multi-objective least-cost path problem (2.4) will have a set of solutions (S^*), each of which is optimal in some respect. Consider a set of *feasible* solutions (those that do not violate the constraints) S to a multi-objective optimization problem. Given a feasible solution $s \in S$, s^* is considered to be an *efficient* or *Pareto-optimal* solution if $f_l(c_{ij}^{l} x_{ij}^{s}) \geq f_l(c_{ij}^{l} x_{ij}^{s^*})$ for $\forall l \in L$ and $f_l(c_{ij}^{l} x_{ij}^{s}) > f_l(c_{ij}^{l} x_{ij}^{s^*})$ for at least one $l \in L$. The corresponding Pareto-frontier $f_l(c_{ij}^{l} x_{ij}^{s^*})$ is termed *non-dominated.* A collection of solutions with exactly one Pareto-optimal solution for each non-dominated solution is termed minimal complete Pareto-optimal set. The maximal complete Pareto-optimal set is a collection in which multiple Pareto-optimal solutions may be corresponded to one non-dominated solution in the objective space.

2.3 Scalarization Techniques

The methods which can be used to solve problem (2.4) can be divided into scalar and Pareto methods (Jozefowiez, Semet, and Talbi 2008; Shi et al. 2017). Scalar methods transform the original problem into a single-objective problem that can be solved many times to estimate the Pareto-optimal set using a range of weighting vectors given to the objectives. A few of the most common scalarization techniques include weighted sum method, epsilon-constraint, Benson's method and weighted max-ordering method (Ehrgott 2006).

2.3.1 Weighted Sum Method

The weighting method is the most common scalarization approach which assigns nonnegative weights w_l to the objectives and adds or subtracts them based on the objective sense. In the weighting method, the objectives are combined into a single minimization problem in which each objective $l \in L$ is assigned a weight $\left(w_l\right)$ as in (2.5) .

$$Minimize \sum_{l=1}^{|L|} w_l f_l(c_{ij}^l x_{ij}) \tag{2.5}$$

Each objective weight has a value of $w_l \in [0,1]$ such that $\sum_{l=1}^{|L|} w_l = 1$. Once solved, the result is a single supported efficient solution. In order to identify multiple Pareto-optimal solutions, some studies consider a few different somewhat arbitrary set of weights (Williams 1998). Although the weighting method is straightforward to apply, its ability to identify the complete set of efficient solutions is typically very limited. Other studies use a systematic approach and use an even distribution of weights, however, it has been noted that such approach still does not generate the complete set of supported efficient solutions and also provides uneven distribution of solutions from the Pareto set (Marler and Arora 2010; Das and Dennis 1997). The NC method has overcome

the second deficiency by possessing the nice property of identifying an even spread of points from the Pareto-optimal set (Messac and Mattson 2004). However, the complete enumeration of supported efficient solutions by the NC method may require extensive computational time and effort given that a prespecified number of points must be identified on the Utopia line or plane (Wang, Lai, and Shi 2011). It should be noted that a larger number of points on the Utopia line or plane would give more accurate estimation of Pareto front but with lower speed of problem solving. While the basic weighting method is simple to implement, there are more structured approaches for identifying the exact set of objective weightings that will yield new non-dominated solutions. In cases in which two objectives are to be optimized, the non-inferior set estimation (NISE) method (Figure 2-1) can be applied to estimate the efficient set (Cohon, Church, and Sheer 1979). This is by far the most common approach for addressing multi-criteria optimization models. This process involves evaluating the solution space between pairs of supported efficient solutions to detect the presence of another supported efficient solution. In the initial stage (Figure 2-1a), two individual minima (S_1 and S_2) are identified. In order to find S_1, a small weight is given to second objective and a large weight to the first objective in (2.5), e.g. $Minimize\ 0.999f_1(x)+0.001f_2(x)$. The other individual minima can be found using the same procedure. Once two individual minima are found, the equation of the connecting line between them is used to weigh objectives and detect a new efficient solution, S_3 (Figure 2-1b). This line search approach is applied to explore the objective space between each new supported efficient solution and its neighboring solutions. In Figure 2-1c, supported efficient solutions S_4 and S_5 are identified by connecting lines between (S_1, S_3) and (S_2, S_3), respectively. In this graphical example, it should be noted that all efficient solutions (if any) at the nonconvex portion of Pareto front between (S_3, S_4) would be unsupported and missed by the NISE method.

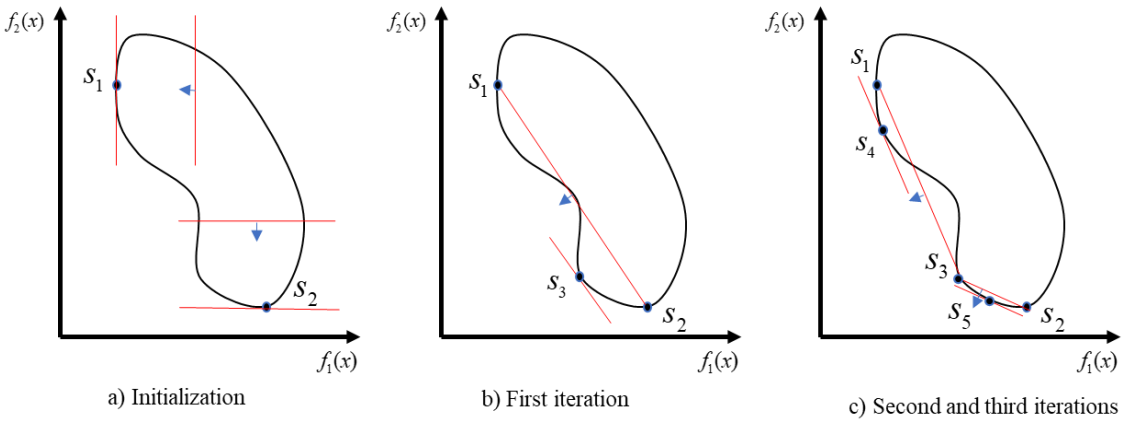

Figure 2-1 Geometric interpretation of NISE method.

Therefore, NISE provides a means for identifying all supported efficient solutions. In the case that more than two objectives are to be considered, the NISE approach becomes more complicated (Huber 1980; Balachandran and Gero 1985). In order to cope with these complexities, MONISE techniques have been proposed to extend the NISE concept to estimate the supported efficient frontier for many criteria (Solanki, Appino, and Cohon 1993; Medrano and Church 2014; Raimundo, Ferreira, and Von Zuben 2020). Similar to NISE, MONISE initializes with identifying individual minima termed anchor points and use them in the next step to find the unit normal vector to the plane or hyperplane traversing anchor points which is termed utopia plane when dealing with three objectives. The utopia plane is used to derive a new weighting vector to generate the first supported efficient solution. In an iterative routine, the feasible space between new efficient solution and neighboring solutions are explored to construct new facets and weighting vectors. This process continues until all feasible region is searched and all efficient solutions have been identified. While both NISE and MONISE are finite methods to efficiently explore the supported

efficient solution set in multi-objective optimization models, they both lack the capability to find unsupported efficient solutions.

2.3.2 Epsilon-Constraint Method

Another approach to find both supported and unsupported efficient solutions is the epsilon-constraint method, where all but one objectives are transformed into constraints (Laumanns, Thiele, and Zitzler 2006; Bérubé, Gendreau, and Potvin 2009). The single objective form of problem (2.5) using epsilon-constraint method can be achieved by retaining one objective (2.6) and returning $|L|-1$ other objectives into Constraints (2.7) and subject to other original Constraints (2.2) and (2.3):

$$Minimize\ f_k(c_{ij}^k x_{ij}) \tag{2.6}$$

s.t.

$$f_m(x) \le \varepsilon_m \qquad m \ne k \tag{2.7}$$

If an optimal solution x^* to this problem is unique, then it is an efficient solution. Otherwise, it is a weakly efficient solution (Ehrgott 2006). If the solution x^* is not unique, problem (2.6)-(2.7) can be adjusted to iteratively minimize other $|L|-1$ objectives, where each optimal solution is used as a constraint in successive runs (Laumanns, Thiele, and Zitzler 2006; Bérubé, Gendreau, and Potvin 2009). In order to identify new efficient solutions, the upper bound of objectives shown as parameter, ε_m, can be reduced by a prespecified constant value (Δ). While small values of Δ may ensure not to miss any efficient solution, it may cause a large number of infeasible solutions. The necessity to choose an appropriate Δ value remains as one of the major drawbacks of the original epsilon-constraint method. Another weakness of epsilon-constraint method is that the scalarized problem is harder than that of the single objective version and the computational effort

needed to identify efficient solutions is highly problem dependent (Laumanns, Thiele, and Zitzler 2006). However, it should be noted that the epsilon-constraint method offers a solution procedure for identify all supported and unsupported efficient solutions, an ability that is lacking in other scalarization methods such as NISE and MONISE.

2.4 Pareto Dominance Approach

Methods based on the notion of Pareto dominance are also commonly used to solve a multi-objective optimization model. For example, ranking and labeling algorithms are basis for many exact and approximate solution methods for identifying non-dominated solutions by the use of Pareto dominance relation (Ishibuchi et al. 2009; Jozefowiez, Semet, and Talbi 2008).

2.4.1 Ranking Algorithms

Among other heuristics, evolutionary and genetic algorithms are usually structured to search for a non-dominated solution set that approximates the entire Pareto front of a multi-objective optimization problem. In evolutionary algorithms, solutions to a given problem are considered individuals of a population and are ranked using a fitness evaluation scheme based on a Pareto approach. In a Pareto approach, the notion of Pareto dominance is used to identify non-dominated solutions within the population by sorting and ranking solutions based on their objective values (e.g., rank 1 for individuals belonging to the Pareto front). Then, ranked solutions are removed from the population to identify a new set of non-dominated solutions among remaining individuals and rank them as such. This ranking process continues until all individuals of population are given a rank, illustrating their position in a set of sorted solutions. The rank given to each solution is coupled with another selection criterion termed a crowding distance to select parents with lower ranks, from less crowded regions of the objective space of current population. Once parents are selected, other evolutionary operators such as mutation and crossover are applied to generate new

offspring and add them to the current population. In the new population, parents and offspring compete to mate and be included in the next generation. This process continues by ranking and selecting best individuals of size N_{pop} in each iteration, improving full population in each passing generation and terminates after a specified number of iterations or when a computation time limit has been exceeded. While only one solution is found in each iteration for methods based on scalarization schemes (e.g., weighted sum), evolutionary algorithms are able to find multiple solutions in each execution of the heuristic (Ishibuchi et al. 2009). In addition to heuristics, the ranking algorithm has been applied to identify partial or entire set of non-dominated paths in multi-objective shortest path problem (Shi et al. 2017). For bi-criterion models having objective functions that are non-linear or cost functions that are non-additive, ranking solution approaches are commonly adopted. In ranking approaches, the shortest path with respect to one criterion is first found and then optimal paths within a certain deviation from the shortest path are explored (Carlyle and Wood 2005). For instance, when minimizing travel time and maximizing route suitability for bicyclists, Ehrgott et al. (2012) define path suitability as the sum of travel time weighted suitability scores of component arcs divided by the total travel time of the path, a formulation that is non-linear and not amenable to a dynamic programming approach. Thus, they utilize an iterative shortest path solution approach for a single OD pair, one which requires complete path enumeration to prove optimality. However, in all but the smallest transportation systems, complete enumeration is likely not computationally viable, necessitating the use of heuristics solution techniques.

2.4.2 Labeling Algorithms

While the applicability of multi-objective least-cost path approaches have been highlighted in literature, the tendency has been to focus on identification of a limited number of the supported

efficient solutions. As such, there are likely many other valid, important, solutions to these problems that are not being evaluated and analyzed that could provide fruitful insights. The other supported and unsupported efficient solutions to multi-objective least-cost path problems can provide more insight on the nuanced tradeoffs between the characteristics of the paths potentially supporting movement. In particular, consideration of the unsupported efficient solutions is especially important given the fact that they can often constitute a major proportion the solutions in the efficient set.

Aside from the ranking method, another Pareto dominance approach is the labeling algorithm, which has been used to identify both supported and unsupported efficient paths in multi-objective shortest path problems (Skriver and Andersen 2000). In instances where objective functions are linear and where cost functions are additive, a dynamic programming approach can be highly efficient (Reinhardt and Pisinger 2011; Matthias Ehrgott et al. 2012). The label correcting and label setting algorithms of Pierre (1980) and Martins (1984) are the most commonly applied solution approaches in this context. The labeling method can be viewed as an extension of Dijkstra's algorithm for single objective shortest path problem (Dijkstra 1959; Shi et al. 2017) and includes two classes of label correcting and label setting algorithms (Martins 1984; Guerriero and Musmanno 2001). Both of these classes are supported by the *principal of optimality* which asserts a non-dominated path is composed of non-dominated sub-paths (Bellman 1954). The label correcting algorithms start by first examining an origin node, iteratively visiting neighboring nodes, and assigning labels representing traversal cost for the tentative paths connecting the origin node to other nodes. Every time a new non-dominated path is found, a node's label is updated, and this process continues until all nodes are visited and labeled, at which point all efficient (supported and unsupported) paths between the origin and destination node are found. While

labeling algorithms are very effective solution methods, they can be applied only if the path cost is separable among its component arcs and if the monotonicity of the cost functions can be guaranteed (Carraway and Morin 1988; Shahabi, Unnikrishnan, and Boyles 2013). In cases where those conditions cannot be satisfied, a subset of the efficient solutions can be heuristically identified by imposing a threshold constraint on one of the objective, enumerating all paths that meet the threshold constraint, and then applying a Pareto filtering technique to retrieve those that are efficient (Matthias Ehrgott et al. 2012).

CHAPTER 3

MODELING BIKEABILITY OF URBAN SYSTEMS

3.1 Introduction

Transportation planning efforts in urban systems involve analyzing how infrastructure characteristics may affect prospects for movement between origins and destinations. In systems supporting bicycle traffic, this involves analysis of characteristics such as those related to safety, comfort, efficiency, and other concerns that may factor into an individual's perception of bikeability (Landis, Vattikuti, and Brannick 1997; Harkey 1998). These characteristics are most often quantified and summarized for individual components of a system (i.e., road *segments*) as a measure of suitability for bike travel. More recently, these measures of suitability have been used to summarize bikeability for paths connecting pairs of origins and destinations (ODs) within a system (Lowry et al. 2012).

Quantifying the suitability of individual components of a transportation system for bike travel is the most basic step in analyzing where and to what extent variations in infrastructure suitability may exist. This involves examining characteristics of road segments thought to have an effect on bikeability, such as their length (Caulfield, Brick, and McCarthy 2012), number of lanes (Landis, Vattikuti, and Brannick 1997), speed limits (Landis, Vattikuti, and Brannick 1997; Harkey 1998), presence of dedicated bike lanes (Akar and Clifton 2009), traffic volumes (Broach, Dill, and Gliebe 2012), number/type of intersections (Menghini et al. 2010; Caulfield, Brick, and McCarthy 2012), etc. Assumptions can then be made regarding how these attributes (or combinations thereof) relate to suitability for bicycling. For example, Landis, Vattikuti, and Brannick (1997) describe the bicycle level of service (BLOS) metric which accounts for a range of factors such as volume of directional traffic, total number of through lanes, posted speed limit

and percentage of heavy vehicles. BLOS is typically structured such that higher value represents greater hazard to bicyclists and hence, less suitability. In another case, Mekuria, Furth, and Nixon (2012) discuss the concept of 'traffic stress', the stress that different roadway conditions can pose to bicyclists. The level of traffic stress (LTS) that can be tolerated can vary for different types of bicyclists (i.e., children, adults, athletes). Their system assigns road segments a LTS between 1.0 and 4.0, where a value of LTS=1.0 reflects the lowest level of stress, (indicating suitability for all types of bicyclists) and a LTS=4.0 reflects the highest level of stress (indicating suitability for only the most capable bicyclists).

Once the suitability of road segments for bicycle travel has been quantified, the suitability of paths connecting origins and destinations within the system can be evaluated. Given any OD path, the suitability of component road segments can be summarized into an overall level of suitability for that path. For example, the length of a path is the sum of the lengths of all road segments traversed in that path. However, in most measures of bikeability, only a single path between an OD pair is considered. For example, after computing BLOS for individual road segments Lowry et al. (2012) identify the path between each OD pair that minimizes a distance-weighted function of road suitability. Bikeability is then measured for each origin as a function of the least-cost paths connecting it to all destinations. After computing the LTS for each road segment, Mekuria, Furth, and Nixon (2012), assess whether or not a least-cost path exists between each OD pair provided different thresholds on LTS in order to examine impacts to network connectivity. Similarly, Lowry, Furth, and Hadden-Loh (2016) identify a least-cost path that meets certain constraints on length and LTS. Following this, they summarize the accessibility of each road segment as the number of times it is used by a least-cost path.

Aside from assessments of bikeability premised on qualities of one OD path reflecting some measure of suitability, multi-criteria optimization models can be applied to help identify a broader set of potential paths representing the tradeoffs among a set of routing objectives. In one such effort, Ehrgott et al. (2012) consider two different routing objectives for cyclist: a) minimize travel time and b) maximize route suitability. Given these two objectives, a set of paths can be identified that are optimal with respect to one or some combination of the two objectives. Therefore, instead of seeking a single path for measuring bikeability between an OD pair, multiple paths can be used to represent different facets of bikeability. Depending on the structure of the objective functions (i.e., additive, non-additive, linear, and non-linear), different solution approaches can be applied to multi-criteria shortest path problems (Reinhardt and Pisinger 2011).

3.2 Methods

In order to move beyond the analysis of one or two routing objectives and provide an analysis of the complete set of Pareto-optimal routing alternatives for many OD pairs within an urban area, a multi-criterion path assessment approach is proposed in Chapter 3. The developed modeling framework is then applied to an urban transportation system to illustrate its practical value for urban planning.

Rather than modeling bikeability relative to a single path premised on a single routing objective, it is desirable to identify paths that are optimal with respect to a suite of objectives. Paths that minimize length, level of stress, and number of intersections are thought to better reflect bikeability. Given that individuals may factor these objectives into their route selection process in many different ways, one approach is to identify the set of paths between each OD pair that represent the best alternatives for any combination of a set of routing objectives – known as Pareto-optimal solutions. In this context, Pareto-optimal refers to the condition that no path in the set is

better than another with respect to all modeled criteria. Included within a Pareto-optimal set of paths are those that are optimal with respect to at least one criterion as well as those that optimize a mixture (or tradeoff) of criterion. To evaluate the tradeoffs between the three routing objectives (minimize distance, LTS, and number of intersections) and identify the set of Pareto-optimal paths for each OD pair, a multi-criterion shortest path model is developed. Next, relevant notation, the proposed multi-criterion model, a solution algorithm, and metrics for summarizing identified routes are detailed.

3.2.1 Notation

Given a network *G* with *N* nodes and *A* arcs, *G (N, A)* and following the notation provided in Table 3-1 the multi-criterion bikeable path model can be formulated.

Table 3-1 Model notation.

Symbol	Description
i, j	Indices for network nodes
N_i	Set of nodes j that can be accessed through node i
c_{ij}	The cost (length) of traversing arc $(i, j) \in A$
s_{ij}	The level of traffic stress on arc $(i, j) \in A$
o	Index for origin nodes $o \in O$
d	Index for destination nodes $d \in D$
x_{ij}	Decision variable: =1 if (i, j) is selected as part of a path, $= 0.0$ otherwise

3.2.2 Multi-criterion Bikeable Path Model

For a given OD pair, the proposed multi-criterion bikeable path model (MCBPM) can be structured as follows:

$$Minimize\ \Phi_1^{od} = \sum_{(i,j)\in A} c_{ij} x_{ij} \tag{3.1}$$

$$Minimize\ \Phi_2^{od} = \sum_{(i,j)\in A} x_{ij} \tag{3.2}$$

$$Minimize\ \Phi_3^{od} = T \tag{3.3}$$

s.t.

$$T \geq s_{ij} x_{ij} \qquad \forall (i,j) \in A \tag{3.4}$$

$$\sum_{j|(i,j)\in A} x_{ij} - \sum_{j|(j,i)\in A} x_{ji} = \begin{cases} 1 & \text{if } i = o, \\ 0 & \text{if } i \neq o,\ d\ (i = 1, \ldots, N) \\ -1 & \text{if } i = d, \end{cases} \tag{3.5}$$

$$x_{ij} = \{0,1\} \qquad \forall (i,j) \in A \tag{3.6}$$

Objective (3.1) minimizes the path length, Objective (3.2) minimizes the number of intersections traversed, and Objective (3.3) minimizes the maximum LTS (s_{ij}) that is encountered on a path. The first two objectives are additive cost functions that accumulate the length of arcs and number of intersections involved in paths. The third objective is non-additive, reflecting the maximum LTS encountered when traversing a path. Constraints (3.4) track the highest LTS of arcs selected for traversal. Constraints (3.5) ensure conservation of flow among network nodes. Constraints (3.6) impose binary-integer restrictions on the arc selection decision variables.

Though Objective (3.4) is non-additive, the optimality principle is satisfied, and a dynamic programing approach can be applied to find the full set of Pareto-optimal paths for a given OD, avoiding the enumeration of paths as required in other cases. To identify optimal solutions, the label correcting algorithm of Martins (1984) can be extended to accommodate the three objective functions. This algorithm (*Multi-objective Paths*), requires a connected graph, two arc attributes (c_{ij}, s_{ij}), one origin node (*o*) and the set of feasible destination nodes $d \in D$. Given these initial conditions, in Step (1), the origin node is labeled with a cost of zero with respect to all criteria and

is added to a queue list for further consideration. Next, the nodes in the queue list are called in a first-in-first-out manner to update the label of adjacent nodes. The first criteria of successor label, Φ_1, is updated by adding the cost (c_{ij}) of the outgoing arc to that of preceding node. The second criteria Φ_2 that accounts for number of intersections, is updated by adding a value of 1.0 to the number of arcs in the preceding node. The conditional statements in Steps (7-10) address criteria Φ_3 such that the s_{ij} value of the successive node is updated only if the s_{ij} of the outgoing arc is greater than that of the preceding node. As in the approach of Martins (1984) and Skriver and Andersen (2000), Steps (11-16) are included for deleting dominated paths and adding nodes with new labels to the queue list for reconsideration. Other steps of the algorithm that are not shown in the pseudo-code include referencing labels of each node and storage of the preceding node in the successor's label to find the optimal paths in a backward process once the queue list is empty and all nodes are labeled. The developed algorithm can identify the complete set of Pareto-optimal paths from one origin to all destinations in a computationally efficient manner. Though the algorithm is structured to find the optimal paths from one origin to all destinations, it can be iteratively executed to find all optimal paths among all OD pairs. According to Tarapata's (2007) schema for classifying multi-objective shortest path models, the proposed model could be considered "$2-SUM\ 1-MAX\ /\ E\ /\ LC$", one that minimizes sums (*2-SUM*), maximizes a quantity (*1-MAX*), and can be solved exactly (*E*) using a label correcting (*LC*) approach.

Multi-objective Paths $(G(N,A), A(c_{ij}, s_{ij}), (o, DestinationNodeList))$

1. *Initialization* : Label$(o) = \{(0,0,0)\}$ & $Queue = \{o\}$
2. While $Queue \neq \varnothing$:
3. $i = Queue$.pop
4. for $j \in N_i$:
5. LabelTemp(j) = [ ]
6. for $(\Phi_{1i}, \Phi_{2i}, \Phi_{3i})$ in Label(i) :
7. if $\Phi_{3i} \geq s_{ij}$:
8. LabelTamp(j).Append($(\Phi_{1i} + c_{ij}, \Phi_{2i} + 1, \Phi_{3i})$)
9. else:
10. LabelTemp(j).Append($(\Phi_{1i} + c_{ij}, \Phi_{2i} + 1, s_{ij})$)
11. *LabelMerge*(j) = Merge (*Label*(j) & LabelTemp(j))
12. *LabelMerge*(j).Remove(all dominated lables)
13. if *LabelMerge*(j) $\neq$ *Label*(j) :
14. *Label*(j) = *LabelMerge*(j)
15. if j not in *Queue* :
16. *Queue*.Append (j)

Figure 3-1 provides an example of what a solution to the multi-criterion model might look like for a single OD pair. In this illustration, the fractional numbers along arcs represent their length and the integer numbers reflect LTS. In Table 3-2, The four Pareto-optimal paths connecting the OD pair are also depicted and are summarized as well. In the solution set, Path 1 is optimal with respect to length (Φ_1) and intersections (Φ_2) while Path 4 is optimal with respect to LTS (Φ_3). Path 3 reflects a tradeoff among the three objectives given that its length and number of intersections is not less than Paths 1 and 2 and its LTS is more than that of Path 4. However, the length of Path 3 is less than that of Path 4 and its LTS is lower than Paths 1 and 2, a set of characteristics that are not jointly dominated by the other paths. Similarly, Path 2 is longer than Path 1 and has higher LTS than Path 3 and 4. However, Path 2 has lower LTS than Path 1, less intersections and is shorter than Path 3 and 4.

Table 3-2 Objective values of Pareto-optimal paths for example OD pair.

Path index	Φ_1	Φ_2	Φ_3
1	0.589	10	4
2	0.590	10	3
3	0.697	12	2
4	0.764	12	1

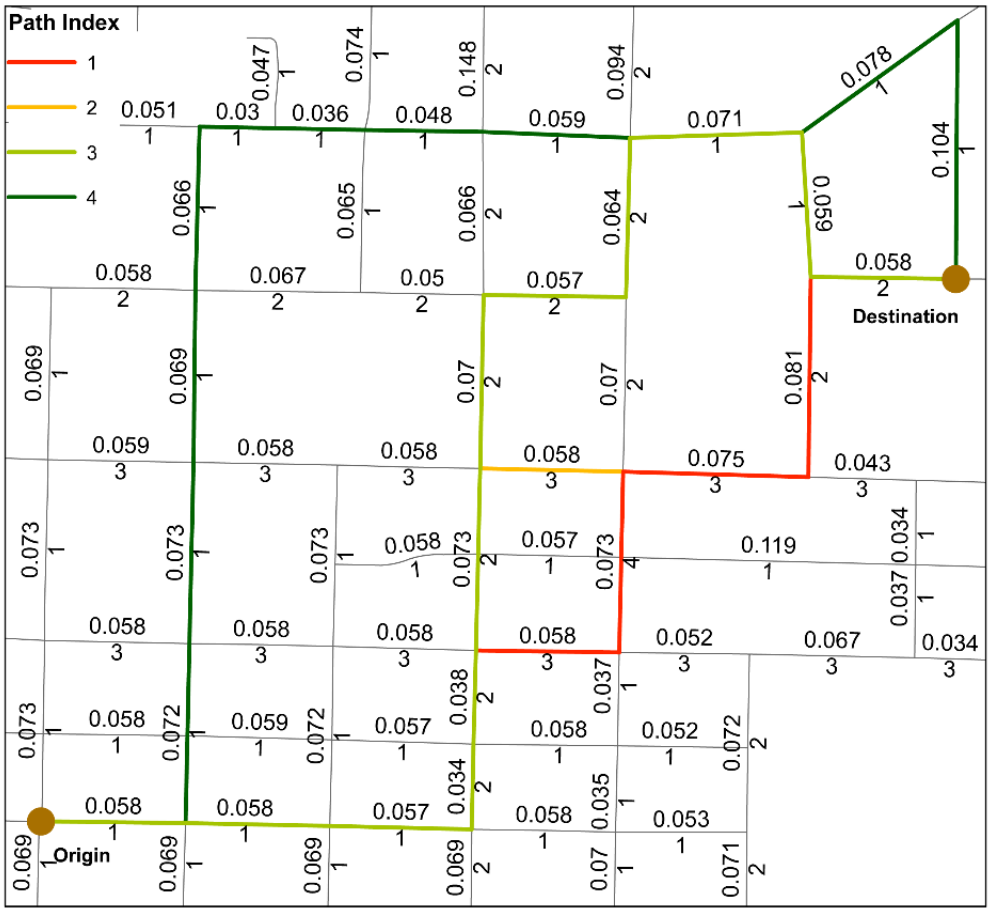

Figure 3-1 Pareto-optimal paths for example OD pair.

3.2.3 Bikeable Route Summary Metrics

While visualization and analysis of alternative paths for a single OD pair is typically relatively straightforward, doing so in applications involving multiple alternative paths for many OD pairs is much more complex. However, in evaluations of urban transportation systems,

assessment of routing possibilities for multiple OD pairs is a necessity. In order to analyze and visualize the results of the multi-criterion model, the characteristics of the set of Pareto-optimal paths identified for each OD pair (P_{od}) can be summarized in a number of ways. For instance, the optimal paths can be summarized by the total number of paths identified (3.7), average length (3.8) , number of intersections (3.9), or LTS (3.10). The set of paths for each OD pair can also be summarized by the range of path length (3.11), number of intersections (3.12), and LTS (3.13) observed. These ranges can be interpreted as the maximum additional increase in one criterion that would be involved in re-routing from a path optimal with respect to that single criterion to another Pareto-optimal path. For instance, range in length (3.11) reflects the difference in length between the longest path and the shortest path in the Pareto-optimal set. Aside from summarizing the paths for each OD pair, the network arcs can also be summarized based on the number of times that they are involved in some subset of the Pareto-optimal paths (i.e., solutions where Φ_1, Φ_2, or Φ_3 is specifically optimized) as detailed in (3.14).

$$\theta_{od} = \left|P_{od}\right|, \qquad o \in O \text{ and } d \in D \tag{3.7}$$

$$\bar{C}_{od} = \frac{\sum_{p \in P_{od}} \Phi_1^{od}}{\theta_{od}}, \qquad o \in O \text{ and } d \in D \tag{3.8}$$

$$\bar{U}_{od} = \frac{\sum_{p \in P_{od}} \Phi_2^{od}}{\theta_{od}}, \qquad o \in O \text{ and } d \in D \tag{3.9}$$

$$\bar{S}_{od} = \frac{\sum_{p \in P_{od}} \Phi_3^{od}}{\theta_{od}}, \qquad o \in O \text{ and } d \in D \tag{3.10}$$

$$\hat{C}_{od} = \max_{p \in P_{od}}\{\Phi_1^{od}\} - \min_{p \in P_{od}}\{\Phi_2^{od}\}, \qquad o \in O \text{ and } d \in D \tag{3.11}$$

$$\hat{U}_{od} = \max_{p \in P_{od}}\{\Phi_2^{od}\} - \min_{p \in P_{od}}\{\Phi_2^{od}\}, \qquad o \in O \text{ and } d \in D \tag{3.12}$$

$$\hat{S}_{od} = \max_{p \in p_{od}} \{\Phi_3^{od}\} - \min_{p \in p_{od}} \{\Phi_3^{od}\}, \quad o \in O \text{ and } d \in D \tag{3.13}$$

$$f_{ij}^{g} = \sum_{o \in O} \sum_{d \in D} \delta_{ijg}, \ \delta_{ijg} = \begin{cases} 1 & (i,j) \in p^g \in P_{od} \\ 0 & (i,j) \notin p^g \in P_{od} \end{cases}, (i,j) \in A, g \in \{\min \Phi_1, \min \Phi_2, \min \Phi_3\} \tag{3.14}$$

3.3 Application

To illustrate the multi-criterion bikeable path analysis framework, it is applied to analyze the bikeability of Columbia, MO, a medium sized city in the Midwestern United States. Columbia is a city that has experienced steady population growth and has a long history of non-motorized transportation development. Columbia has also been designated as a non-motorized transportation pilot program (NTPP) community and has received federal funding for improving bikeability and walkability through infrastructure developments and educational campaigns and programs. Therefore, it is of interest in urban areas such as Columbia to understand the impact that changes to non-motorized transport policy and infrastructure may have (or have had) on bikeability.

A total number of 167 traffic analysis zones (TAZs) are used to represent potential origins and destinations (27,722 OD pairs) for bicycle travel in the city (Figure 3-2a). The centroids of TAZs are connected to the closest intersection on the roadway using dummy connectors at no cost. Given that TAZs at peripheral areas are quite large, smaller administrative areas (e.g., Census blocks) can be used or additional points (e.g., location of bike sharing stations) can be added to the road network to more precisely account for start and end point of bike trips. The existing transportation network involves 5,009 nodes and 6,042 undirected arcs. Table 3-3 provides additional summary characteristics of the transportation system. The length of arcs was used as a measure of the cost incurred in their traversal. While some revealed and stated preference studies report bicyclists' preference for routes involving less than five signalized intersections (Menghini

et al. 2010; Caulfield, Brick, and McCarthy 2012), all intersections with other roads (signalized and non-signalized intersections) are given equal consideration in this application.

Table 3-3 Study site characteristics.

Data	Attribute	LTS Category				Total number of components
		1	2	3	4	
Transportation Network	Total arc length (miles)	340.12	119.99	53.75	50.82	6,042 arcs, 5,009 nodes
	Number of arcs	3,914	1,280	435	413	
Traffic Analysis Zones	Area (sq. miles)	Mean	Min		Max	167 areal units
		0.42	0.02		3.24	

LTS (Table 3-4, Figure 3-2b) was assigned to each road segment by local planning staff using the four-level classification scheme similar to the method proposed by Mekuria, Furth, and Nixon (2012), in which LTS was assessed based upon roadway speed limit, number of lanes, presence/absence of a bike lane, as well as the personal experience of the planning staff with the transportation system. Under this classification scheme, components of the transportation system that are generally suitable for all types of bicyclists are considered to be Level 1, the least stressful. In the study area, these involved local roads with a speed limit of 25 mph or less and only one lane of traffic in each direction as well as dedicated bikeways, physically separated from motor vehicle traffic (Table 3-4). Locations at which dedicated bike lanes are frequently present, having two or less lanes of vehicular traffic per direction and speed limits of 35 mph or lower are categorized as Level 2 stress. However, infrastructure having meeting the same speed limits and traffic lanes, but without dedicated bike lanes is categorizes as Level 3 stress (Table 3-4). In cases where the posted speed limit is 45 mph or less, having two or more lanes of vehicular traffic in each direction

is considered to be Level 3 stress where bike lanes are frequently available or Level 4 when bike lanes are rarely present (Table 3-4). Situations in which the speed limit of a roadway is 55 mph or greater and where a dedicated bike lane is present are categorized as presenting the highest level of stress to bicyclists, Level 4. Roadways without dedicated bike lanes having posted speed limits of 55 mph or more are considered to be unsuitable for most regular bicycle-based commutes and are not assigned a LTS.

Table 3-4 Criteria for assigning LTS to transportation system components.

Level of traffic stress	Speed limit (miles per hour)	Number of lanes (in each direction)	Presence of dedicated bike lane
1	10 to 25	1	Rare/Frequent/Always
2	15 to 35	2 or less	Frequent/Always
3	15 to 35	2 or less	Rare
3	15 to 45	2 or more	Frequent/Always
4	15 to 45	2 or more	Rare
4	20 to 55	2 or more	Always

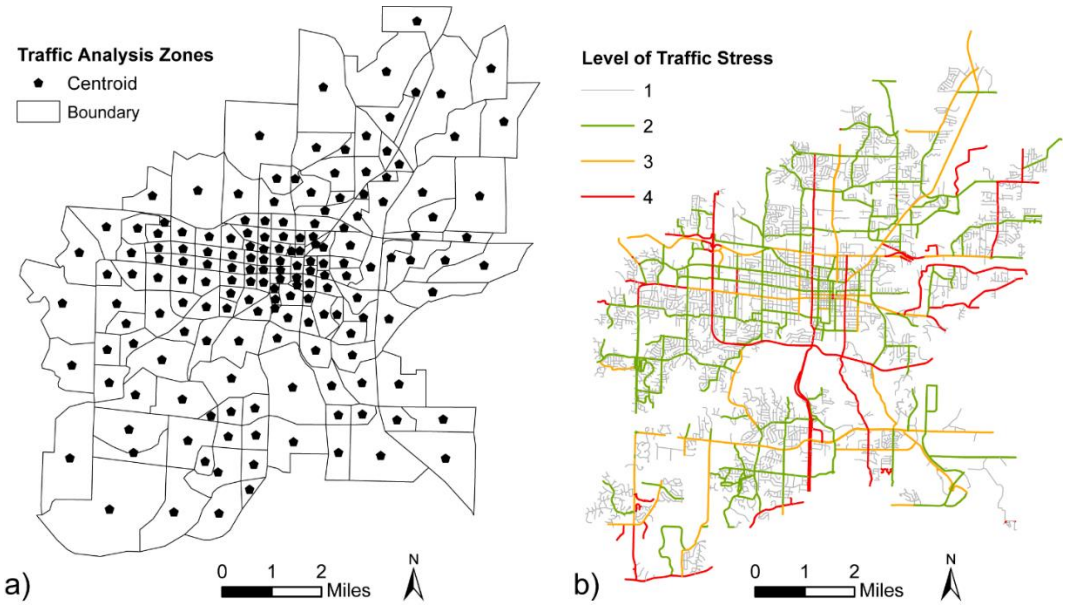

Figure 3-2 Study area: (a) ODs, (b) level of traffic stress.

Given the LTS of each component of a transportation system, the LTS of paths connecting origins and destinations can be determined. In particular, the LTS of a path is equal to the highest LTS of its component road segments. That is, for any path $p \in P_{od}$ involving arcs $(i, j) \in p$, $LTS_p = \max_{(i,j)\in p} s_{ij}$. For example, a path comprised of five road segments with LTS values of 1.0, 2.0, 2.0, 4.0, 2.0 respectively, would have an overall LTS of 4.0. Based on the inputs described above, the *Multi-Objective Paths* algorithm was implemented using Python 2.7 on a Windows 10 64bit workstation with four 2.53GHz processors and 16GB RAM. The solution algorithm was iteratively executed 167 times to identify Pareto-optimal paths from each TAZ to the other 166 TAZs. All 329,931 Pareto-optimal paths among the 27,722 OD pairs were identified in approximately 284 minutes.

3.4 Assessing Urban Bikeability

Table 3-5 summarizes the characteristics of the 329,931 paths identified by the solution algorithm. The number of Pareto-optimal paths between each pair of TAZs ranged from 1.0 to 79.0, with an average (θ) of 11.8 paths per OD pair. Over all pairs of TAZs, the Pareto-optimal OD paths on average involve 45.06 intersections $(\bar{U})$, a LTS $(\bar{S})$ of 3.16, and 5.13 miles of roadway $(\bar{C})$. The range of one measure of path suitability observed over the set of Pareto-optimal paths for an OD pair can provide insight on the level of separation among the solutions. The range in path length over all OD pairs $(\hat{C})$ on average varies 1.01 miles, which given an average trip length of 5.13 miles, equates to an average of 19.6% ((1.01*100)/5.13) variance in trip length. This variance in trip length is in the range of the 10 to 20 percent additional distance that bicyclists have been reported to find acceptable relative to a shortest path (Winters et al. 2010). The range in the number of intersections $(\hat{U})$ involved in the Pareto-optimal paths for OD pairs is on average

16.29, which indicates up to how many additional intersections bicyclists might encounter relative to a path involving the minimum number of intersections. The range in LTS over all OD pairs ($\hat{S}$) was on average 0.82, suggesting that the alternative paths involve up to 0.82 additional LTS relative to the path with minimum LTS.

Table 3-5 Summary of identified paths.

Variable	Mean	SD	Min	Max
All OD pairs				
θ	11.88	10.23	1	79
$\bar{C}$	5.13	2.86	0.20	20.03
$\bar{U}$	45.06	22.14	2	151
$\bar{S}$	3.16	0.62	1	4
$\hat{C}$	1.01	0.93	0.00	5.15
$\hat{U}$	16.29	13.29	0.00	71
$\hat{S}$	0.82	0.70	0.00	3
OD pairs connected by a path less than 2.0 miles				
θ	3.97	3.11	1	19
$\bar{C}$	1.49	0.56	0.20	3.81
$\bar{U}$	18.31	6.84	2	46
$\bar{S}$	2.64	0.72	1	4
$\hat{C}$	0.31	0.52	0.00	3.41
$\hat{U}$	5.09	7.19	0.00	50
$\hat{S}$	0.96	0.85	0.00	3

Figure 3-3 illustrates average objective values for all Pareto-optimal paths connecting each origin to all destinations based upon further aggregation of the summary measures described in (3.8)-(3.10). Centrally located TAZs tend to have lower average path length (Figure 3-3a) and involve fewer intersections (Figure 3-3b). However, the central TAZs tend to involve more intersections per mile (Figure 3-3c), likely due to the higher road density in those areas. TAZs having lower average LTS (Figure 3-3d) seems to have a strong correlation with portions of the city having bike lanes and bicycle-friendly streets.

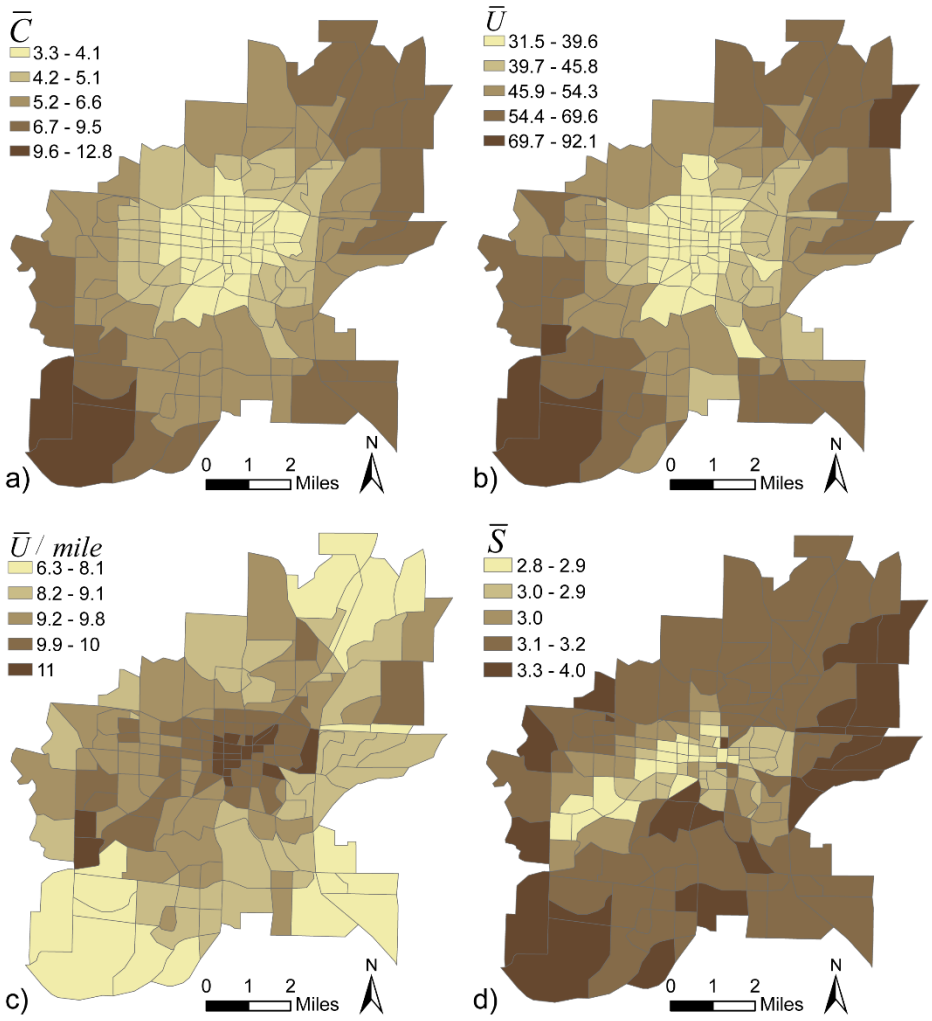

Figure 3-3 Average characteristics of Pareto-optimal paths: a) length, b) number of intersections, c) number of intersections per mile, and d) LTS.

Some of the paths identified when considering movement between all pairs of TAZs were quite long, up to 20.03 miles. While such paths are optimal with respect to the modeled criteria, their relative ability to effectively serve bicycle-based trips could be limited. Analysis of the 2009 National Household Survey indicates that most bicycle-based commutes are less than 2.0 miles and regardless of the mode of travel, approximately 40% of all urban trips are less than 2.0 miles. As such, 2.0 mile thresholds on feasible paths/trips are commonly assumed in assessments of

bikeability (Lowry, Furth, and Hadden-Loh 2016). To account for this practical limitation (Table 3-5), paths between for OD pairs that were less than 2.0 miles in length are summarized separately. Application of this threshold on length indicates lack of bikeability between 24,622 OD pairs (88.6% of the OD pairs). Likewise, the average number of Pareto-optimal paths (θ) for connected OD pairs decreased from 11.88 to 3.97 and these paths are on average 1.49 miles long ($\bar{C}$), involve an average of 18.31 intersections ($\bar{U}$) and an average LTS ($\bar{S}$) of 2.64. Furthermore, path length ranges from 0.0 to 3.41 miles with an average of 0.31 over the OD pairs, which is within the range of 0.5-0.75 miles over the length of the shortest path found to be acceptable by bicyclists evaluated in other studies (Shafizadeh and Niemeier 1997).

The average objective values for paths that are optimal specifically with respect to Φ_1, Φ_2 or Φ_3 as well as those for paths that represent tradeoffs between the three objectives are presented in Table 3-6. Considering all OD pairs, paths optimal with respect to length are on average 4.7 miles long, those of minimal intersections involve on average 38.8 intersections, while those optimal with respect to LTS have an average LTS = 3.0. The average objective values for the tradeoff solutions are always higher than those optimal with respect to any single objective ($\Phi_1 = 5.1$, $\Phi_2 = 47$, $\Phi_3 = 3.5$). The objective values of the tradeoff paths are on average the second lowest with respect to all criteria, simultaneously. Pairwise comparison of (Φ_1, Φ_2) indicates that paths optimized with respect to number of intersections are on average 13.9% longer than the shortest paths, but involve 24.0% fewer intersections. Comparing (Φ_2, Φ_3), paths optimized with respect to LTS involve on average 20.2% more intersections, are 1.8% longer, but involve 23.5% less LTS compared to those minimizing number of intersections. Similarly, for

(Φ_1, Φ_3), the paths minimizing length have on average 23.5% higher LTS and 4.1% more intersections, but are 15.7% shorter compared to those minimizing LTS.

Considering only paths less than two miles, average objective values for paths optimizing Φ_1, Φ_2 or Φ_3 decrease to 1.3, 16.0 and 2.4 respectively. While the tradeoff paths do not minimize any of the individual criteria, they on average have the second-best objective value only with respect to Φ_3. The second lowest average objective values with respect to Φ_1 are associated with paths optimizing Φ_2 ($\Phi_1 = 1.4$ for optimal Φ_2 paths), and with respect to Φ_2, the second lowest average objective values are associated with paths optimizing Φ_1 ($\Phi_2 = 17.9$ for optimal Φ_1 paths). Thus, the pairwise difference between (Φ_2, Φ_3) and (Φ_3, Φ_1) is higher than that of (Φ_2, Φ_1). Therefore, it appears that paths optimizing Φ_1 and Φ_2 tend to align considering paths less than or equal to two miles in length, affecting the average value of the tradeoff paths.

Table 3-6 Comparison of Pareto-optimal paths for OD pairs.

Path	All OD pairs			OD pairs (paths <= 2.0 miles)		
	Φ_1	Φ_2	Φ_3	Φ_1	Φ_2	Φ_3
	Average objective values					
Optimal Φ_1	4.7*	49.4	3.8	1.3*	17.9**	3.2
Optimal Φ_2	5.4	38.8*	3.8	1.4**	16.0*	3.2
Optimal Φ_3	5.5	47.5	3.0*	1.6	19.6	2.4*
Tradeoff	5.1**	47.0**	3.5**	1.5	18.3	2.6**
Pair-wise path comparison	Percentage difference in cost (%)					
Optimal (Φ_1, Φ_2)	13.9	-24.0	0.0	7.4	-11.2	0.0
Optimal (Φ_2, Φ_3)	1.8	20.2	-23.5	13.3	20.2	-28.6
Optimal (Φ_3, Φ_1)	- 15.7	4.1	23.5	-20.7	-9.1	28.6

Note: * and ** indicate first and second-best average objective values.

Figure 3-4 depicts the average number of Pareto-optimal paths (3.7) originating from each TAZ. For distant OD pairs, which involve longer paths and larger number of component arcs, a more diverse set of paths can be found. The geographic distribution of the average ranges associated with each objective is detailed in Figures Figure 3-4b-d. The ranges of path length and number of intersections are similar to the distribution of the number of paths identified for each origin as they become greater for origins located more peripheral to the urban core. Conversely, origins located closer to the city center and western portion of the city tend to have a higher range of LTS. From a network structure perspective, Φ_1 and Φ_2 appear to be more dominant in routes originating from and destined to peripheral locations (greater average range in those areas) since those paths either traverse the city center to minimize path length or circumvent it to minimize number of intersections encountered. Conversely, a greater number of options for minimizing Φ_3 seem to be available in areas with more bicycle-friendly infrastructure where bicyclists can better avoid roads of higher LTS.

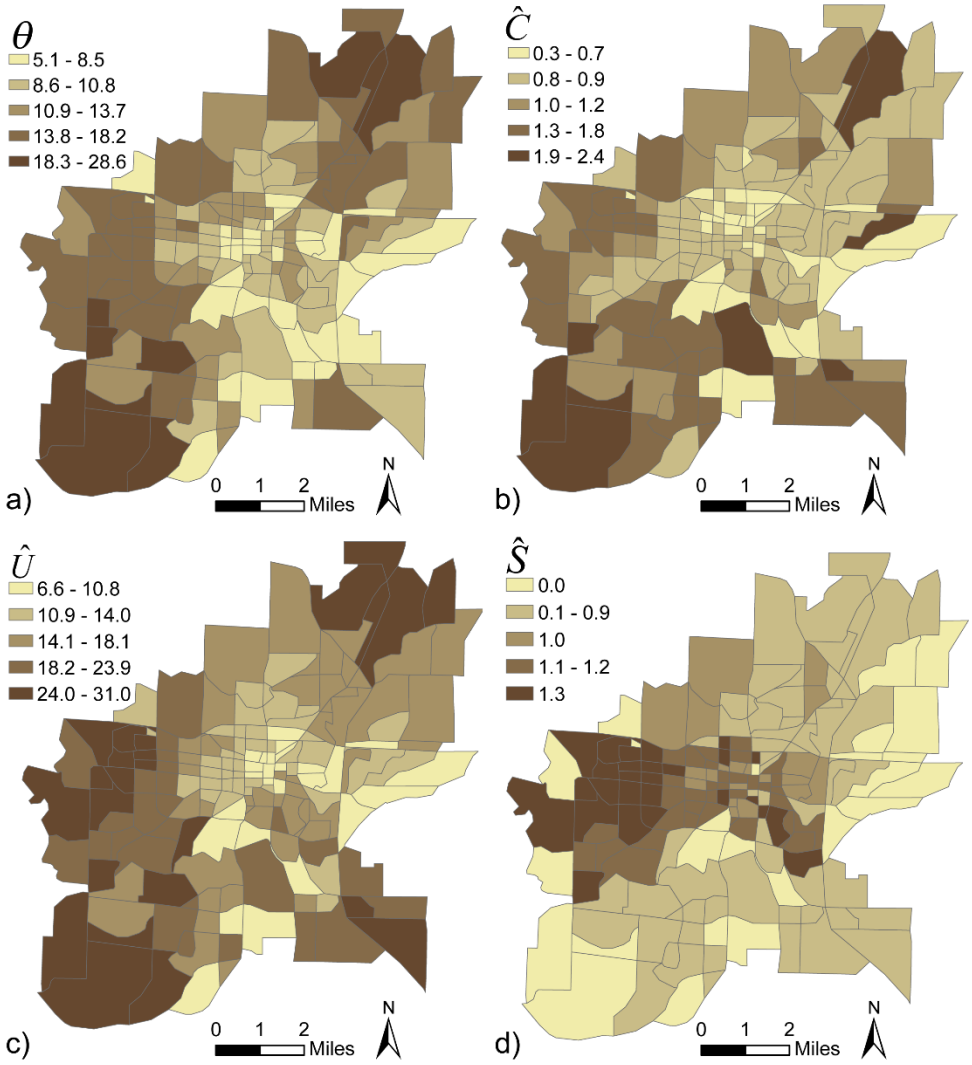

Figure 3-4 Pareto-optimal paths: a) number of paths; marginal benefit with respect to b) Φ_1, c) Φ_2, and d) Φ_3.

3.4.1 Location of Pareto-optimal Paths

While summaries of the path characteristics for urban origins and destinations provide some insight on the relative bikeability that may be present for portions of a city, knowledge of where those paths are located is also important. Eq. (3.14) can be applied to summarize where the Pareto-optimal paths can be found in the network (Figure 3-5). Out of the 329,931 paths identified, 77,418 (23.5%) are optimal specifically with respect to Φ_1, Φ_2 or Φ_3. Figure 3-5a depicts paths optimal

with respect to length, showing that they make heavy use of infrastructure in the city center. Figure 3-5b renders paths optimal with respect to number of intersections, indicating that they tend to circumvent the road dense portions of the city center. Figure 3-5c illustrates the location of paths optimal with respect to LTS. The remaining 252,513 (76.5%) paths represent tradeoffs among the three objectives. Figure 3-5d depicts the location of these tradeoff paths and shows that a larger portion of the transportation system could indeed be viewed as suitable for some bicyclists. While a single criterion shortest path model could easily be applied with respect to each of the three individual objectives to find three optimal routes for each OD pair (Figure 3-5a-c), this large number of paths optimizing tradeoffs among the objectives would be ignored, highlighting the importance of a multi-criterion approach.

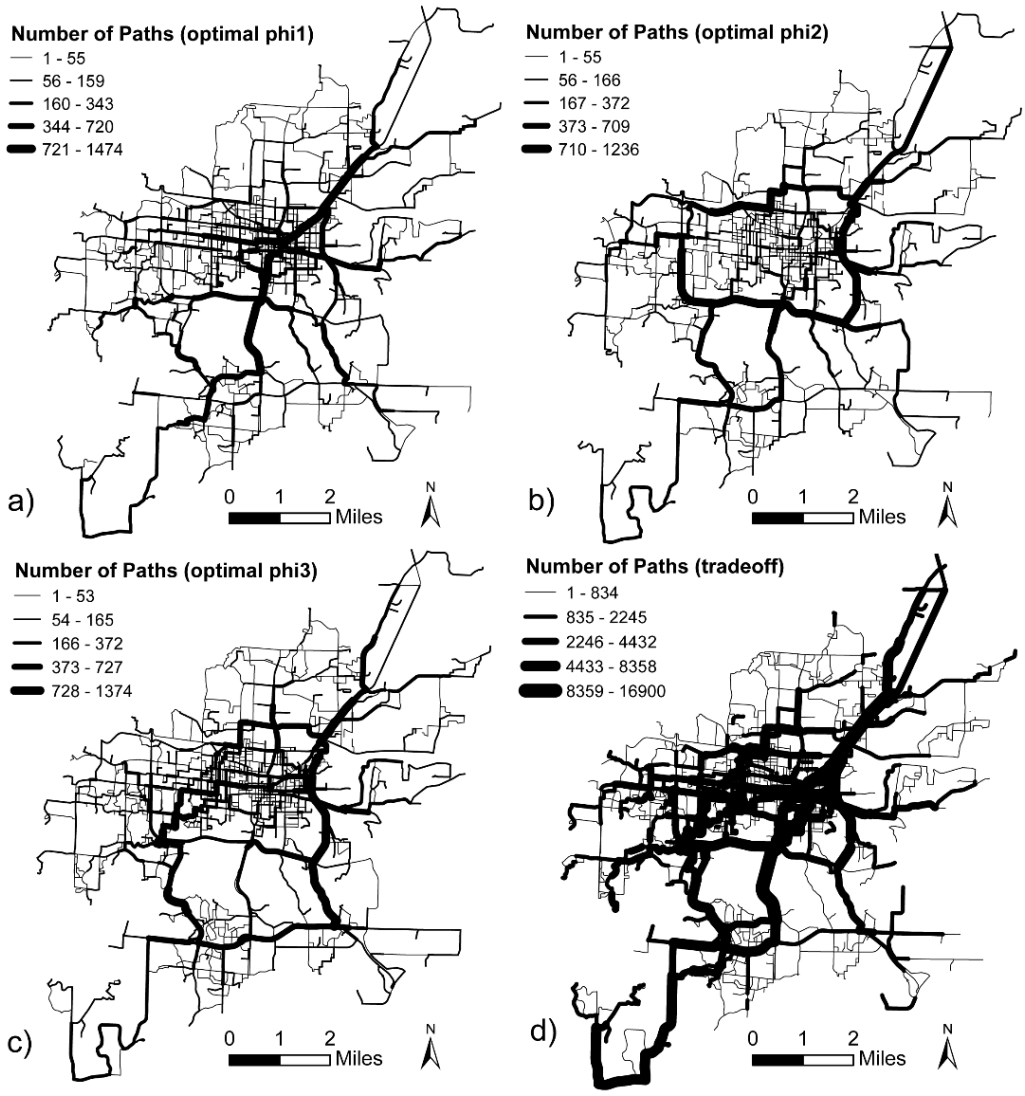

Figure 3-5 Number of Pareto-optimal paths identified: a) Φ_1, b) Φ_2, c) Φ_3 and d) $f(\Phi_1, \Phi_2, \Phi_3)$.

3.5 Summary

There are characteristics of urban transportation infrastructure that are thought to influence use by bicyclists given their perceived effect on safety, comfort, and efficiency. Therefore, it is important to explore the extent to which these characteristics of urban infrastructure may affect prospects for bikeability. Prior research has primarily focused on assessing the qualities of

individual road segments and has considered only a few alternative routes and routing criteria for a limited number of origins/destinations. To address these limitations, a multi-criterion shortest path framework is proposed for evaluating the characteristics of alternative routes in their entirety and measuring the tradeoffs between alternative paths with respect to three routing objectives thought to be important to bicyclists – minimizing route cost, number of intersections encountered and level of traffic stress. A label correcting algorithm and dynamic programming approach is used to identify the complete set of routes optimal with respect the three objectives and bikeability metrics are developed to summarize variations in bikeability within an urban environment. The proposed methods are applied to a case study to illustrate a practical implementation of the framework and the types of insights that can be obtained in support of transportation planning efforts.

CHAPTER 4

PLACEMENT OF INFORMATION IN NETWORKS

Transportation systems can serve a diverse range of needs, collection of data and/or providing information to users of the systems becomes complicated given variations in travel behavior and the planning objectives of interest. For example, in the case of information provision, the value of information to travelers can be fraught with uncertainty as it depends upon how it relates to their activities and supporting path(s) of movement as well as their ability/desire to receive and utilize additional information in their decision-making process (Yang, Mao, and Metcalf 2019; van Essen et al. 2020). Likewise, in the case of information collection, the value of the collected information for a particular need, such as origin-destination (OD) flow estimation, depends on how well it represents the nature of movements in a transportation system as well as how it affects the performance of the analytical task (Gentili and Mirchandani 2012).

Intelligent Transportation Systems (ITS) employ many technologies for the collection and distribution of information regarding the state of a transportation system. For example, variable message signs (VMS) provide visual traffic information and guidance to drivers at specific sites within a system. VMS can be used to disseminate a variety of information regarding incidents, detours and alternative routes, general information and warnings, road condition and weather, special events, high occupancy vehicle and contraflow lane designations, and reversible lane control (Jindahra and Choocharukul 2013; G. Zhang et al. 2014; Romero et al. 2020). While VMS are usually stationary, the information content that is distributed can be tailored to the needs of those traversing the site. Aside from VMS, there are other intelligent transportation system technologies that are being explored for providing vehicles with relevant information such as vehicular ad hoc networks (VANETs). Like VMS, VANETs involve locating facilities in a

transportation system. However, the facilities serve to provide a virtual connection between the vehicles and the infrastructure (Lu, Qu, and Liu 2019). Along with providing vehicles with information in support of travel decisions, intelligent transportation systems are increasingly employing data driven applications such as detection of traffic parameters and characteristics of individual vehicles that rely upon intensive data collection from sensors in the network (Zhang et al. 2011). For example, traffic data collected via cameras, speed sensors, and automated vehicle counters are often used to explore many social problems (Zheng et al. 2016). In the context of ITS though, collected data is increasingly being used to provide real-time estimates of traffic conditions and insight into the number of trips between system origins and destinations (Yim and Lam 1998; Anderson and Souleyrette 2002).

Given that providing and collecting information are expensive, resource constrained tasks, minimizing the cost associated with the facilities required to effectively conduct these tasks is an important planning consideration. It can be difficult though to predict exactly how the transportation system will be utilized at any time and when and where the need for information (dissemination or collection) will arise. Therefore, instead of assuming a single traffic assignment protocol when modeling system usage, a variety of assignment scenarios should be considered. As adequate resources for providing and/or collection information are likely to be lacking, various provision/collection service thresholds may also need to be considered. In this chapter, an optimization methodology is proposed to address these problems. First, background literature related to the proposed modeling approach is reviewed. Next, a probabilistic flow capture problem is proposed for siting facilities in a network. Following this, a multi-objective version of the model is applied to the siting of VMS to illustrate the tradeoffs between minimizing system cost and maximizing benefit to the system.

4.1 Flow Capturing Location Model (FCLM)

A variety of models have been proposed to assist in siting facilities in transportation systems to serve flow moving among network origins and destinations. In the context of providing information to travelers via facilities such as VMS, maximizing exposure to sited facilities is an important goal. To address such planning concerns, Hodgson (1990) details the FCLM, a linear-integer model that maximizes coverage of flows traversing network given a limitation on the number of facilities that can be sited. In this sense, vehicle/passenger flows would be detected by sensors located along the paths they traverse. In the basic FCLM, it is assumed that *all* flow between an origin and destination are assigned to a *single* path and facilities can be located at nodes anywhere along a path. Facilities are also considered to provide equivalent service, regardless of where they are positioned along the path. Variates of the FCLM have been described to address a range of planning problems. For instance, Kuby and Lim (2005) modify the basic FCLM to locate refueling stations for alternative fuel vehicles which sometimes require the availability of multiple fueling sites along a path. Matisziw (2019) also details a version of the FCLM in which multiple facilities can be sited along a path, however, the ability of each facility to serve flow is probabilistic. As such, the objective of their model becomes one of maximizing expected coverage of flow.

Another important objective when planning for the provision of information in a transportation system is the minimization of costs associated with configuring the system and/or those incurred by the users of the transportation system. For example, Huynh, Chiu, and Mahmassani (2003), Henderson (2004) and Boyles and Waller (2011) minimize system travel time and Chiu and Huynh (2007) minimize life cycle costs (initial installation and operating costs) as well as user costs associated with randomly occurring incidents. In such context, the more flow

that can benefit from the provided information, the more efficient the transport system becomes. In a slightly different planning problem, that of locating signs to help travelers navigate a transportation system, Toi et al., (2005) propose a model that minimizes the extent to which travelers would be expected to deviate from a route (a measure they term the 'straying index'). While most information siting approaches have focused on minimizing some form of cost, a budget constraint is typically used to limit the extent to which facilities can be sited (Huynh, Chiu, and Mahmassani 2003; Henderson 2004; Toi et al. 2005; Chiu and Huynh 2007; Boyles and Waller 2011).

4.2 Location Set Covering Problem (LSCP)

Another planning goal is to determine the minimum number (or cost) of facilities needed to ensure that a specified level of service is provided. To address this planning goal, Berman, Larson and Fouska (1992) detail LSCP to address cases in which a proportion of all flows must be covered or captured. In their formulation, some proportion $\lambda = [0,1.0]$ of the total system flow must be served by a set of sited facilities (indexed $i \in I$). The set of nodes R_m comprising each path $m \in M$ is known. A binary-integer variable X_i is defined for each candidate facility to reflect the decision to site $(X_i = 1)$ or not to site $(X_i = 0)$. Their flow set covering formulation is as follows:

$$Minimize \sum_{i \in I} X_i \tag{4.1}$$

s.t.

$$\sum_{i \in R_m} X_i \geq Y_m \qquad \forall m \in M \tag{4.2}$$

$$\sum_{m \in M} f_m Y_m \geq \lambda \sum_{m \in M} f_m \tag{4.3}$$

$$X_i = \{0,1\} \qquad \forall i \in I \tag{4.4}$$

$$Y_m = \{0,1\} \qquad \forall m \in M \tag{4.5}$$

Objective (4.1) minimizes the number of facilities needed and Constraints (4.2) ensures demand cannot be captured unless at least one facility capable of providing exposure to it is sited. Constraint (4.3) ensures that at least some proportion λ of the total network flow is served by the set of sited facilities. Constraints (4.4) and (4.5) are binary/integer restrictions on the decision variables.

In the context of locating sensors to collect information about a transportation system, a variety of applications exist for such flow covering models. For example, in order to help estimate the flows between origins and destinations, traffic flows are commonly recorded at locations throughout a transportation system. Given that there are practical limitations as to how many sensors can be at work at any one time, a variety of approaches for identifying the best locations for traffic sensors have been proposed. For example, Yang, Yang and Gan (2006) describe an integer model that minimizes the number of sensors to be located such that at least one sensor is placed along every path in the network. This condition equates to $\lambda = 1$ in (4.3) and replacing Constraints (4.2) with Constraint (4.6).

$$\sum_{i \in R_m} X_i \geq 1 \qquad \forall m \in M \tag{4.6}$$

Gentili and Mirchandani (2012) also seek to minimize the number of sensors needed to ensure that flow along network paths can be accurately estimated and employ a similar flow covering model. In their case, enough arcs need to be equipped with sensors such that a unique solution to the path flow estimation problem can be identified. To accomplish this, they devise

new constraints to ensure that the selected set of arcs are sufficient to obtain a unique estimation of OD flows.

Coverage of demand by sited facilities in many instances though can be uncertain. That is, although a facility has been sited within a given service standard of a demand location, the probability facility i can effectively serve demand location $m(p_{im})$ can vary. Haight, Revelle and Snyder (2000) and ReVelle, Williams and Boland (2002) incorporate such a condition on demand coverage in the form of a probabilistic threshold Constraint (4.7).

$$\prod_i (1-p_{im})^{X_i} \le (1-\alpha_m)^{Y_m} \qquad \forall m \in M \tag{4.7}$$

For each demand location m, Constraints (4.7) state that the probability that m is not served must be less than some acceptable probability of non-service (α_m). While this probabilistic threshold constraint is inherently non-linear, Haight, Revelle and Snyder (2000) demonstrate that linearization can be achieved through a log transformation as in (4.8).

$$\sum_i \log(1-p_{im}) X_i \le \log(1-\alpha_m) Y_m \qquad \forall m \in M \tag{4.8}$$

In efforts to provide or collect information in a transportation system, it is important to determine how much flow would be served by the configuration of sited facilities as well as the respective origins and destinations of the flows. Provided estimates of demand for movement between OD pairs are available (i.e., OD flows), there are a variety of ways in which those flows could be assigned to paths. For example, all flow between an OD can be assigned to the shortest path, *k*-shortest paths or any set of paths thought to support movement between the OD (Lam and Chan 2001). Once relevant OD paths are identified, flows are assigned to the paths accordingly and the potential impact of a facility configuration can then be evaluated. In some applications, a

single assignment of flow is considered (Henderson 2004; Matisziw 2019). In others, the assignment of flow to paths can be allowed to vary, reflecting dynamic traffic conditions (Chiu and Huynh 2007; Basu and Maitra 2010). Some studies have specifically explored methodologies for addressing recurrent congestion (Yang 1999; Li et al. 2016) whereas others have focused on non-recurrent congestion (Huynh, Chiu, and Mahmassani 2003; Chiu and Huynh 2007), addressing the placement of information to best assist with the diversion of traffic alternative routes.

All of the facility siting approaches detailed in this section in some way address the way demand for a service is met by a configuration of facilities. In planning for information provision and/or collection, minimizing the number of facilities needed to serve demand is critical given the expenses involved in such infrastructure development. Given that provision of information to flow between all OD pairs in a network may not be feasible due to resource constraints and that certain OD pairs may require differing levels of information, being able to ensure a base level of service is available is also an important consideration (i.e., a threshold constraint on flow coverage). In order for information to be of use to network flow, aside from being observable, the information needs to be effectively conveyed. However, given any range of variables, conveying information is rife with uncertainties that need to be accounted for in the siting process (i.e., probabilistic threshold constraint). Further contributing to the complexity of this problem is the fact that typically more than one path supporting movement from an origin to a destination exists. Thus, the OD flow or demand needing service is distributed over the network in some fashion. In a bulk of the flow capturing literature, only a single path among each OD pair is considered. Only in a few cases are multiple paths supporting flow among each OD pair postulated (Riemann, Wang, and Busch 2015; Matisziw 2019). Moreover, most applications only consider either a single

assignment of flow in a system over one or more planning periods. However, given that the ways in which OD flow utilizes the system is constantly changing, there is a need to consider multiple potential assignments of flow in a system when making decisions regarding facility placement. Next, to better account for the various conditions described above, a modeling approach for identifying optimal sites for provision and/or collection of information in a transportation system is proposed. Following the introduction of this model, an application to truck flow in a highway network is provided to highlight its computational characteristics.

4.3 Probabilistic Flow Capture Problem (PFCP)

Consider a transportation system represented as a directed graph G with N nodes and A arcs $G(N, A)$. This system supports flows (α_{od}) among pairs of origin nodes $(o \in O \in N)$ and destination nodes $(d \in D \in N)$. It is assumed that the flows between each origin and destination are distributed over a set of viable network paths N_{od} according to some network assignment strategy. That is, each path $m \in M$, supports a certain amount of flow $f_m \in \alpha_{od}$. Facilities *i* can be sited along arcs (e.g., $i \in A$) (and/or at nodes) at a cost of δ_i. In keeping as much as possible with the notation presented earlier, a probabilistic flow capture problem is now formulated.

$$\Psi = Minimize \sum_{i \in A} \delta_i X_i \tag{4.9}$$

s.t.

$$\sum_{m \in N_{od}} f_m Y_m \geq \lambda_{od} \sum_{m \in N_{od}} f_m \qquad \forall o \in O, d \in D \mid a_{od} \neq 0 \tag{4.10}$$

$$\sum_{i \in R_m} X_i \ln(1 - p_{im}) \leq Y_m \ln(1 - \alpha_m) \qquad \forall m \in M \tag{4.11}$$

$$X_i = \{0,1\} \qquad \forall i \in I \tag{4.12}$$

$$Y_m = \{0,1\} \qquad \forall m \in M \tag{4.13}$$

Objective (4.9) minimizes cost of equipping network arcs with facilities that provide (and/or collect) information to traffic flows. Constraints (4.10) stipulate that at least λ_{od} percent of each OD flow is exposed to a facility and is akin to threshold constraint utilized by Berman, Larson and Fouska (1992). Thus, when $\lambda_{od} = 1.0$, 100% of flow must be served by the sited facilities as the formula is a location set covering problem. When $0 \le \lambda_{od} < 1$, only λ_{od} percent of flow is guaranteed to be covered. Constraints (4.11) follow the structure of the probabilistic threshold constraints (4.8) and state that path m cannot be confidently served unless the probability of non-exposure to sited facilities is less than $1-\alpha_m$. Given that multiple facilities may be needed to ensure the probability of exposure for flow along a path exceeds the probabilistic threshold, the path reduction techniques of Berman, Larson and Fouska (1992) no longer are applicable. Constraints (4.12) and (4.13) are binary/integer restrictions on all decision variables.

While model (4.9)-(4.13) addresses the coverage of OD pairs individually, it is also possible to do so in aggregate. For instance, an origin-specific approach can be adopted whereby a certain proportion of total outflow from an origin to all destinations may require coverage. This situation can be readily accommodated in the model. Let $\Omega_o =$ the set of paths m originating at node o, then:

$$\sum_{m \in \Omega_o} f_m Y_m \ge \lambda_o \sum_{d \ne o \in N} \alpha_{od} \qquad \forall o \in O \tag{4.14}$$

In the proposed formulation, the way in which flow is assigned to a path connecting an OD

is an input to the model. In other words, it is assumed that the way in which the network will be utilized is known. This is in fact a very common assumption in the flow capturing literature. In many models, only the shortest path connecting an OD is considered (Upchurch and Kuby 2010). More recently, variants of the flow capturing models have been proposed that consider multiple, alternative paths of movement among ODs (Gzara and Erkut 2009; Matisziw 2019). Regardless of how flow is modeled to utilize a network at any given time, there will always be uncertainty as if and to what extent that representation of network use will actually manifest over time. Therefore, instead of considering one or a few alternative representations of network flow, it may be worth exploring many potential ways in which flow could be assigned to paths within a system. This facet can be addressed in the model by identifying and comparing solutions for many alternative flow assignment scenarios.

To explore the robustness of a siting solution to multiple scenarios of flow assignment, the following experimental framework can be employed. First, derive a representative set of flow assignment scenarios $s \in S$. While an infinite set of such scenarios no doubt exists, scenarios could be selected based on factors such as observed or hypothesized locations of disruption (e.g., accidents, congestion, etc.), different assignment strategies (e.g., all-or-nothing, user equilibrium, etc.), proportion of flow to be served and different levels of likelihood for observing information on each path. Next, the model can be in turn solved for each flow assignment scenario and the resulting siting configurations can then be examined.

4.4 Empirical study

In this section, the PFCP is applied to identify VMS siting configurations for providing information to truck flows utilizing the Interstate highway system in the state of Ohio, USA. This system supports truck flow among 15 metropolitan statistical areas (MSAs) (210 OD pairs). 68

directed arcs (Figure 4-1), representing 4,698.14 miles of roadway, function to provide connectivity among the OD pairs. For this experimental network, a minimum of 210 paths are needed to connect the OD pairs while at maximum, 119,582 paths could theoretically function to support OD flow (Matisziw, Murray, and Grubesic 2007). In all likelihood though, the number of paths that actually serve to support flow among origins and destinations in this network is somewhere in between these two extremes.

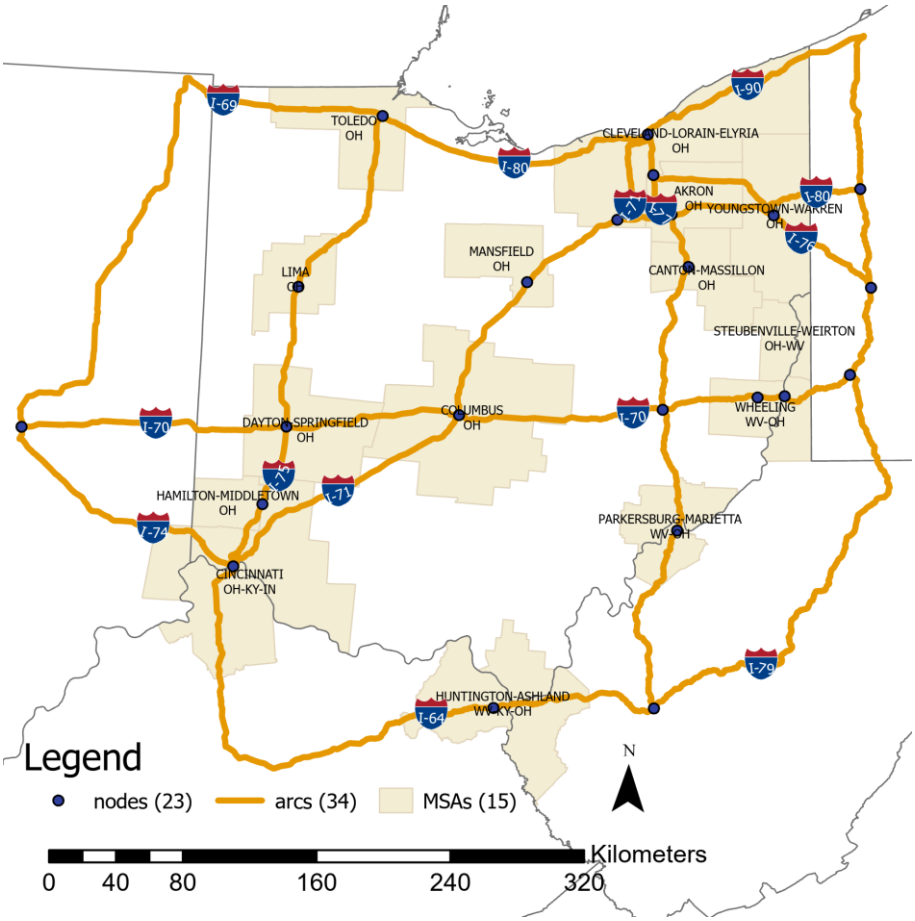

Figure 4-1 Ohio, USA interstate highway network.

In the transportation sciences, many different ways of assigning OD flow to network paths have been proposed based on the hypothesized travel behavior. Rather than focus on any one particular network assignment, this paper explores a range of assignments for flow between each

OD pair in an attempt to better understand the solution characteristics of the model. Although 119,582 OD paths do exist in the system, only 118,114 connect OD pairs having non-zero truck flows. Out of these paths, three subsets of paths were selected to represent viable alternatives for movement between the OD pairs. First, to model the influence of travel cost on flow assignment, the inverse cost for each path is powered by a coefficient β and is evaluated relative to the sum of powered inverse path costs of all paths serving an OD pair as shown in Eq. (4.15). Therefore, when β is high, assignment of flow will be more highly influenced by less costly paths and distributed over a small set of paths. Conversely, when β is low, assignment of flow will be less influenced by path cost and distributed over a larger set of paths.

$$f_m = a_{od}\left(\frac{(1/c_m)^{\beta}}{\sum_{l\in N_{od}}(1/c_l)}\right) \tag{4.15}$$

Second, after an initial proportional assignment of flow, all paths allocated less than 1.0 unit of flow, are removed from consideration and f_m is recomputed. Next, in increasing order of path costs c_m, flows assigned to paths are rounded down to integer values and the fractional remainders are tracked. Whenever at least 1.0 unit of remainder becomes available, it is added to the flow of the incumbent path. Using this process ensures an integer assignment of OD flow on viable paths while also ensuring that total OD flow (a_{od}) is conserved. In this study, these steps were repeated for $\beta = 4$ (generates 4,017 total paths, many alternatives for each OD,), $\beta = 8$ (generates 970 total paths, a moderate number of alternatives for each OD), and $\beta = 12$ (generates 599 total paths, a few alternative paths for each OD).

The likelihood that information sited along a particular arc i will be observed by flow along

a path $m(p_{im})$ could be based upon many different assumptions. Here, it is assumed that flow on an arc will have a higher likelihood of observing the VMS and integrating the content into their decision-making process given a longer arc (i.e., greater opportunity to utilize info). To account for the greater likelihood of exposure given longer arc length, for arcs $i \in R_m$ in path m, $p_{im} = 0.7 + \left(\left(\frac{c_i}{c_m} 0.75 \right) / 4 \right)$. Therefore, all arcs are assigned a likelihood of exposure of at least 0.7 and up to an additional ~19% likelihood could be added based on the length of the arc in relation to the length of the entire path.

The PFCP also requires selection of values for the λ_{od}, and α_m which would be determined based on the planning goals of those managing the infrastructure. Since these parameters can vary in practice, a range of parameters settings are explored in this paper to examine their general influence on the model solution characteristics and output. For the sets of OD paths obtained for each β, three values of λ_o (the proportion of flow leaving each origin to be served) are examined $(\lambda_o = 0.20, \lambda_o = 0.60, \lambda_o = 1.0)$ as are three values of α_m (the probabilistic threshold on exposure that needs to be met before a path can be considered covered) $(\alpha_m = 0.78, \alpha_m = 0.82, \alpha_m = 0.86)$. Thus, for each β, 9 model parameterizations are considered, for a total of 27 different parameterizations.

In this application, the cost of deploying VMS in network is considered as a function of length of the arc on which VMS is to be installed $\delta_i = c_i$. Thus, the objective of the PFCP is to minimize the total roadway length that is to be outfitted with VMS. However, one shortcoming of threshold-based optimization models is that once the threshold for coverage has been met, there is no incentive to further benefit flow. For instance, should there exist more than one way to cover

at least 20% of the flow out of each origin through outfitting three arcs with VMS, from a modeling standpoint, any of the alternative optima will suffice, even if one results in more flow coverage than the others. To explore the tradeoffs that may occur between achieving a probabilistic threshold and incentivizing the coverage of flow, the PFCP cost minimization Objective (4.9) is paired with the opportunity for path diversion objective of Matisziw (2019).

$$\Omega = Maximize \sum_{i \in A} b_i X_i \tag{4.16}$$

Objective (4.16) maximizes the benefit that the facilities can present to flow in terms of providing information that can assist flow in identifying alternative ways of proceeding to the destination (i.e., options for rerouting/diversion). The set of arcs R_m comprising path m can then be evaluated to assess their relative benefit for diverting path flows. The benefit (b_i) of locating information on a particular arc $i \in R_m$ along a path m can be measured as the percent of flow weighted path cost that could be avoided given that opportunities for diversion exists upon exiting arc i. In this way, more benefit will be accrued when a greater proportion of flow weighted path cost can be avoided given information is provided at an arc i.

Given a bi-objective formulation, Pareto-optimal solutions can be identified by way of the NISE method (Cohon, Church, and Sheer 1979). First, a weighted combination of Objectives (4.9) and (4.16) can be formed as in Objective (4.17) so as to identify the noninferior solutions that do best in terms of each individual objective. Given a weight $w = [0,1]$ on Objective (4.9), a weight of $(1-w)$ can be applied to Objective (4.16) as shown in Eq. (4.17).

$$Minimize\ Z = w\Psi - (1-w)\Omega \tag{4.17}$$

For example, one could first optimize Ψ $(w = 0.999)$, with the corresponding objective values being (Ψ_1, Ω_1). Likewise, one could next optimize Ω $(w = 0.001)$, with the corresponding objective values being (Ψ_2, Ω_2). Once a pair of adjacent noninferior solutions are found, such as (Ψ_1, Ω_1) and (Ψ_2, Ω_2), the equation of the line (4.18) connecting two noninferior solutions of (Ψ_1, Ω_1) and (Ψ_2, Ω_2) subject to the original constraints on the problem can be optimized to identify any intervening noninferior solution (e.g., (Ψ_3, Ω_3)).

$$Z = \left(-\frac{\Psi_1 - \Psi_2}{\Omega_1 - \Omega_2} \right) \Omega + \Psi \tag{4.18}$$

For each of the 27 experimental parameterizations, the biobjective specification was solved using the NISE approach with Gurobi 9.0 on a Windows 10 64-bit laptop with four 1.8 GHz processors and 16 GB RAM.

4.5 Discussion

In total 1,311 supported efficient solutions were identified for the various model parameterizations, for which the individual number of solutions (NS) are documented in Table 4-1. Figure 4-2 shows the tradeoffs between cost and benefit to path diversion for all supported efficient solutions for the 9 model parameterizations in which the probability of exposure to information must be at least 78% for flow to be considered covered by the VMS (i.e., $\alpha = 0.78$). Among the solutions for each combination of $\alpha = 0.78$, β and λ, there is a solution at which cost is the lowest (optimizing Objective (4.9)) and at which benefit to path diversion is the highest (optimizing Objective (4.16)). All other solutions, represent tradeoffs between the two objectives. For example, the set of selected arcs for three Pareto-optimal solutions for the $\beta = 4$, $\alpha = 0.78$, $\lambda = 0.2$ parameterization, labeled A, B, and C in Figure 4-2, are depicted in Figure 4-3. Solution

A represents a complete focus on optimizing the cost minimization objective (Figure 4-3a). 14 arcs need to be outfitted with VMS in order to ensure that at least 20% of the outflow from the origin nodes is covered at 78% probability of exposure to the VMS. The selected arcs form three subgraphs in different portions of the state. In all but two instances, arcs representing movement for both directions between pairs of nodes were selected. Solution B (Figure 4-3b) provides nearly 75% more benefit for path diversion than solution A, but involves outfitting 37 arcs with VMS at more than 4 times the cost of solution A. The arcs in this solution form a single subgraph in the central portion of the network. Solution C (Figure 4-3c) represents an intermediate tradeoff between cost and benefit. The 22 selected arcs build upon the three clusters in solution A, entailing about twice as much cost as A and about half that of B while providing approximately 42% more benefit to diversion than A and about 23% less benefit than B. Figure 4-4 illustrate the number of times that each network arc appears in the 115 supported efficient solutions for $\beta = 4$, $\alpha = 0.78$, $\lambda = 0.2$ to provide a better perspective as to which arcs tend to be selected as relevant to more solutions.

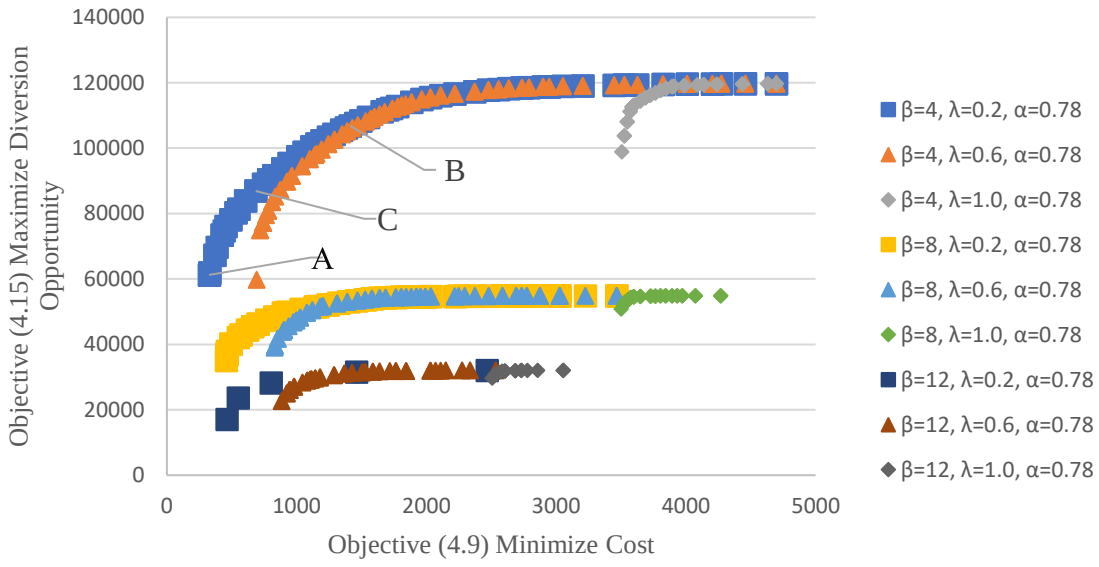

Figure 4-2 Supported efficient solutions for $\alpha = 0.78$ varying β and λ.

Table 4-1 Number of supported efficient solutions and paths for model parameterizations

β	λ	α			# paths with flow
		0.78	**0.82**	**0.86**	
		NS[a]	NS[a]	NS[a]	
4	**.20**	115	113	113	4017
	.60	107	97	95	
	1.0	45	21	15	
8	**.20**	91	89	78	970
	.60	81	71	2	
	1.0	33	23	13	
12	**.20**	5	2	22	599
	.60	45	2	2	
	1.0	17	11	3	

[a]NS = Number of supported efficient solutions.

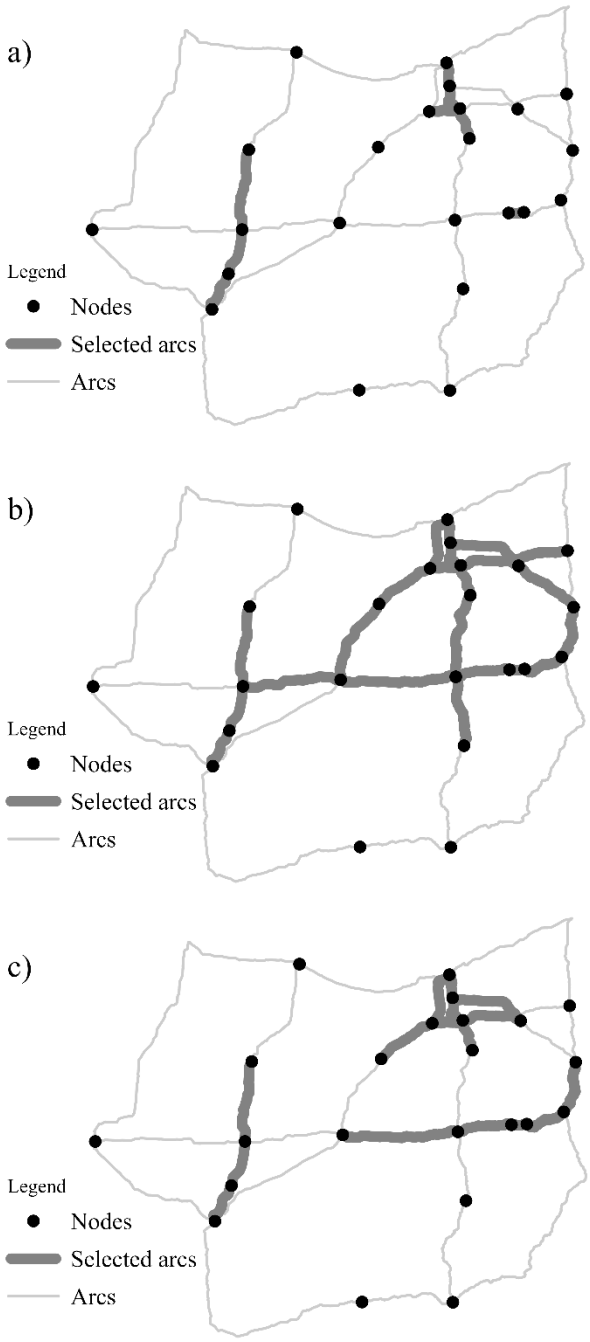

Figure 4-3 Arcs selected in supported efficient solutions for model parameterization $\alpha = 0.78$, $\lambda = 0.2$ and $\beta = 4$: a) solution A, b) solution B, and c) solution C.

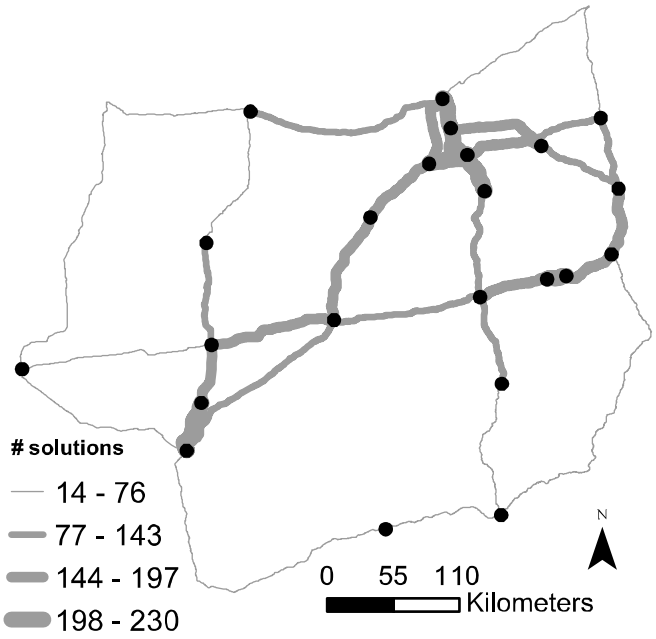

Figure 4-4 Number of times arcs are selected over the 115 supported efficient solutions for model parameterization $\alpha = 0.78$, $\lambda = 0.2$ and $\beta = 4$.

As mentioned earlier, smaller β values generated a greater number of paths for each OD pair. A greater number of paths in turn provide more alternatives to flow and more opportunity for diversion. Thus, all solutions for parameterizations where $\beta = 4$ entail more opportunity for diversion than those where $\beta = 8$ and $\beta = 12$. When a minimum of 20% of the outflow from each origin must be covered $(\lambda = 0.2)$, a variety of lower cost solutions are found. However, as the threshold for coverage of flow out of each origin increases to 60% $(\lambda = 0.6)$ and 100% $(\lambda = 1.0)$, the initial cost of simply satisfying the threshold becomes much more, prior to benefit for diversion becoming a major consideration. For example, while 693 miles of roadway (14.8% of the system) would be involved in a VMS plan to serve 60% of origin outflows for $\beta = 4$, $\alpha = 0.78$, $\lambda = 0.6$ solutions, 3,505 miles of roadway (74.6% of the system) would be involved in order to ensure 100% of flows were covered in $\beta = 4$, $\alpha = 0.78$, $\lambda = 1.0$ solutions.

To examine the characteristics of the PFCP solutions (Objective (4.9)) more specifically, Table 4-2 summarizes solutions optimal with respect to $(w = 0.999)$ for the 27 different model parameterizations. For each combination of β, λ and α, the cost of the selected network arcs relative to the total cost of arcs in the network (MC), the level of benefit for path diversion relative to the maximum benefit for diversion that could be obtained (DB), and amount of flow covered relative to total flow in the system (FC) are reported. For any given α and β combination in Table 4-2, both the MC and DB increase for higher λ coverage thresholds. For instance, for $\alpha = 0.78$ and $\beta = 4$, the MC increases from 6.9 to 14.7 percent as the λ increases from 20 to 60 percent. Since λ is a minimal threshold on the flow that should be served, the proportion of flow actually covered (FC) by the facility configuration can be larger than the threshold in practice. Again, in the case of $\alpha = 0.78$, $\beta = 4$ solutions, when the coverage threshold is $\lambda = 0.2$, 44.5% of system flow is actually covered and when the threshold is $\lambda = 0.6$, 67.3% of system flow is actually covered. For model parameterization involving less paths such as $\beta = 12$, even greater amounts of flow are covered given that the OD flow is assigned to smaller set of shorter paths. As the threshold on the level of confidence that the flow could receive the information from the facilities increased from $\alpha = 0.78$ to $\alpha = 0.86$, MC slightly increased in most instance as did DB except when $\beta = 8$ for $\lambda = 0.2$ and $\lambda = 0.6$. However, in nearly all cases, the proportion of flow (FC) that was actually covered decreased as the α threshold increased.

Table 4-2 Characteristics for solutions optimal with respect to cost minimization objective

β	λ	α								
		0.78			**0.82**			**0.86**		
		MC[a]	DB[a]	FC[a]	MC[a]	DB[a]	FC[a]	MC[a]	DB[a]	FC[a]
4	**.20**	6.9	51.1	44.5	6.9	51.1	43.5	6.9	51.1	42.5
	.60	14.7	49.9	67.3	17.3	60.3	69.3	17.8	62.9	68.5
	1.0	74.6	74.6	100.0	86.3	90.1	100.0	88.3	95.7	100.0
8	**.20**	9.8	63.9	47.6	10.1	68.0	43.3	10.1	64.3	43.8
	.60	17.7	71.0	68.5	21.1	76.1	69.8	21.1	73.9	70.5
	1.0	74.5	92.6	100.0	80.9	97.1	100.0	83.6	99.7	100.0
12	**.20**	9.9	53.4	49.7	10.1	60.7	43.0	10.4	61.1	42.2
	.60	18.8	70.9	70.9	21.2	70.8	72.7	21.2	70.8	72.6
	1.0	53.4	92.8	100.0	59.8	97.5	100.0	60.7	99.8	100.0

[a]MC = % of total system cost, DB = % of maximum diversion benefit, FC = % to total system flow covered.

It should be noted that while in our application arc length was used to represent the cost of siting facilities to provide (or collect) information to network flows, there are alternative ways in which facility costs could be operationalized in this type of modeling approach. For instance, arcs could be split into smaller management units. Alternatively, the number of facilities that would be needed to effectively serve an arc could be explicitly calculated (e.g., based on some recommended minimum facility spacing).

CHAPTER 5

MULTI-OBJECTIVE HABITAT CONNECTIVITY

5.1 Introduction

Research has widely reported changes in species persistence over the past 30 years (Sherman and Morton 1993; Pounds and Crump 1994; Pounds et al. 1997; Ron et al. 2003; Stuart et al. 2004; Wake and Vredenburg 2008). Urbanization, infrastructure, and habitat transformation are frequently cited as among the leading factors responsible for these changes (Hamer 2018; Scroggie et al. 2019; Numminen and Laine 2020; Trombulak and Frissell 2000; Marsh et al. 2017). Given the rapid pace of environmental and landscape change, it is important to understand the factors and mechanisms that may influence habitat connectivity to address management and conservation concerns (Nathan et al. 2008). For example, preserving or creating inter-habitat corridors that best meet the needs of species for dispersal events (e.g., natal dispersal) as well as part their regular migration (e.g., mating, foraging, and summer-winter habitat) is critical to the persistence of species, especially in human-dominated landscapes (Gamble, McGarigal, and Compton 2007; Semlitsch 2008; Lowe 2009).

5.1.1 Landscape Connectivity and Conservation of Biodiversity

The extent to which the landscape supports species movement among habitats is often referred to as landscape or habitat connectivity (Baguette and Dyck 2007; Saura and Pascual-Hortal 2007). Connectivity in this sense is a complex function of landscape and species-specific characteristics. As such, a wide array of metrics for quantifying connectivity have been proposed, many of which are rooted in network theory given its ability to link the spatial structure of complex systems to prospects for movement therein (Galpern, Manseau, and Fall 2011). In network models

of landscape systems, habitat areas (i.e., patches) are represented as nodes and the direct linkages between the habitat nodes are represented as arcs. Connectivity between a pair of habitat areas can therefore be modeled as the set of arcs a species traverses enroute from one habitat to another, often termed a path or corridor. In networked systems though, a multitude of paths between a pair of nodes may exist. Therefore, decisions need to be made as to which paths are actually viable alternatives capable of supporting a particular type of movement. For example, a common assumption in modeling movement is that travel in a system involves costs and hence, efficient movements with respect to those costs are more desirable. A frequently utilized measure of connectivity among habitats in this respect is the shortest or least- cost path (Adriaensen et al. 2003; Sawyer, Epps, and Brashares 2011). In this sense, the relative cost of movement associated with traversing arcs connecting landscape features for a particular species is quantified based upon how different landscape and ecological factors are thought to impede or facilitate movement (Zeller, McGarigal, and Whiteley 2012). Once the cost of traversing arcs in the landscape system has been established, the most efficient inter-habitat path(s) is then often sought as a measure of habitat connectivity (Dijkstra 1959; Floyd 1962). That is, it is assumed that paths (or corridors) that have the lowest cumulative cost (i.e., resistance or impedance) from a species' perspective are more likely to be important in supporting inter-habitat movements (Beier, Majka, and Newell 2009; Gurrutxaga, Lozano, and Barrio 2010).

5.1.2 Modeling Ecological Networks – Least Cost Paths

Modeling the paths (or corridors) that could represent reasonable alternatives for landscape traversal is one approach to reasoning about ecological corridors. While a variety of methods have been proposed for modeling movement, central to many of them is the concept of cost minimization. That is, it is assumed that paths (or corridors) that have the lowest cumulative cost

(i.e., resistance or impedance) from a species' perspective are more likely to be important in supporting ecological corridor over the landscape (Beier, Majka, and Newell 2009; Gurrutxaga, Lozano, and Barrio 2010). The mathematical model used for identifying paths of minimal costs in a network is known as the Shortest Path Problem or more generally as the Least-cost Path Problem.

In order to derive a least-cost path, the cost of moving through each portion of the landscape (i.e., the arcs) must first be quantified. In many ecological applications, the landscape is represented as a grid of systematically sized cells (i.e., a raster). In such applications, each cell is assigned a cost reflecting the relative resistance to movement through that cell. The cost of traversing a cell is usually derived based on the assumed contribution of different landscape characteristics present within the area bounded by the cell. When modeling ecological corridor, combinations of landscape characteristics such as forest canopy, land use and land cover, habitat quality, elevation, road density and proximity to water are frequently used in deriving landscape traversal cost (Adriaensen et al. 2003; Sutcliffe et al. 2003; Parks, Mckelvey, and Schwartz 2012; Matos et al. 2019) . After each cell has been assigned a cost and origin/destination cells have been selected, the raster can be rendered as a network in which a node represents each cell and arcs represent the relationship between neighboring cells. The arcs can then be attributed with the cost values from the corresponding raster cells and the least-cost path model can be applied. The least-cost path problem can then be solved, yielding a single optimal path. It should be noted that while raster-based representations of landscapes are frequently used as a basis for ecological networks, vector-based (e.g., point, line, polygon) representations can also be effectively used (Matisziw et al. 2015).

While least-cost paths based on composite measures of cost have been widely explored, such cost representations have been viewed as lacking a robust biological or empirical foundation (Sawyer, Epps, and Brashares 2011). While there is some evidence that species utilize some sort of decision-making framework when navigating the landscape, the exact nature of the framework and the combination of factors upon which it is premised has not been well established. For example, there are many objectives that have been postulated regarding the amphibian decision-making processes, such as: minimizing distance, minimizing elevation change, maximizing exposure to moist environments, and maximizing likelihood of successful traversal (Bowler and Benton 2005; Todd and Winne 2006; Lowe et al. 2006; Giordano, Ridenhour, and Storfer 2007). Further, the exact combination(s) of objectives that may be underlying movement decisions is unknown. In addition to empirical complexities, other complications can emerge in the interpretation of least-cost paths. The location and characteristics of least-cost paths are highly influenced by the resistance parameterization of landscape. Since several factors are often combined to generate a composite resistance surface, the weights associated with each factor and resistance values assigned to each class within each factor pose enormous uncertainty in the estimates (Beier, Majka, and Newell 2009). In addition, the tradeoffs among different factors cannot be investigated since only one least-cost path is identified. As an example, depending on how the cost function is formulated, in some cases longer paths with relatively low cumulative resistance would be valued more than much shorter paths having higher cumulative resistance (Parks, Mckelvey, and Schwartz 2012). The fact that there are essentially an infinite number of ways in which cost of movement can be derived is perhaps one of the most challenging obstacles to application of least-cost path problems and interpretation thereof. Given these limitations, Parks, Mckelvey, and Schwartz (2012) propose explicitly accounting for biological and

conservational objectives when studying landscape connectivity, and Rayfield, Fortin and Fall (Rayfield, Fortin, and Fall 2010) suggest identifying multiple low cost paths instead of one least cost path. In this study, we propose a methodological approach to account for multiple movement objectives that are known to affect species navigation on the landscape, resulting in many Pareto-optimal paths each optimized with respect to one or combination of objectives. Such approach not only increases the size of decision support but also can be easily adapted to accommodate the movement characteristics of multiple species in natural conservation efforts.

5.2 Multi-objective Habitat Connectivity Problem

A multi-objective *habitat connectivity* problem (MOHCP) is proposed for accounting for a general set of objectives that could be modeled in a least-cost path framework. In particular, three objectives assumed to influence the inter-habitat movement of a species are integrated in the model: a) minimize the total risk associated with movement (Tischendorf and Fahrig 2000; Saura and Pascual-Hortal 2007), b) minimize the total length of movement (Urban and Keitt 2001; Parks, Mckelvey, and Schwartz 2012), and c) minimize change in environmental conditions during movement (Lowe et al. 2006; Giordano, Ridenhour, and Storfer 2007; Cosentino, Schooley, and Phillips 2011). To model these objectives, each arc (i, j) in the network is associated with attributes reflective of environmental change $\left(z_{ij}\right)$, corridor length $\left(c_{ij}\right)$, and risk associated with traversal $\left(\pi_{ij}\right)$. For each origin-destination $\left(o,d \in N\right)$ pair in the network, the MOHCP can be formulated as follows:

$$Minimize\ \Omega_1^{od} = 1 - \Pi_{(i,j)\in A}(1-\pi_{ij})^{x_{ij}} \tag{5.1}$$

$$Minimize\ \Omega_2^{od} = \sum_{(i,j)\in A} c_{ij}x_{ij} \tag{5.2}$$

$$Minimize\ \Omega_3^{od} = \sum_{(i,j)\in A} z_{ij} x_{ij} \tag{5.3}$$

s.t.

$$\sum_{j|(i,j)\in A} x_{ij} - \sum_{j|(j,i)\in A} x_{ji} = \begin{cases} 1 & \text{if } i = o \\ 0 & \text{if } i \neq o, d (i = 1,...,N) \quad i \neq j \\ -1 & \text{if } i = d, \end{cases} \tag{5.4}$$

$$x_{ij} = \{0,1\} \qquad \forall (i,j) \in A \tag{5.5}$$

Objective (5.1) minimizes the risk $(\pi_{ij} = [0,1])$ of traversal failure assuming independence of traversal probability among arcs. This objective is analogous to maximizing the likelihood of successful traversal. Objective (5.2) minimizes the total corridor length. Objective (5.3) minimizes the total change in environmental conditions. Constraints (5.4) and (5.5) are applied as in regular least-cost path problem.

Given that the probability of successful traversal of each arc is $(1-\pi_{ij}) = [0,1]$, Objective (5.1) is monotonically increasing, a sufficient condition for Bellman's principal of optimality (Carraway and Morin 1988). Thus, all sub-paths of a Pareto-optimal path with respect to Objective (5.1) are also Pareto-optimal. Objectives (5.2) and (5.3) are also monotonic, therefore, all sub-paths of Pareto-optimal solutions with respect to these objectives are Pareto-optimal as well. While Objective (5.1) is nonlinear and non-additive, it can be re-stated in an additive and linear form by modifying the transformation function proposed by Reinhardt and Pisinger (2011) as in (5.6).

$$Minimize\ \Omega_1^{od} = \sum_{(i,j)\in A} x_{ij} \ln \left(\frac{1}{1-\pi_{ij}}\right) \tag{5.6}$$

5.3 Solution Methodologies

As discussed earlier, the weighting method is commonly used to identify some of the supported efficient solutions to problems like the MOHCP. However, the extent to which those supported efficient solutions represent the complete set of efficient solutions cannot be determined. Thus, alternative methods for characterizing the efficient set should be explored. In this spirit, a MONISE routine is described for identifying the set of supported efficient solutions and an exact multi-criteria labeling routine is detailed for identifying the complete set of efficient solutions to the MOHCP.

5.3.1 NISE for Biobjective Optimization Models

In cases in which two objectives are to be optimized, NISE method (Figure 5-1) can be applied to estimate the efficient set. This process involves evaluating the solution space between pairs of supported efficient solutions to detect the presence of another supported efficient solution. In Stage B, given Ω_1 and Ω_2, one would first solve for y^{*1} and then y^{*2} in steps 5 and 6. Then, the equation of the line connecting two already found solutions (Lines 12 and 13 in Stage C) could be used to identify intermediate solutions by weighing objective function as of step 18 in Stage D. When new supported efficient solutions are found in Step D, the solution space between them and their neighboring supporting solutions is in turn evaluated for the presence of additional supported efficient solutions. This process continue until all regions of the frontier are explored and returns the supported efficient paths and their objective values in step 32.

NISE Supported Non-dominated Least-cost Paths ($G(N,A), l \in L, o \in N, d \in N$, $\delta = 0.0001,\ k = 0$)

A: Initialization

1. $\bar{W} = ()$ list of criteria weight vectors
2. $Y^* = ()$ list of vectors of Pareto frontiers
3. $U^* = ()$ list of vectors of $|L|$ Pareto frontiers
4. $SEP = ()$ list of arcs for non-dominated path

B: Identify two individual minima

5. for each criterion v in L:
   for each criterion l in L:
   if $v \neq l$: $w_l = \delta$; else: $w_l = (1-\delta)$
   $k = k+1$
6. $s^* \Leftrightarrow y^{*k} = Min\ w_1\Omega_1^{od} + w_2\Omega_2^{od} + w_3\Omega_3^{od}$
   s,t (2) & (3)
7. $SEP.insert\ (\{(i,j) \mid x_{ij}^{s^*} = 1\})$
8. $Y^*.insert(y^{*k})$
9. $U^*.insert(y^{*1}\ \ y^{*2})$

C: Identify new weighting vector

10. $y^{*1} = U^*[|U^*|][1]$
11. $y^{*2} = U^*[|U^*|][2]$
12. $n_1 = -\dfrac{y^{*2}[2] - y^{*1}[2]}{y^{*2}[1] - y^{*1}[1]}$
13. $n_2 = 1.0$
14. $\bar{W}.insert((n_1\ \ n_2))$

D: Solve and explore new facets

15. $r = 1$
16. $While\ |\bar{W}| \geq (r)$:
17. $(w_1, w_2) = \bar{W}[r]$
18. $s^* \Leftrightarrow y^{*r} = Min\ w_1\Omega_1^{od} + w_2\Omega_2^{od}$
    s.t. (2) & (3)
19. If $\{(i,j) \mid x_{ij}^{s^*} = 1\}$ not in *SEP*:
20. $SEP.insert\ (\{(i,j) \mid x_{ij}^{s^*} = 1\})$
21. $Y^*.insert(y^{*r})$
22. $k = k+1$
23. for $q = 1$ to $q = 2$:
24. $U^*.insert(U^*[r])$
25. $U^*[|U^*|][q] = y^{*r}$
26. $y^{*1} = U^*[|U^*|][1]$
27. $y^{*2} = U^*[|U^*|][2]$
28. $n_1 = -\dfrac{y^{*2}[2] - y^{*1}[2]}{y^{*2}[1] - y^{*1}[1]}$
29. $n_2 = 1.0$
30. $\bar{W}.insert((n_1\ \ n_2))$
31. $r = r+1$
32. Return SEP, Y^*

Figure 5-1 NISE algorithm for the biobjective optimization model.

5.3.2 MONISE for MOHCP

To identify the supported efficient solutions for the MOHCP, a MONISE algorithm for identifying supported non-dominated paths is now outlined in Figure 5-2. The *MONISE Supported Non-dominated Least-cost Paths* algorithm requires a network, attributes for each arc that can be used to measure the objectives (e.g., traversal risk, corridor length, level of change) and a pair of

origin and destination nodes (o,d) as input. In Stage A, lists for vectors of objective weights to be applied $(\bar{W})$, vectors of the objectives comprising the Pareto frontier for each solution (Y^*), vectors tracking sets of Pareto frontiers (U^*), as well as storing the arcs comprising the non-dominated paths associated with efficient solutions are initialized. MONISE works by identifying weights for the objectives that will give rise to supported efficient solutions. That is, Objectives (5.1), (5.2) and (5.3) are combined into a single weighted Objective (5.7) where each weight (w_l) has a value [0,1] such that $w_1 + w_2 + w_3 = 1.0$.

$$Minimize\ w_1\Omega_1^{od} + w_2\Omega_2^{od} + w_3\Omega_3^{od} \tag{5.7}$$

In Stage B, a set of initial weights are given to the Objective (5.7) in order to find the three individual minima (e.g., $w_1 = 1.0$, $w_2 = 0.0$, $w_3 = 0.0$ to optimize objective Ω_1^{od}) known as anchor points Messac and Mattson. When identifying anchor points for each objective using Eq. (5.7), there may exist multiple individual minima, all having same values with respect to the objective being optimized using weight $(w_l = 1.0)$ but different values with respect to other objectives $(w_l = 0.0)$. In such a case, some of these solutions are dominated, therefore should be avoided in the solution procedure by giving a small weight $(\delta = 0.0001)$ to the other objectives (step 5). Objective (5.7) subject to Constraints (5.4) and (5.5) can then be solved (step 6) and the arcs associated with the solution (s^*) is stored in the list of supported efficient paths *SEP* (step 7) and the Pareto frontier (y^{*k}) stored in list Y^* (step 8). The Utopia plane defined by the initial three solutions (y^{*1}, y^{*2}, y^{*3}) is then stored in list U^* (step 9). In Stage C, the Utopia plane can then be

used to derive a new set of objective weights (n_1, n_2, n_3) (steps 10-12) which are stored in list $\bar{W}$ (step 13). Now that a new set of objective weights has been found, they can be used in Stage D in an iterative routine (step 15) to generate and solve a new model (step 16-17). The solution to the new model is then evaluated to see whether or not it has already been found (step 18). If it isn't present in the set of identified supported efficient paths, it is added to that set (step 19) and is its Pareto frontier (step 20). Next, the Pareto frontier of the new solution is then iteratively swapped into the plane of solutions used to derive the weights used in the model to construct three new planes to add to list U^* (step 23-24). Each of those planes in turn are used to derive three new weighting schemes (steps 26-27) which are added to the list of objective weights to consider (step 28). Any new objective weightings that are found are likewise used to generate and solve additional models (steps 16-17), find new supported efficient solutions (steps 18-20), and generate new weighting schemes to consider until all supported efficient solutions and associated non-dominated paths have been found (step 30).

MONISE Supported Non-dominated Least-cost Paths $(G(N,A), l \in L, o \in N, d \in N,$ $\delta = 0.0001,\ k = 0)$

A: Initialization

1. $\bar{W} = ()$ list of criteria weight vectors
2. $Y^* = ()$ list of vectors of Pareto frontiers
3. $U^* = ()$ list of vectors of $|L|$ Pareto frontiers
4. $SEP = ()$ list of arcs for non-dominated path

B: Identify anchor points and Utopia plane

5. for each criterion v in L:
   for each criterion l in L:
   if $v \neq l$: $w_l = \delta$; else: $w_l = (1-2\delta)$
   $k = k+1$
6. $s^* \Leftrightarrow y^{*r} = Min \sum_{l \in L} w_l \Omega_l^{od}$
   s.t. (2) and (3)
7. $SEP.insert\ (\{(i,j) \mid x_{ij}^{s^*} = 1\})$
8. $Y^*.insert(y^{*k})$
9. $U^*.insert((y^{*1}\ \ y^{*2}\ \ ...\ y^{*k}))$

C: Identify new weighting vector

10. $R = (0,0), i = 1$
    for h =1 to $|L|$:
    if $(h \neq 1)$:
    $y^{*h} = U^*[|U^*|][h]$
    $y^{*l} = U^*[|U^*|][1]$
    $R[i] = \overrightarrow{y^{*l} y^{*h}} = y^{*h} - y^{*l}$
    $i = i+1$
11. $\vec{m} = R[1] \times R[2]$
12. $(n_1\ n_2\ ...\ n_{|L|}) = \dfrac{\vec{m}}{|\vec{m}|}$
13. $\bar{W}.insert((n_1, n_2 ... n_{|L|}))$

D: Solve and explore new facets

14. $r = 1$
15. *While* $|\bar{W}| \geq (r)$:
16. $(w_1, ..., w_{|L|}) = \bar{W}[r]$
17. $s^* \Leftrightarrow y^{*r} = Min \sum_{l \in L} w_l \Omega_l^{od}$
    s.t. (2) and (3)
18. If $\{(i,j) \mid x_{ij}^{s^*} = 1\}$ not in *SEP*:
19. $SEP.insert\ (\{(i,j) \mid x_{ij}^{s^*} = 1\})$
20. $Y^*.insert(y^{*r})$
21. $k = k+1$
22. for $q = 1$ to $|L|$:
23. $U^*.insert(U^*[r])$
24. $U^*[|U^*|][q] = y^{*r}$
25. $R = (0,0), i = 1$
    for $h = 1$ to $|L|$:
    if $(h \neq 1)$:
    $y^{*h} = U^*[|U^*|][h]$
    $y^{*l} = U^*[|U^*|][1]$
    $R[i] = \overrightarrow{y^{*l} y^{*h}} = y^{*h} - y^{*l}$
    $i = i+1$
26. $\vec{m} = R[1] \times R[2]$
27. $(n_1\ n_2\ ...\ n_{|L|}) = \dfrac{\vec{m}}{|\vec{m}|}$
28. $\bar{W}.insert((n_1, n_2 ... n_{|L|}))$
29. $r = r+1$
30. Return SEP, Y^*

Figure 5-2 MONISE algorithm for the MOHCP.

5.3.3 Multi-Criteria Labeling Algorithm for MOHCP

The multi-criteria labeling algorithm of Martins (1984) can be adapted to accommodate the three objectives in the MOHCP problem to retrieve the full set of efficient solutions (supported and unsupported) from one origin to all destination nodes (Figure 5-3). The *Multi-criteria All Non-dominated Least-cost Paths* algorithm for MOHCP requires a graph, $G(N, A)$, with arcs attributed with the measures needed to evaluate the objectives (e.g., a_{ij}^1, a_{ij}^2, a_{ij}^3), as well as an origin node and a set of destination nodes. In Stage A, empty list Q is initialized to track nodes that have been labeled and need to be reconsidered later in the solution procedure. The origin node is then labeled with a set of initial values, a 5-tuple in which the first three elements reflect objective values when traveling from origin node to the labeled node and the last two referencing the index of the preceding node and an id for the label, respectively. These initial values are to assist with computing objective values at the first move when departing the origin node toward an adjacent node. The labeled origin node is then added Q (step 1). In Stage B, for each labeled node i in Q (step 3), the objective values of the neighboring nodes $\{ j \mid (i, j) \in A \}$ are re-computed as accessed through node i (steps 5-9), with their labels updated accordingly. Each label is representing objective values for one path connecting origin node to the labeled node. Therefore, some of these labels are associated with dominated paths and some are associated with non-dominated paths. Dominated paths are those that have equal or higher cost with respect to all modeling objectives comparing to a non-dominated path. A filtering technique is applied to drop dominated paths whenever a set of labels is updated or changed (step 10). Whenever a new node $\{ j \mid (i, j) \in A \}$ is visited, its label set is evaluated to check if the set of non-dominated paths from origin node to that node have changed or not. Should a node's label be updated, it is added to Q

for reconsideration (steps 11-12). Finally, the incumbent node i is removed from Q (step 13) and the process continues until all nodes are visited and labeled. In Stage C, the supported and unsupported non-dominated paths are retrieved by tracking labels, from each destination node back to the origin node using the reference index to the predecessor node embedded in each label (steps 18-27) and placed into the list AEP.

Multi-Criteria Least-Cost Path Labeling $(G(N,A), A(a_{ij}^1, a_{ij}^2, a_{ij}^3), (o \in N, d \in D))$

Step A: Initialization

1. $\text{Label}(o) = \{(1,0,0,o,1)\}$ & $Q = \{o\}$

Step B: Start from origin node and label all network nodes

2. While $Q \neq \varnothing$:
3. $i = Q[1]$
4. for $j \mid (i, j) \in A$:
5. if Label(j) does not exist, Label(j) $= \varnothing$
6. TempLabel=$\varnothing$
7. for g in Label(i):
8. TempLabel.insert$\left(\left(g[1] \times a_{ij}^1, g[2] + a_{ij}^2, g[3] + a_{ij}^3\right)\right)$
9. Label(j)=Label(j).merge(TempLabel)
10. Label(j).remove(dominated labels)
11. if j not in Q:
12. Q.insert(j)
13. Q.remove(i)

Step C: Construct non-dominated paths

14. $AEP = \varnothing$
15. for $d \in D$:
16. for l in Label(d):
17. path $= \varnothing$
18. path.insert(d)
19. $\theta = l[4]$
20. $\theta \neq o$:
21. path.insert(θ)
22. index = Label[θ][5]
23. preceding = Label[θ][index][4]
24. path.insert(o)
25. AEP.insert(path)
27. Return AEP

Figure 5-3 Multi-criteria least cost path labeling algorithm for the MOHCP.

5.4 Application to Amphibian Habitat Connectivity

The MOHCP is now applied to model paths/corridors that could support amphibian habitat connectivity to illustrate the applicability of the multi-objective optimization framework and solution approaches.

5.4.1 Factors Affecting Amphibian Habitat Connectivity

The persistence of amphibians depend on aquatic and terrestrial habitat, and the ability to successfully migrate and disperse (Heard, Scroggie, and Malone 2012; Sinsch et al. 2012). There is some doubt as to the amphibians' ability to accurately orient themselves with respect to prospective new habitat (Patrick, Aram, and Malcoln 2007; Semlitsch 2008). However, there is evidence that movements toward and away from breeding sites are nonrandom. For instance, Walston and Mullin (2008) report that the initial orientation of juveniles from breeding ponds may be influenced by the width of surrounding forested habitat. Diego-Rasilla, Luengo, and Phillips (2008) discuss the potential role of geomagnetic fields in the movement of palmate newts. There is an increasing body of research that has noted the effects that different types of landscape conditions may have on the ability of amphibians to traverse the landscape. For example, Lowe et al. (2006) report slope between habitat having a negative effect on gene flow and dispersal. In another study, Giordano, Ridenhour, and Storfer (Giordano, Ridenhour, and Storfer 2007) report limited gene flow between high-altitude and low-altitude sites, highlighting the negative impact of elevation change on dispersal. Amphibian movement is known to be influenced by changes in moisture conditions, perhaps in attempts to minimize risk of desiccation and depredation (Todd and Winne 2006). Corridor Length has also been reported as a factor affecting the movement of amphibians (Semlitsch 2008; Pittman, Osbourn, and Semlitsch 2014) and is viewed as an important factor when modeling cost and likelihood of successful dispersal over the landscape

(Bowler and Benton 2005). Therefore, three objectives that may be relevant to amphibian habitat connectivity that fit into the general MOHCP framework are: a) minimize traversal risks associated with land use/land cover types, b) minimize distance and deviation from ideal moisture conditions, and c) minimize change in elevation, which relate to Objectives (5.1)-(5.3) in the MOHCP respectively.

5.4.2 Study Area and Experimental Design

The MOHCP and solution methodologies outlined earlier are applied to model landscape paths supporting amphibian habitat connectivity in a portion of Pershing State Park, located in the state of Missouri, USA (Figure 5-4). This area hosts a variety of wetland types and other landscape features including woody-dominated wetland, deciduous forest, deciduous woody, grassland, cropland, open water and impervious surface. The study site contains 12 wetlands which are considered to be viable origin and destination amphibian habitats.

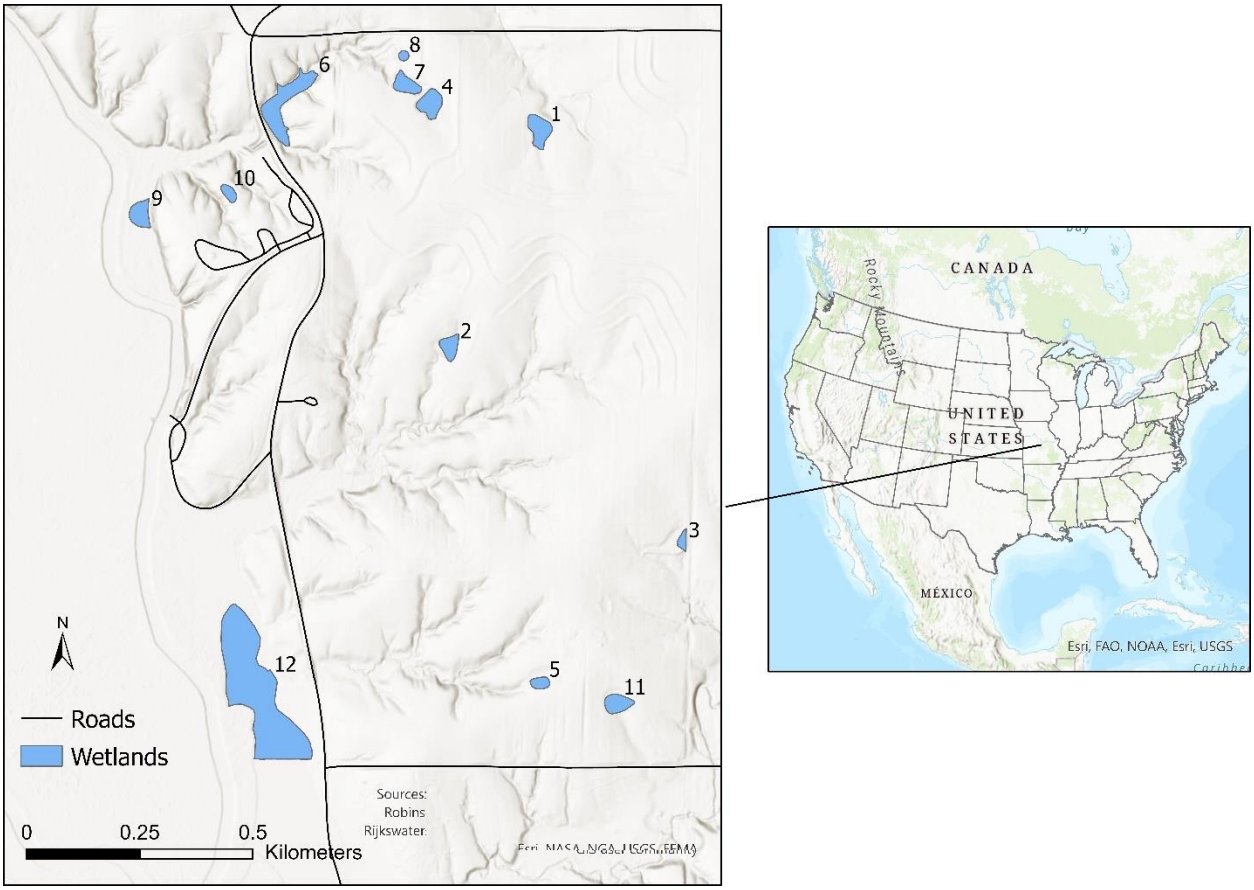

Figure 5-4 Study site.

While many studies of habitat connectivity utilize a raster-based model of the landscape as a basis for the network, vector-based models can be used as well (Matisziw et al. 2015), especially when the landscape characteristics exhibit homogeneity over larger areas as is the case with the current study site. To represent the landscape to be traversed, each wetland was rendered as a network node. The areas intervening the wetlands were also rendered as nodes located to represent the spatial variation in land use/ land cover in the region and arcs were added between neighboring nodes. Nodes were then added at locations where the network arcs intersected land use/ land cover polygon boundaries to ensure each arc only traverses one land use/ land cover category. More specifically, a total number of 200 nodes were randomly positioned in the study area, 12 of which

specifically located inside of wetlands in order to serve as origin and destination nodes. The remaining 188 nodes were distributed among 7 land use types proportional to their areal unit of total study area (0.74 square mile). Next, 200 Thiessen polygons covering the full study area were created, and point features were connected using the neighboring relation among Thiessen polygons, resulting an initial network with 200 nodes and 567 undirected arcs shown in Figure 5-5. Since the network arcs may cross different land use types or/and both terrestrial and aquatic habitat, it wouldn't be possible to assign one single traversing cost to each arc when modeling risk associated with amphibian movement on each type of land use or habitat. Therefore, the initial network layer was intersected with the wetland and land use/land cover layers to find points of geometric intersection and split network arcs at those points so as to ensure one single value can represent risk associated with movement on each arc. The resulting network (Figure 5-6) consists of 909 nodes and 1277 arcs, and seems similar to the initial network (Figure 5-5) but with 709 additional junctions (breakpoints) located along the arcs at their geometric intersection with land use/ land cover and wetlands layers.

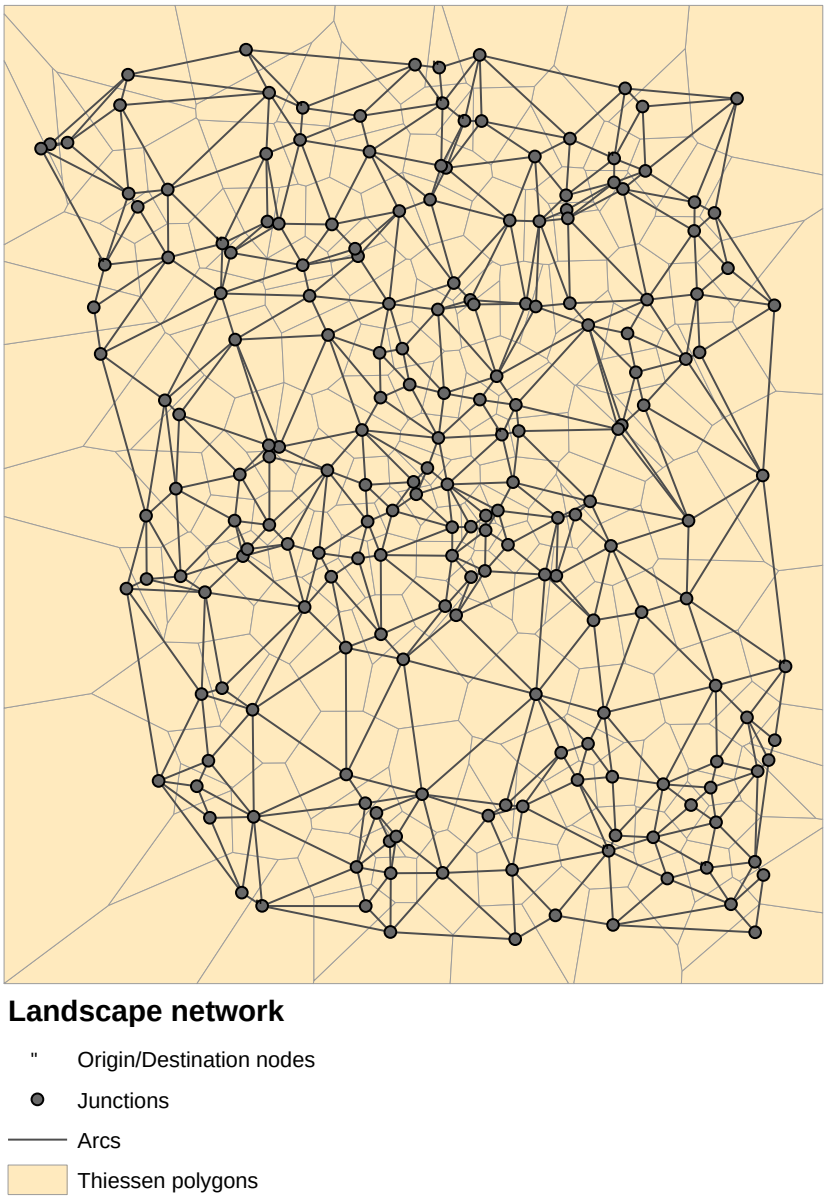

Figure 5-5 Thiessen polygons and the network G created for modelling terrestrial movement.

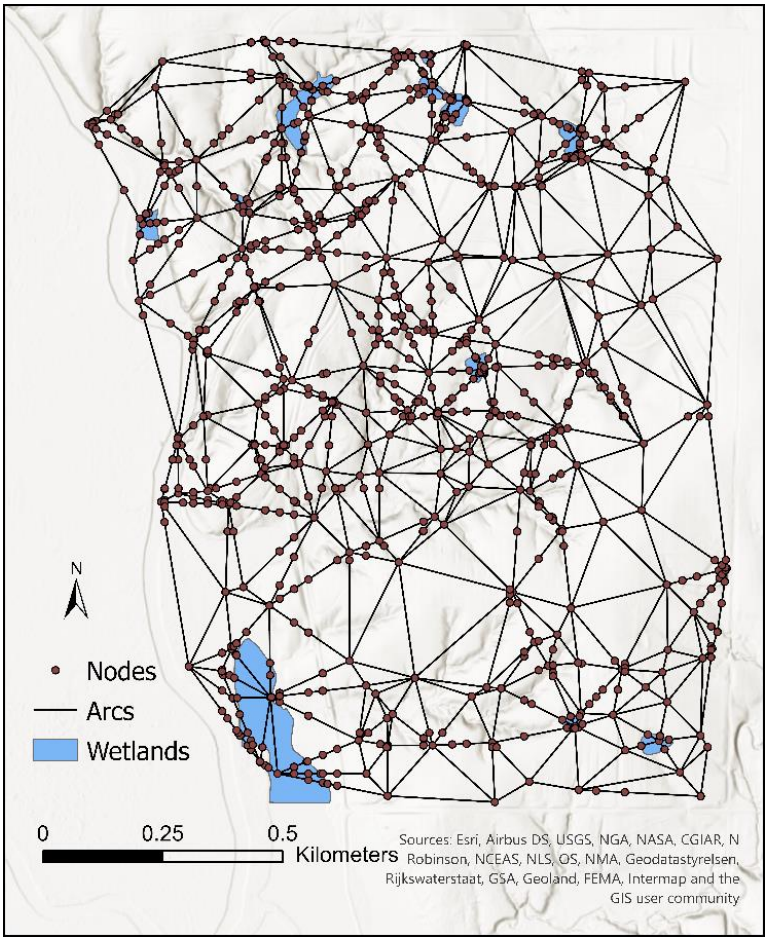

Figure 5-6 Network representation of wetland system.

The arc attributes needed to assess Objectives (5.1), (5.2) and (5.3) were then derived from supplementary layers of geographic data. The elevation of each node was extracted from a digital elevation model (DEM) (MSDIS 2019) (Figure 5-7). The effects of elevation change were calculated for each arc by subtracting elevation of the end nodes e_j from that of starting nodes e_i. Elevation change was classified as either uphill or downhill where uphill movements were weighted twice as high as downhill movements based on their perceived negative impact as in (5.8) to compute z_{ij}.

$$z_{ij} = \begin{cases} w_p(e_j - e_i), & \text{if } e_j \geq e_i \\ w_n(e_i - e_j), & \text{if } e_j < e_i \end{cases} \quad \forall (i, j) \in A \tag{5.8}$$

Surface moisture was estimated using the topographic wetness index (TWI) index of Beven and Kirkby (1979). The TWI is formulated as $TWI = \ln(\alpha / \tan(\beta))$, where α is the drainage area and β is local slope. Drainage area (α) and local slope (β) were derived from the DEM. When calculating the TWI index, locations having zero slope and a non-zero drainage area were given the maximum meaningful TWI value $(TWI = 21.77)$ over the study area, and locations having zero slope and zero drainage area were given the lowest meaningful value $(TWI = -0.66)$. TWI for the study region is shown in Figure 5-7b. The cost weighted deviation of the soil moisture m_{ij} along an arc (as measured using TWI) from ideal surface moisture conditions for amphibians (M) was then computed as $\left((M - m_{ij} + 1)c_{ij}\right)$. That is, when soil moisture is low relative to the ideal level, the greater the deviation and associated cost to traversal. Land use/land cover was used as a basis for characterizing traversal risk (Figure 5-7c). To do this, each arc was associated with its underlying land use/ land cover (MSDIS 2019). Land use/land cover categories were assigned a base level of risk (π^b) (Table 5-1). Since longer arcs pose higher exposure to a risk category, an adjustment function was applied $\left(\pi_{ij} = \pi^b + c_{ij}\pi^b / 2c_{\max}\right)$ such that the base risk level is increased up to 50.0 % based on the length of an arc c_{ij} relative to the longest arc $c_{\max}$ in the network. While in this study we use expert opinion to assign discrete risk values in Table 5-1, surrogate models or curve fitting can be applied to build a functional output of underlying data representing the rate of species loss when exposed to different land use/land cover categories. Finally, arcs that are within wetland polygons were attributed with zero costs given that characteristics within each wetland

were assumed to be homogenous. Should significant variations exist within a habitat area, the habitat would best be represented as multiple polygons/nodes. A summary of the arc attributes used to represent the three objectives is provided in Table 5-2.

Table 5-1 Relative risk associated with traversal of various types of land use/land cover

Land use/land cover class	Relative risk (π^b)	Area (sq. km)
Woody-dominated wetland	0.060	0.183
Deciduous forest	0.065	0.531
Deciduous woody/Herbaceous	0.070	0.095
Grassland	0.075	0.572
Open water (river)	0.085	0.085
Cropland	0.090	0.428
Impervious surface	0.095	0.035
		Total = 1.929

Table 5-2 Summary of arc attributes

Variable	Mean	SD	Min	Max
π_{ij} *	0.080	0.012	0.060	0.135
m_{ij} **	3.31	3.77	- 0.66	21.77
z_{ij} ***	1.645	1.906	0.0	13.293
c_{ij} ***	49.879	49.043	0.006	305.195

*% likelihood, **TWI, ***meters.

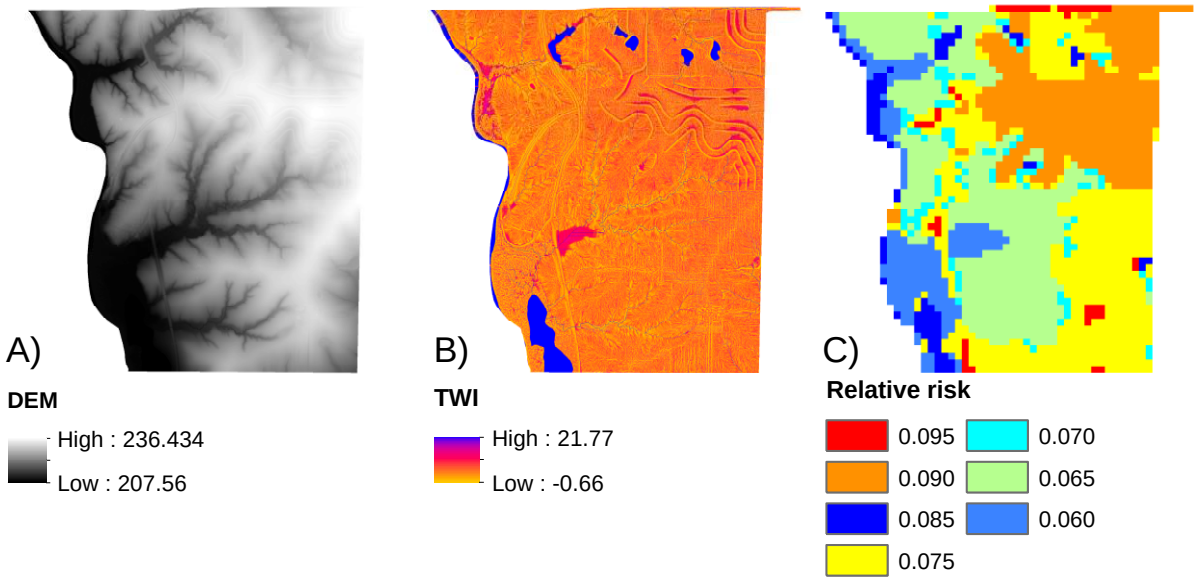

Figure 5-7 Elevation, TWI, and relative risk.

5.5 Results and Discussion

Both the *MONISE Supported Non-dominated Least-cost Paths* algorithm and the *Multi-Criteria All Non-dominated Least-cost Paths* algorithm were applied to solve the MOHCP for the landscape network representing prospects for amphibian movement in the study site. The algorithms were implemented using Python 3.6.6 on a Windows 10 64-bit with five 1.80 GHz processors and 16.0 GB RAM. The optimization solver Gurobi 9.0 was used to find the optimal solution to weighted models in the MONISE routine (steps 6 and 17 in Figure 5-2).

The *MONISE Supported Non-dominated Least-cost Paths* algorithm was executed 132 times, once for each origin-destination pair, identifying all 620 supported efficient solutions in 13.40 minutes. The *Multi-Criteria All Non-dominated Least-cost Paths* routine was executed 12 times, once for each origin, identifying all 3,550 efficient solutions and associated non-dominated paths (supported and unsupported) in 34.46 minutes. Therefore, it is easy to see that the unsupported

paths constitute more than 82% of the non-dominated paths, paths that would be ignored in other estimation procedures such as the weighting method and MONISE. For individual origin-destination pairs of wetlands, the number of supported non-dominated paths range from 1-25, while the number of all non-dominated paths (both supported and unsupported) range between 1-183. Our results suggest that majority of efficient paths in multi-objective optimization are located at the nonconvex portion of objective space. In this application, we applied an exact labelling algorithm to identify both supported and unsupported paths, however, approximate procedures such as MONISE can be adapted to find the unsupported paths as well, a possibility that can be explored in future studies. For instance, one approach could be prohibiting already found supported paths in next iterations so as to push unsupported paths to the frontier of objective space and identify them by iterative execution of MONISE. In corridor planning, finding several alternative paths in single objective optimization model has been of special importance, and K-shortest path, K-similar paths, near shortest paths, gateway and multi-gateway shortest paths are only some examples of prior attempts in literature for increasing the number of alternative paths (Scaparra, Church, and Medrano 2014). In a similar context, our analysis indicates that comprehensive exploration of frontier in multi-objective optimization models propose a great opportunity to substantially increase options for decision-making in corridor planning.

5.5.1 Solution Characteristics

Table 5-3 reports the number of non-dominated paths originating from and destined to each wetland. In general, wetlands with a larger number of supported non-dominated paths also tend to have larger number of unsupported non-dominated paths. The number of arcs entering each wetland vary based on their size, shape, and relationship with other land use/ land cover areas. The smallest wetland (perimeter = 70.8 m) has only three entrance arcs while the largest wetland

(perimeter = 957.2 m) has 14 entrance/exit nodes. As such, some wetlands are going to have more prospective paths given that more opportunities for entrance/exit may exist.

Table 5-3 Number of supported and unsupported non-dominated paths identified for each wetland

Wetland ID	Perimeter (m)	# entrance /exit nodes	# supported		# unsupported		# all	
			Incoming	Outgoing	Incoming	Outgoing	Incoming	Outgoing
1	214.8	9	34	27	139	128	173	155
2	166.5	6	43	43	154	122	197	165
3	117.4	5	43	41	163	162	206	203
4	194.4	8	52	48	158	166	210	214
5	113.7	8	54	56	204	173	258	229
6	524.1	9	50	46	194	204	244	250
7	181.9	7	32	34	203	250	235	284
8	70.8	3	38	35	216	257	254	292
9	190.3	5	45	50	262	280	307	330
10	116.2	6	67	84	305	263	372	347
11	172.8	5	74	70	293	296	367	366
12	957.2	14	88	86	639	629	727	715
Sum	3020.1	85	620	620	2930	2930	3550	3550

For supported non-dominated paths, the average objective values with respect to likelihood of successful traversal, deviation from ideal soil moisture weighted distance (cost and moisture level shown separately), and elevation change are detailed in Table 5-4. In aggregate, the supported non-dominated paths tend to have better average objective values with respect to all modeled objectives than the unsupported paths. One reason for this is that there are many more unsupported paths between distant wetlands given more diverse opportunities for routing exist. As discussed earlier, the supported non-dominated paths are only a subset of the full non-dominated set. While the computational time required to identify the supported set using the MONISE algorithm is approximately 37% of that needed to identify the complete set of non-dominated paths, the supported non-dominated solutions only constitute 17% of the full set of non-

dominated paths (supported and unsupported). Considering the smaller size of supported non-dominated set and larger standard deviation among the routing objectives in those solutions, it is clear that analysis and decision-making based upon only consideration of the supported efficient solutions (or a subset thereof) is rather limiting given those solutions represent such a small proportion of the efficient set.

Table 5-4 Summary of movement objectives for supported and unsupported non-dominated paths

Path attribute	Supported efficient paths			
	Mean	SD	Min	Max
$1-\pi_{ij}$ *	0.24	0.16	0.02	0.91
m_{ij} **	23404.05	9455.75	1096.88	46028.09
z_{ij} ***	42.74	21.91	0.52	110.42
c_{ij} ***	1329.47	551.45	50.31	2401.98
	Unsupported efficient paths			
$1-\pi_{ij}$ *	0.14	0.09	0.02	0.70
m_{ij} **	29215.34	7585.58	5318.42	47667.66
z_{ij} ***	53.47	19.86	5.25	115.59
c_{ij} ***	1641.89	443.12	278.58	2693.71

*% likelihood, **TWI, ***meters

Each panel in Figure 5-8 depicts the Pareto frontier for paths from one origin wetland to six of the destination wetlands (wetland ids correspond with those in Figure 5-4). The circles represented characteristics of supported non-dominated paths while the squares represent characteristics of unsupported non-dominated paths. For example, Figure 5-8a shows the frontier for paths originating at wetland 7 destined to wetlands 1 through 6. There is only one non-dominated path (which is a supported path) between wetland 7 and 4 and it has the lowest weighted distance, lowest elevation change, and highest probability of successful traversal. That is reasonable given that the wetlands are extremely close together. Wetland 7 is a little further from

wetlands 6 and 1 and there are two supported and two unsupported non-dominated paths connecting it to both. Again, without using the label correcting approach, 50% of the non-dominated paths would have been missed. In cases in which wetlands are separated by greater distance and more diverse network structure, options for movement can exhibit much more variation. For example, wetlands 7 and 5 are both relatively small and far apart. However, there are many more non-dominated paths 3 of which are supported with the other 15 being unsupported. All of these paths have relatively low probabilities of traversal success (0.11-0.21%), but have quite a bit of variation in elevation change (24.6-59.8m) and a small amount of variation in their weighted distance (25,391-30,962). Figure 5-8f shows the frontier for paths originating at wetland 12 destined to wetlands 1 through 6. Wetland 12 is relatively large and has multiple entrance/exit points to the landscape network. As such, there are more opportunities for finding competitive combinations of objectives. A majority of the non-dominated paths in this case are unsupported and the diverse nature of the tradeoffs between the objectives can be seen. Consider for instance the frontier for paths between wetlands 12 and 1. In this case, there are three supported and 79 unsupported non-dominated paths. So again, if one were to only identify the supported non-dominated paths in this example, more than 96% of the other non-dominated paths would be ignored. Among these paths, the probability of successful traversal ranges from 0.02 to 0.19%, with elevation change ranging from 50.4m to 111.2m and weighted distance ranging from 28,790 to 44,815.

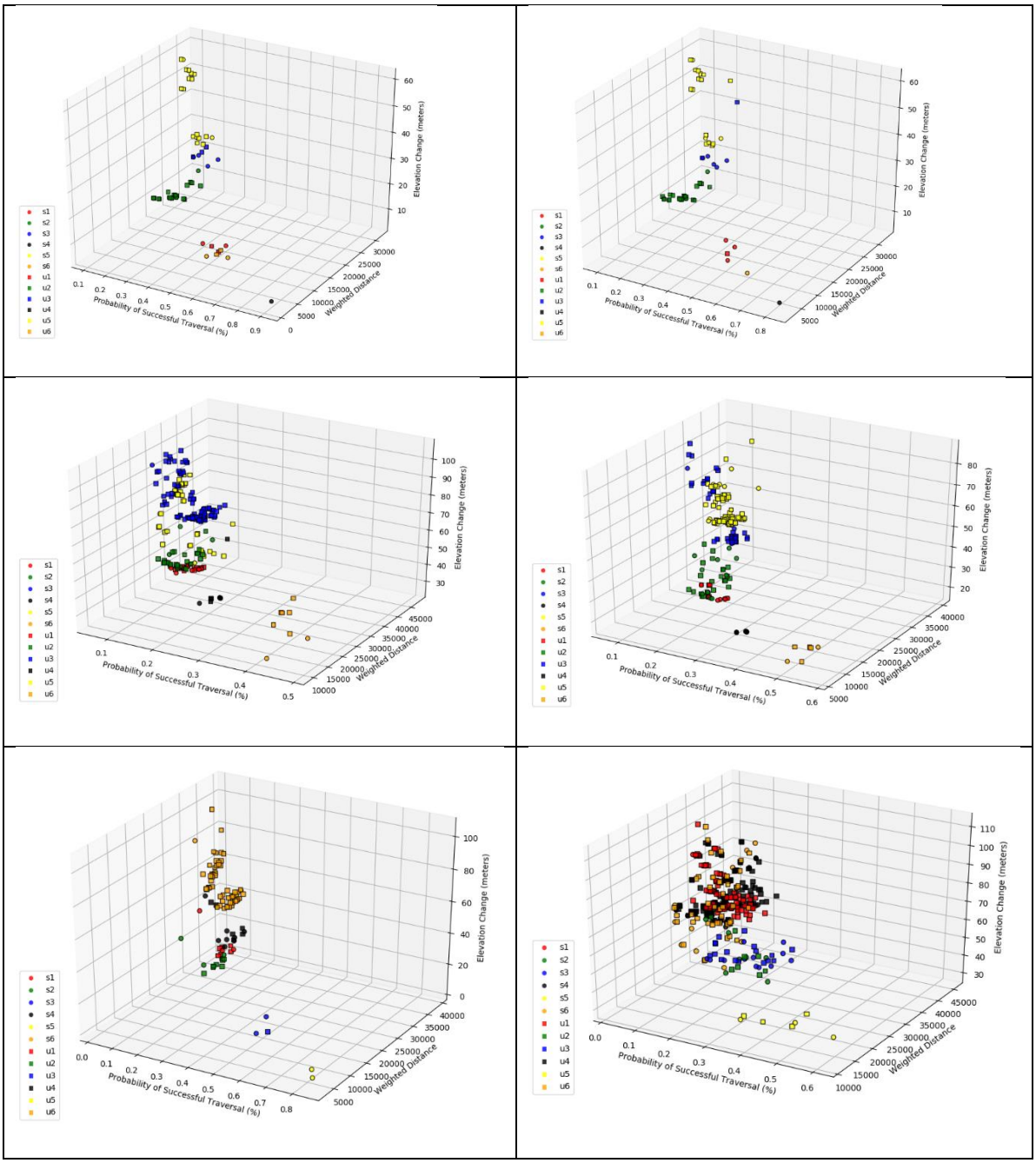

Figure 5-8 The Pareto frontier for paths destined to wetlands 1, 2, 3, 4, 5, and 6 from: a) wetland 7, b) wetland 8, c) wetland 9, d) wetland 10, e) wetland 11, and f) wetland 12.

Figure 5-9 classifies each arc by the number of supported non-dominated paths traversing it in the anchor point solutions (those optimizing each individual objective as in steps 5-6 in Figure

5-2). In this sense there are 132 non-dominated paths for each objective (one path between each pair of wetlands). When optimizing the probability of successful traversal (Figure 5-9a) only 293 of the 1,277 network arcs (22.9%) were traversed by a non-dominated path. The majority of those (162) were traversed by 6 or less paths with only 13 being traversed by 19 or more paths. When optimizing weighted distance (Figure 5-9b) 37.7% of the network arcs were traversed by a non-dominated path, indicating that more arcs were favorable in some way toward that objective. A majority of those (344) were still traversed by 6 or less paths. Figure 5-9c shows the non-dominated paths resulting from optimizing the elevation change objective. In this case, only 22% of the arcs are traversed by a path and there are more arcs (52) that are traversed by 19 or more paths indicating greater consolidation of utility among the wetlands. It should be noted that for any of the three objectives (Figure 5-9a-c), there are instances in which arcs traversed by non-dominated paths according to that objective are not utilized at all by paths non-dominated with respect to one or both of the other objectives. The efficient paths found in our application are suitable for amphibian species movement, but movement costs and objectives in MOHCP can be easily modified to account for multiple species. Given that species have limited travel distance range, the location of arcs traversed by many paths can be factored into locating prospective constructed/compensatory wetlands with the aim of facilitating multistep and generational inter-habitat species movement.

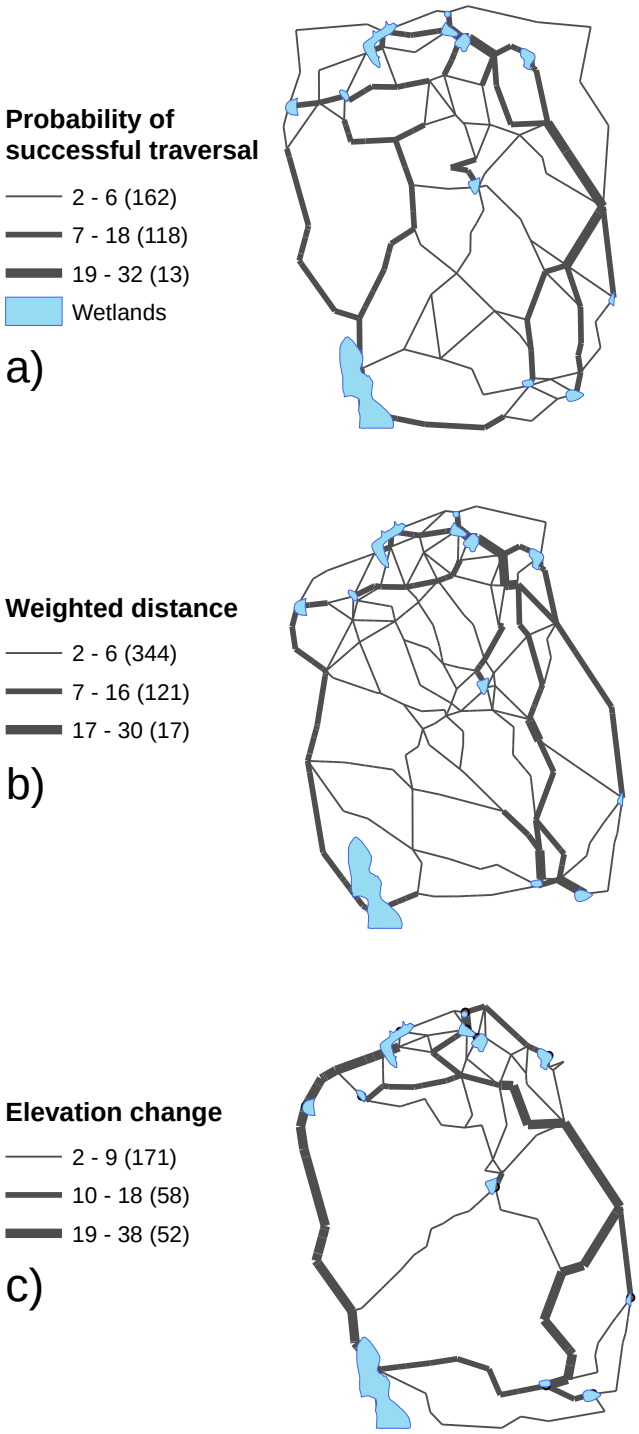

Figure 5-9 Number of non-dominated paths using arcs in anchor solutions with respect to a) Ω_1 (probability of successful traversal), b) Ω_2 (moisture weighed distance), c) Ω_3 (elevation change).

The spatial distribution of the supported and unsupported non-dominated paths is shown in Figure 5-10. Figure 5-10a shows the number of supported paths that traversed each arc. In this case, approximately 55% of the arcs are traversed by at least one supported path (unused arcs are not shown). There are clearly some portions of the network that are much more utilized than others. Figure 5-10b shows the number of unsupported paths traversing each arc. These unsupported paths traverse approximately 75% of the arcs in the network, making use of 20% more of the system than the supported paths. Many of the arcs that were heavily traversed by supported paths are also heavily traversed by unsupported paths, emphasizing their role in the system. However, there are also some arcs that were used to a lesser extent by the supported paths that are used much more by the unsupported paths. For some additional perspective, Figure 5-10c shows the spatial distribution of all of the non-dominated paths (supported and unsupported) as well as the arcs that are never traversed by a non-dominated path. These unused arcs account for 25% of the network arcs, many of which occur near the periphery of the wetland system.

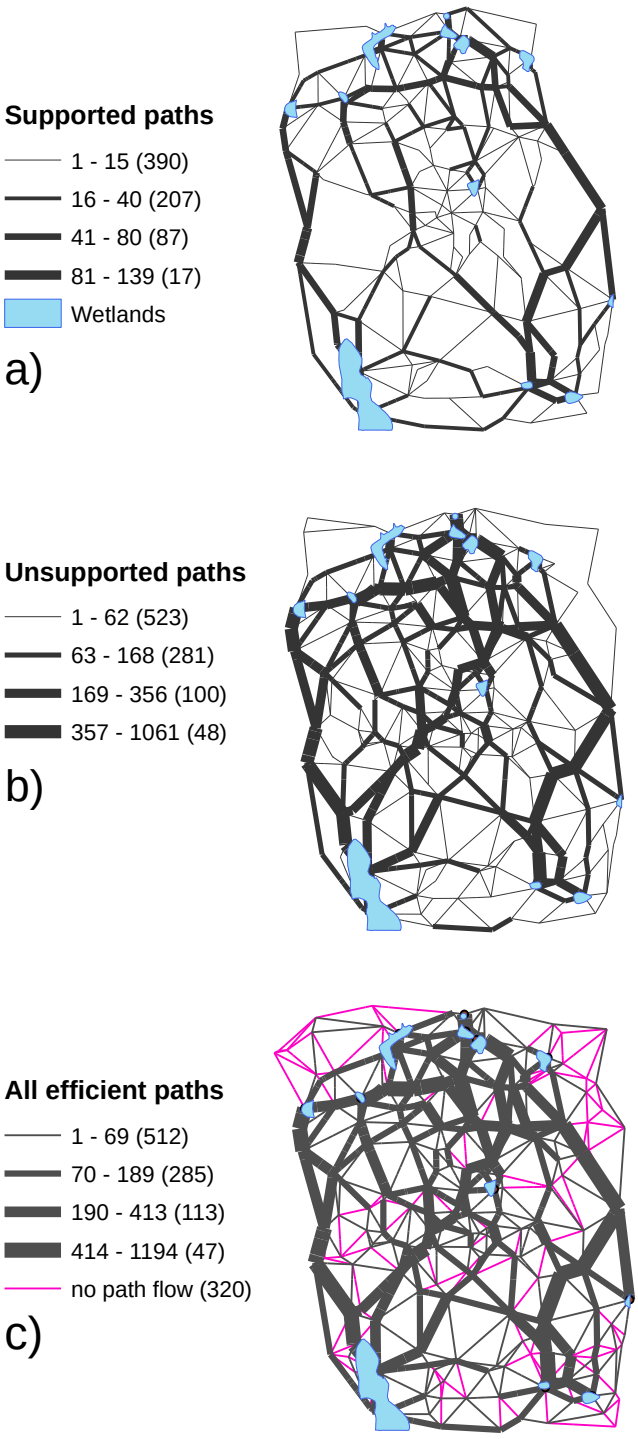

Figure 5-10 Non-dominated paths: a) supported, b) unsupported, and c) all.

CHAPTER 6

VULNERBILITY ASSESSMENT OF ECOLOGICAL SYSTEMS

6.1 Modeling System Change

In practice, changes to networks can be induced due to a variety of phenomena such as industrial accidents, natural disasters, and intentional or unintentional human intervention (Grubesic and Matisziw 2013; Edara and Matisziw 2015). As detailed earlier, there is a need for contextualizing relative impacts to connectivity in a habitat network over time, such as those that may result from landscape alterations due to infrastructure development or landscape management projects. In such cases, a planning agency may have limited resources available for altering the landscape (e.g., road construction, landscape drainage, urban development, etc.) over a set of planning periods. Once the resources for landscape modifications have been used for one planning period, the functionality of the landscape from the perspective of a species may be changed. Even though the impact to landscape connectivity for a species may not be extreme in one period, the cumulative impacts over time have the potential to compound the effects of connectivity loss.

A variety of mathematical models have been proposed for identifying scenarios of change in networks (Matisziw and Murray 2009; Losada, Scaparra, and O'Hanley 2012; Matisziw, Grubesic, and Guo 2012; Q. Li and Savachkin 2013; Starita and Scaparra 2016; Jiang and Liu 2018). In some instances, the worst-case and/or best-case scenario(s) of network change is sought (Church, Scaparra, and Middleton 2004). The reason for this is that knowledge of the best and worst-case outcomes provides context for any other scenarios that could arise (e.g., proximity to best and/or worst-case scenarios). In cases where there are several entities acting upon a network in different, perhaps opposing ways, the process of network change over time can be modeled as a two player game (e.g., Stackelberg game) (Shen, Smith, and Goli 2012; Lei, Shen, and Song 2018). In such

approaches, one entity makes a decision to use/modify the network to optimize their planning objective(s) which is then followed by the other entity making a decision to use/modify the network to optimize their planning objective(s) in light of the actions of the other entity. For example, Acevedo et al. (2015) and Sefair et al. (2017) develop optimization models for identifying a set of sites to protect given future disturbance to some unprotected sites. In their modeling approach, the protected sites are determined by maximizing the minimum life expectancy resulting from disturbance stage, and the effects of disturbance and protection on a population of interest are captured by discrete-time Markov chain. Changes to the landscape and the impact on habitat connectivity can be examined using this type of game theoretical approach. One problem reflects an effort to modify the landscape. The other problem reflects how habitat connectivity from the perspective of a species is changed in light of the modified landscape. The interplay between these two competing interests can then be evaluated over time. That is, in one period landscape connectivity for the species is evaluated and the set of paths that provide optimal connectivity with respect to the current landscape configuration are identified. In the next period, an entity modifies the landscape in some way (e.g., damaging or improving the characteristics of the network arcs/nodes). Landscape connectivity is then reassessed for the species and changes to connectivity can be documented to assess the impact of the landscape alterations to the species. This process can be played out over many periods to examine the long-term impacts of landscape changes to the species. In this way, alternative scenarios of landscape changes over time can be better evaluated with respect to their impact on habitat connectivity. Next, a bilevel optimization framework is described for identifying the worst-case set of landscape alterations for habitat connectivity. The developed methodology is then applied to a wetland system of origins and destinations supporting amphibian species movement.

6.2 Connectivity Degradation Problem (CDP)

Consider a directed graph G^t in time period $t \in T$ comprised of a set of N^t nodes and A^t arcs $\left(G^t(N^t, A^t)\right)$ in which connectivity among a set of origin $o \in N^t$ and destination nodes $d \in N^t$ is of interest. Connectivity between origin and destination habitats is assumed to exist whenever a viable path, comprised of arcs $(i, j) \in A^t$ is present. The subset of network G^t that can be traversed by a species in time t is denoted $\hat{G}^t(\hat{N}^t, \hat{A}^t)$ and the set of viable paths connecting pairs of habitats in time t, EP_{od}^t, are known. The worst-case scenario of network change for species connectivity given that up to τ_t arcs can be lost in a period can then be modeled. Given the set of arcs in $\hat{G}^t$, the decision as to whether an arc is targeted for alteration $\left(Q_{ijt} = 1\right)$ or left unaltered $\left(Q_{ijt} = 0\right)$ must be made as is whether each path is viable $\left(Y_{odtk} = 1\right)$ or no longer of use $\left(Y_{odtk} = 0\right)$, as well as if connectivity between each OD pair remains $\left(Z_{od}^t = 0\right)$ or been lost $\left(Z_{od}^t = 1\right)$. These decisions can be modeled in a manner similar to that of Matisziw, Murray and Grubesic (2007).

$$CDP: \ Maximize \ \Gamma_t = \sum_o \sum_d Z_{od}^t \tag{6.1}$$

s.t.

$$\sum_{k \in EP_{od}^t} Y_{odtk} + Z_{od}^t \geq 1 \qquad \forall o, d \in \hat{N}^t \tag{6.2}$$

$$Z_{od}^t \leq (1 - Y_{odtk}) \qquad \forall o, d \in \hat{N}^t, \forall k \in EP_{od}^t \tag{6.3}$$

$$Y_{odtk} \geq 1 - \sum_{(i,j) \in \Psi_{odtk}} \left(Q_{ijt} + Q_{jit}\right) \qquad \forall o, d \in \hat{N}^t, \forall k \in EP_{od}^t \tag{6.4}$$

$$Y_{odtk} \le \left(1 - Q_{ijt} - Q_{jit}\right) \qquad \forall o,d \in \hat{N}^t, \forall k \in EP_{od}^t, \forall (i,j) \in \Psi_{odtk} \tag{6.5}$$

$$\sum_{(i,j)\in \hat{A}^t} Q_{ijt} \le \tau_t \tag{6.6}$$

$$Y_{odtk} = \{0,1\} \qquad \forall o,d \in \hat{N}^t, \forall k \in EP_{od}^t \tag{6.7}$$

$$Z_{od}^t = \{0,1\} \qquad \forall o,d \in \hat{N}^t \tag{6.8}$$

$$Q_{ijt} = \{0,1\} \qquad \forall (i,j) \in \hat{A}^t \tag{6.9}$$

Objective (6.1) maximizes the connectivity loss between origin and destination habitats. Constraints (6.2) and (6.3) state that connectivity between an origin and destination habitat cannot be lost unless all efficient paths $k \in EP_{od}^t$ in that time period are lost. Constraints (6.4) and (6.5) ensure that at least one arc of each efficient path $(i,j) \in \Psi_{odtk}$ is lost to be considered disrupted $\left(Y_{odtk} = 0\right)$, and it is assumed that the loss of an arc in one direction $\left(Q_{ijt} = 1\right)$ or $\left(Q_{jit} = 1\right)$ disables connectivity of both directions. Constraint (6.6) tracks the number of arcs being interdicted, and Constraints (6.7)-(6.9) are binary integer restrictions on decision variables. Given that interdiction resources are limited in each time interval (limited to τ_t) and unused resources can be transferred into next time interval, if the optimal solution Γ_t^* is not unique, then it is essential to identify the solution with lowest $p_t = \sum_{(i,j)\in \hat{A}^t} Q_{ijt}$. Similar to epsilon-constraint method where multiple objectives are optimized in turn and their optimal solutions are added as constraints in subsequent runs (Laumanns, Thiele, and Zitzler 2006; Bérubé, Gendreau, and Potvin 2009), model (6.1)-(6.9) can be modified to find an efficient solution with maximum number of OD connectivity loss Γ_t^* and minimum number of arc loss p_t^*. In the modified model, Objective (6.1) is replaced with

Constraint (6.6) in a minimization problem (6.10) subject to optimal connectivity loss Constraint (6.11), and other original constraints in the CDP model.

$$Minimize\ p_t = \sum_{(i,j)\in \hat{A}^t} Q_{ijt} \tag{6.10}$$

s.t.

$$\sum_{o\in \hat{N}^t} \sum_{d\in \hat{N}^t} Z_{od}^t = \Gamma_t^* \tag{6.11}$$

For each period, unused resources are tracked $s_t = \tau_t - p_t$ and added to the next interval $\tau_{t+1} = \tau_0 + s_t$ where τ_0 is an input parameter, base upper bound for arc loss, and reflects the pace of landscape change. While the CDP can theoretically be used to identify the worst-case scenario of connectivity loss in a habitat system, its ability to do so depends upon determining which paths constitute viable alternatives for movement. In this respect, research has shown that alternative paths depend on the objectives that are considered for movement. The *Multi-objective Habitat Connectivity Problem (MOHCP)* can be used to identify these paths given the state of a habitat system at a particular period (Matisziw, Gholamialam, and Trauth 2020). Given a network G^t in time t, traversal of arc $(i,j)\in A^t$ is associated with a cost c_{ijt}^l relative to each objective $l \in L$ thought to factor into movement decisions. For an origin $o \in N^t$ and destination node $d \in N^t$, the decision as to which arcs should $\left(X_{ijt}=1\right)$ and should not be traversed $\left(X_{ijt}=0\right)$ must be made. Therefore, the total cost of moving between an OD pair relative to a particular objective is $\Phi_l^t = \sum_{(i,j)\in A^t} c_{ijt}^l X_{ijt}$. The MOHCP for any period t can be structured as follows.

$$MOHCP:\ Minimize\ (\Phi_l^t,...,\Phi_{|L|}^t) \tag{6.12}$$

s.t.

$$\sum_{j|(i,j)\in A^t} X_{ijt} - \sum_{j|(j,i)\in A^t} X_{jit} = \begin{cases} 1 & \text{for } i = o \\ 0 & \forall i \in N^t \setminus \{o, d\} \\ -1 & \text{for } i = d \end{cases} \tag{6.13}$$

$$X_{ijt} = \{0,1\} \qquad \forall (i, j) \in A^t \tag{6.14}$$

Objective (6.12) minimizes traversal cost with respect to an array of routing objectives $l \in L$ in each time period $t \in T$. Constraints (6.13) ensure that if an arc on $\hat{G}^t(\hat{N}^t, \hat{A}^t)$ enters node i then one will exit node i, unless node i is the origin or destination node. Constraints (6.14) are integer binary restrictions on arc decision variables. The input for MOHCP is a set of origin $o \in N^t$ and destination nodes $d \in N^t$, and a directed graph $\left(G^t(N^t, A^t)\right)$ with multiple cost attributes associated with each arc $(c_{ijt}^1, ..., c_{ijt}^{|L|})$. The model can be solved using approaches such as the Multicriteria All Non-dominated Least Cost Paths or MONISE Supported Non-dominated Least Cost Paths algorithms to identify a set of efficient solutions EP_{od}^t for each OD pair given the state of the network in time t (Matisziw, Gholamialam, and Trauth 2020). In order to track overall network connectivity degradation over time, the change in connectivity can be modeled as in Matisziw and Murray (2009).

$$\theta_t = \frac{\lambda_t}{\lambda_{t-1}} \qquad t \in T \tag{6.15}$$

Where λ_t is the number of OD pairs that are connected in MOHCP, and θ_t ranges from zero to one with lower values indicating more dramatic impact to connectivity. Another measure for assessing connectivity can be total number of paths found in each period $\alpha_t = \sum_{o\in\hat{N}^t} \sum_{d\in\hat{N}^t} EP_{od}^t$.

Whereas θ_t and α_t are measures reflecting prospects for movement, another measure is introduced to evaluate the change in objective values for Pareto-optimal paths after each arc loss scenario. This measure β_t is defined as the ratio of Pareto-optimal paths from current period t that exists in the prior period $t-1$ as described in (6.16). Given that Pareto-optimal paths found in earlier periods have the same or less traversing cost than those found in subsequent periods, the higher values of β_t indicate less negative impact to the quality of supporting paths for connectivity.

$$\beta_t = \frac{\left|\left\{EP_{od}^{t-1} \mid o,d \in \hat{N}^{t-1}\right\} \bigcap \left\{EP_{od}^{t} \mid o,d \in \hat{N}^{t}\right\}\right|}{\left|\left\{EP_{od}^{t} \mid o,d \in \hat{N}^{t}\right\}\right|} \qquad t \in T \tag{6.16}$$

6.3 Simulation Framework

The CDP and MOHCP can be used in tandem to determine upper bound of habitat connectivity loss that can potentially occur due to landscape alterations. As illustrated in Figure 6-1, the initial input is network topology, cost attributes for different movement objectives, origin/destination habitats and arc loss limit τ_0 which reflects the pace of landscape change. For each period, a set of efficient paths optimizing multiple routing objectives reflecting species navigation decision when traversing the landscape are identified in Stage 2. In the initial period $t=0$, the MOHCP is applied to the full network G^t and connectivity metrics and objective values for Pareto-optimal paths are computed and reported. Next, CDP and its counterpart as detailed in (6.1)-(6.11) are applied to identify a set of arcs p_t^* whose loss maximizes degradation of connectivity. Should an arc be lost in one period, it is assumed that it is also no longer viable in subsequent periods. The set Ω_t denotes all arcs that have been completely lost up to period t. The

set of arcs being disrupted in each period can be explicitly tracked by adding Constraint (6.17) to the MOHCP.

$$\sum_{(i,j)\in\Omega_t} X_{ijt} = 0 \qquad \forall (i,j) \in \Omega_t \tag{6.17}$$

Once a scenario of arc loss has been determined for time t, the set of efficient paths for the modified network G^{t+1} can then be modeled and the process is repeated. The iterative arc loss and re-establishment of efficient paths approach results in appearing a completely or partially new set of efficient paths between each origin and destination pair in each subsequent stage, likely with higher average traversing costs in comparison to those found in earlier stages. For each origin and destination pair, there will eventually be a period in which no viable path will exist (i.e., zero connectivity), meeting the stopping criteria in Stage 3.

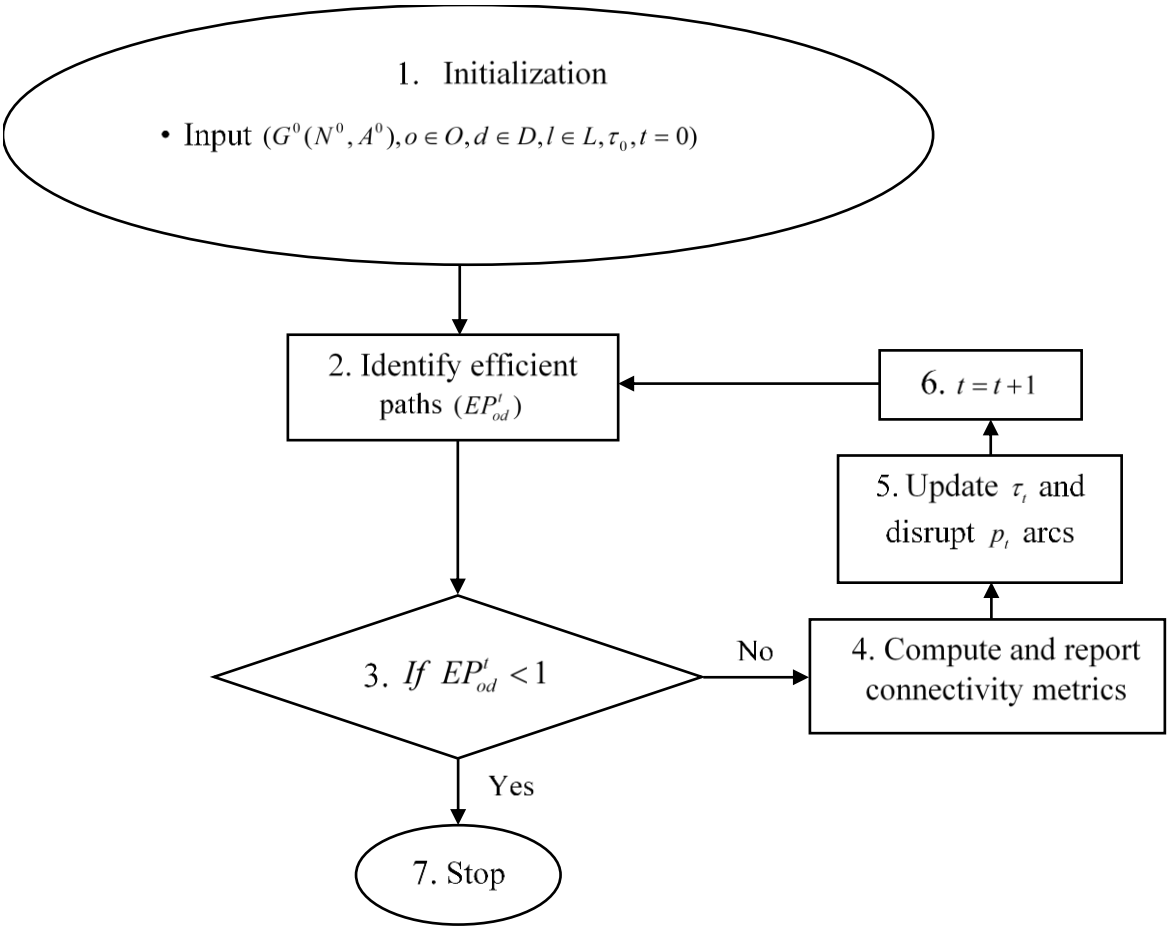

Figure 6-1 Simulation framework for assessing habitat network degradation.

6.4 Results and Discussion

The habitat vulnerability assessment approach is applied to the wetland system described in previous chapter, Section 5.4.3. The results for 24 model parameterizations are reported in Table 6-1. In general, given lower levels of resources for landscape change, the habitat network connectivity sustains higher number of periods $|T|$. For instance, considering the all efficient paths represent the best options for connectivity, it takes 23 periods to eliminate connectivity when five arcs can be rendered inoperable in each period, whereas it takes only 8 periods to eliminate

connectivity given that thirty five or more arcs can be rendered inoperable in each period. As another example, considering the shortest paths represent the best options for connectivity, it takes 62 periods to eliminate connectivity when five arcs can be rendered inoperable in each period, whereas it takes only 10 periods to eliminate connectivity given that twenty or more arcs can be rendered inoperable in each period. The computation time has a direct relationship with the size of path set and is significantly lower when using the shortest path comparing to the other two efficient sets.

Table 6-1 Computation time and total arcs rendered inoperable given different levels of landscape change τ_0

τ_0	All Efficient Paths			Supported Efficient Paths			Shortest Path		
	# of arcs selected for redevelopment	$\|T\|$	solution time (min)	# of arcs selected for redevelopment	$\|T\|$	solution time (min)	# of arcs selected for redevelopment	$\|T\|$	solution time (min)
5	85	23	424.8	100	23	152.9	122	62	33.7
10	85	12	297.5	90	14	72.1	88	15	9.6
15	85	12	227.4	74	7	44.5	91	16	9.6
20	86	10	232.4	77	6	37.8	80	10	6.3
25	78	8	131.8	76	9	40.3	80	10	6.3
30	71	6	104.9	76	9	40.3	80	10	6.3
35	79	8	157.2	76	9	40.9	80	10	6.3
40	79	8	155.5	76	9	40.4	80	10	6.3

6.4.1 Assessment and Visualization of Connectivity Change

The change in inter-habitat connectivity using three different sets of paths and two levels of resources for landscape development is presented using network measures previously defined. The gap between Γ_t and λ_t reflects the number of wetland pairs that remains connected after each landscape alteration scenario and before constructing system connectivity again in the next period, Stages 2 and 5 of the framework (Figure 6-1). The change in quality of paths after each landscape

alteration scenario is evaluated using metric β_t, which fluctuates between 0.0 and 1.0, tending to be higher in earlier periods. Initially for $t=0$, there are 132 shortest paths (12*12-12=132), and 3,550 supported and unsupported efficient paths in which 659 of them are supported. When using all efficient paths and given $\tau_0=15$ (Table 6-2), all of 94 disconnected wetland pairs in initial Period $t=0$, become connected in Period 1 $(\theta_1=1.0)$. However, from Period 2 to Period 6 some wetland pairs become permanently disconnected $(\theta_t<1)$. The number of paths reaches the maximum value of 7,244 in Period 2 in which 145 of them are found in Period 1 as well $(\beta_2=0.02)$. Also, out of 3,871 paths found in Period 1, 697 paths are in common with those found in the initial Period $(\beta_1=0.18)$. In Periods 3 and 4, there are very few common paths but there is no common path between subsequent periods $(\beta_t \le 0.01)$. Wetlands 9 and 10 are the only connected wetlands in the last three periods and are permanently disconnected after redevelopment of one arc in Period 11.

Table 6-3 details the connectivity change to all efficient paths given $\tau_0=35$. Given that $\beta_t=0.0$ in all six periods, the worst-case scenario of landscape change occurs in each individual period. That is, all efficient paths providing connectivity are disabled in every period and completely new set of paths are found in subsequent periods for those wetlands that are still connected. In Figure 6-2, the number of paths and location of arcs selected for redevelopment given $\tau_0=35$ are visualized. In Figure 6-2a, the location of 32 arcs in initial Period $t=0$ indicates that redevelopment of arcs traversed by many paths imposes highest damage to the landscape connectivity. 10 out of 32 arcs selected for redevelopment are subset of 58 arcs traversed by many paths (17.2%), 13 are subset of 279 arcs traversed by medium number of paths (4.7%), and 9 are subset of 620 arcs traversed by few paths (1.4%). A similar trend can be examined in the next

periods. As another example in Period 1 (Figure 6-2b), 13.1% of arcs traversed by many paths, 2.9% of arcs traversed by medium number of paths, and only 0.9% of arcs traversed by few paths are selected for redevelopment. In the next two periods, redevelopment of 10 arcs impacts 56 pairs in Period 2 (Figure 6-2c), and redevelopment of seven arcs impacts 42 pairs in Period 3 (Figure 6-2d). Three Wetlands 1, 5 and 7 remain connected through 319 efficient paths in Period 4 and are temporarily disconnected through redevelopment of four arcs (Figure 6-2e). In Period 5, three Wetlands 1, 5 and 7 still form the six pairs which are connected by 635 efficient paths but four of these six pairs become permanently disconnected through redevelopment of four arcs (Figure 6-2f). The last connected pair, Wetlands 1 and 5 sustain two more periods and become permanently disconnected after redevelopment of one arc in Period 7 (Figure 6-2h). The model output for supported efficient paths and $\tau_0 = 15$ in Table 6-4 shows it takes seven periods for the habitat network to collapse. The maximum number of supported efficient paths shows up in Period 1 where complete connectivity among 132 wetland pairs can be still guaranteed $\theta_1 = 1$. In terms of quality of paths, there are some common paths between the first three periods (less than 5%) but in all subsequent periods there is no common path between any two periods. Given $\tau_0 = 35$, the habitat network sustains nine periods as visualized in Figure 6-3 (Table 6-5). Out of 25 redeveloped arcs in the initial Period $t = 0$ (Figure 6-3a), 8 arcs are subset of 59 arcs traversed by many paths (13.5%), 11 are subset of 241 arcs traversed by medium number of paths (4.6%), and 6 are subset of 401 arcs traversed by few paths (1.5%). For the next period $t = 1$ (Figure 6-3b), 14.3% of arcs traversed by many paths, 3.6% of arcs traversed by medium number of paths, and only 0.2% of arcs traversed by few paths are selected for redevelopment. In Figure 6-3c, connectivity among 90 pairs of wetlands in Period 2 is disabled through redevelopment of 14 arcs. Out of these 90 pairs, 42 of them are reconnected in the next Period $t = 3$ and the remaining 48

pairs become permanently disconnected (Figure 6-3d). Out of these 7 connected wetlands, four of them are still connected in Period 4, and the remaining three wetlands become permanently disconnected (Figure 6-3e). Three Wetlands 1, 5 and 7 form the six connected pairs in Period 5 and are impacted by the redevelopment of three arcs (Figure 6-3f). Two Wetlands 1 and 5 remain connected in the last three periods and are impacted by redevelopment of 5 arcs in total. The spatial distribution of arcs selected for redevelopment over different periods in Figure 6-2 and Figure 6-3 indicates that damages to arcs located at the vicinity of wetlands has the most detrimental impact to connectivity. In addition, Wetlands 1, 5 and 7 present greater level of resilience to landscape alteration because they survive many periods and are supported by a large number of backup paths located at the Eastern portion of the study area. When the shortest path is used for wetlands connectivity, the network sustains 16 periods for $\tau_0 = 15$ and 10 periods for $\tau_0 = 35$ (Table 6-6 and Table 6-7). Given that one new shortest path is found in each period for each pair, the metric β_t is not applicable and not reported. Also, the total number of paths is equal to the total number of connected wetland pairs in each period $\alpha_t = \lambda_t$, therefore, only λ_t is reported. In Figure 6-4, the location of shortest paths and arcs selected for redevelopment given $\tau_0 = 35$ are visualized for ten periods. The central Wetland 2 plays an important role in connecting northern and southern portion of the study area, and paired with Wetlands 5 and 10 form the only connected wetlands in the last four periods. Given that wetlands' resilience to landscape change is identified now, our modeling approach can be used to prioritize protection plans and target them toward those wetlands that are more vulnerable and become isolated in the earlier stages of landscape change.

Table 6-2 Model output for each period t given $\tau_0 = 15$ and using all efficient paths

t	τ_t	p_t	α_t	β_t	θ_t	λ_t	Γ_t
0	15	15	3550	-	-	132	94
1	15	15	3871	0.18	1.00	132	108
2	15	15	7244	0.02	0.83	110	102
3	15	14	2001	0.01	0.40	44	40
4	16	9	1204	0.01	0.73	32	32
5	22	7	950	0.00	0.69	22	22
6	30	3	9	0.00	0.18	4	4
7	42	2	4	0.00	1.00	4	4
8	55	2	12	0.00	1.00	4	4
9	68	1	2	0.00	1.00	2	2
10	82	1	4	0.00	1.00	2	2
11	96	1	14	0.00	1.00	2	2

Table 6-3 Model output for each period t given $\tau_0 = 35$ and using all efficient paths

t	τ_t	p_t	α_t	β_t	θ_t	λ_t	Γ_t
0	35	32	3550	-	-	132	132
1	38	19	5376	0.00	1.00	132	132
2	54	10	2446	0.00	0.42	56	56
3	79	7	1660	0.00	0.75	42	42
4	107	4	319	0.00	0.14	6	6
5	138	4	635	0.00	1.00	6	6
6	169	2	132	0.00	1.00	2	2
7	202	1	326	0.00	1.00	2	2

Table 6-4 Model output for each period t given $\tau_0 = 15$ and using supported efficient paths

t	τ_t	p_t	α_t	β_t	θ_t	λ_t	Γ_t
0	15	15	659	-	-	132	112
1	15	15	939	0.03	1.00	132	112
2	15	15	645	0.05	0.83	110	110
3	15	12	820	0.00	0.82	90	90
4	18	9	450	0.00	0.47	42	42
5	24	5	101	0.00	0.28	12	12
6	34	3	114	0.00	1.00	12	12

Table 6-5 Model output for each period t given $\tau_0 = 35$ and using supported efficient paths

t	τ_t	p_t	α_t	β_t	θ_t	λ_t	Γ_t
0	35	25	659	-	-	132	132
1	45	18	937	0.00	1.00	132	132
2	62	14	701	0.00	0.68	90	90
3	83	8	310	0.00	0.47	42	42
4	110	3	67	0.00	0.29	12	12
5	142	3	57	0.00	0.50	6	6
6	174	2	38	0.00	0.33	2	2
7	207	2	68	0.00	1.00	2	2
8	240	1	60	0.00	1.00	2	2

Table 6-6 Model output for each period t given $\tau_0 = 15$ and using the shortest path

t	τ_t	p_t	θ_t	λ_t	Γ_t
0	15	15	-	132	126
1	15	15	1.00	132	126
2	15	14	1.00	132	132
3	16	11	0.68	90	90
4	20	9	0.80	72	72
5	26	6	0.42	30	30
6	35	5	1.00	30	30
7	45	3	0.40	12	12
8	57	2	0.50	6	6
9	70	2	1.00	6	6
10	83	2	1.00	6	6
11	96	2	1.00	6	6
12	109	2	1.00	6	6
13	122	1	0.33	2	2
14	136	1	1.00	2	2
15	150	1	1.00	2	2

Table 6-7 Model output for each period t given $\tau_0 = 35$ and using the shortest path

t	τ_t	p_t	θ_t	λ_t	Γ_t
0	35	18	-	132	132
1	52	17	1.00	132	132
2	70	14	0.83	110	110
3	91	11	0.82	90	90
4	115	9	1.00	90	90
5	141	4	0.22	20	20
6	172	2	0.30	6	6
7	205	2	1.00	6	6
8	238	2	1.00	6	6
9	271	1	0.33	2	2

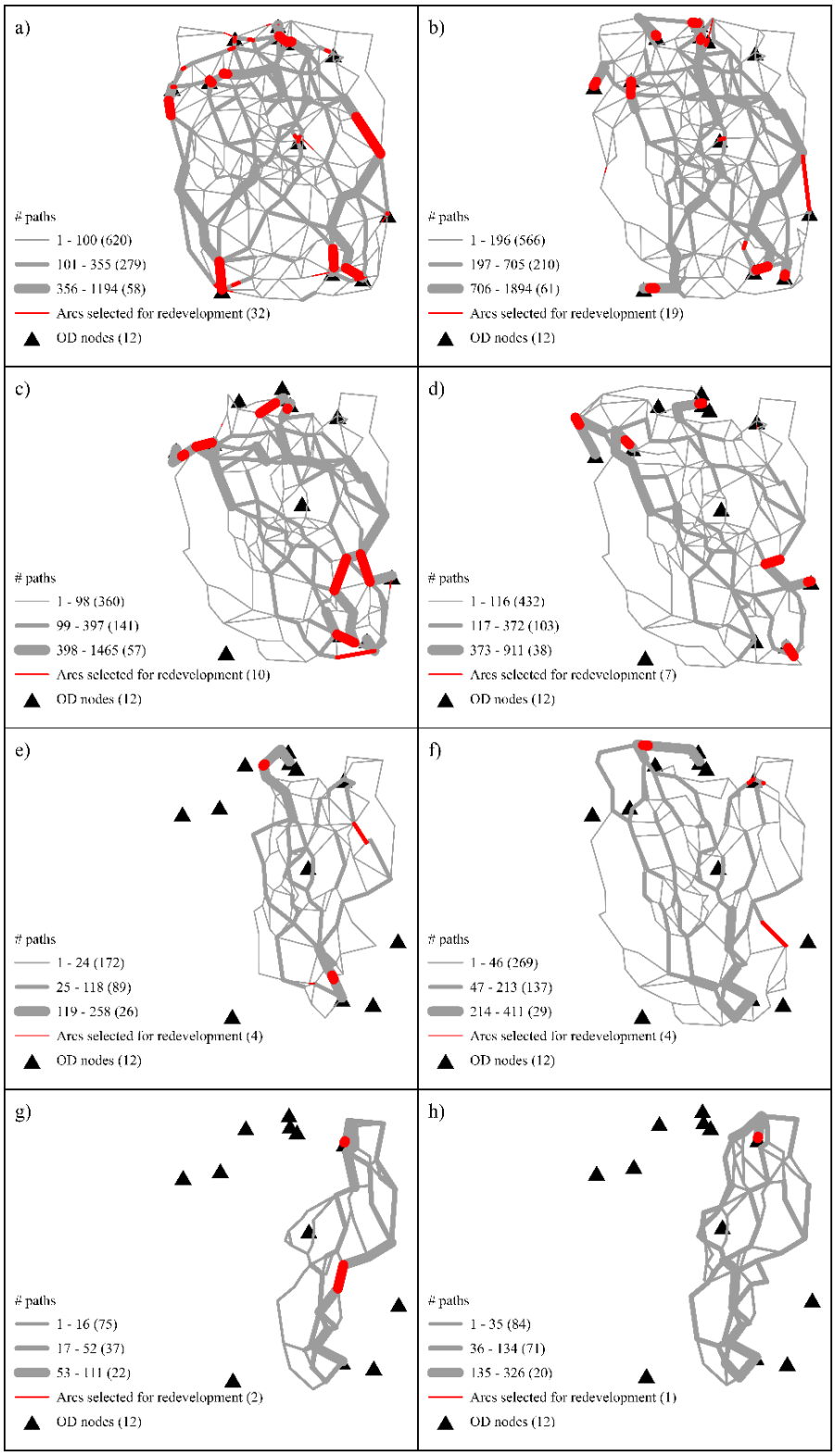

Figure 6-2 Habitat network connectivity degradation given $\tau_0 = 35$ and using all efficient paths: a) $t = 0$, b) $t = 1$, c) $t = 2$, d) $t = 3$, e) $t = 4$, f) $t = 5$, g) $t = 6$ and h) $t = 7$.

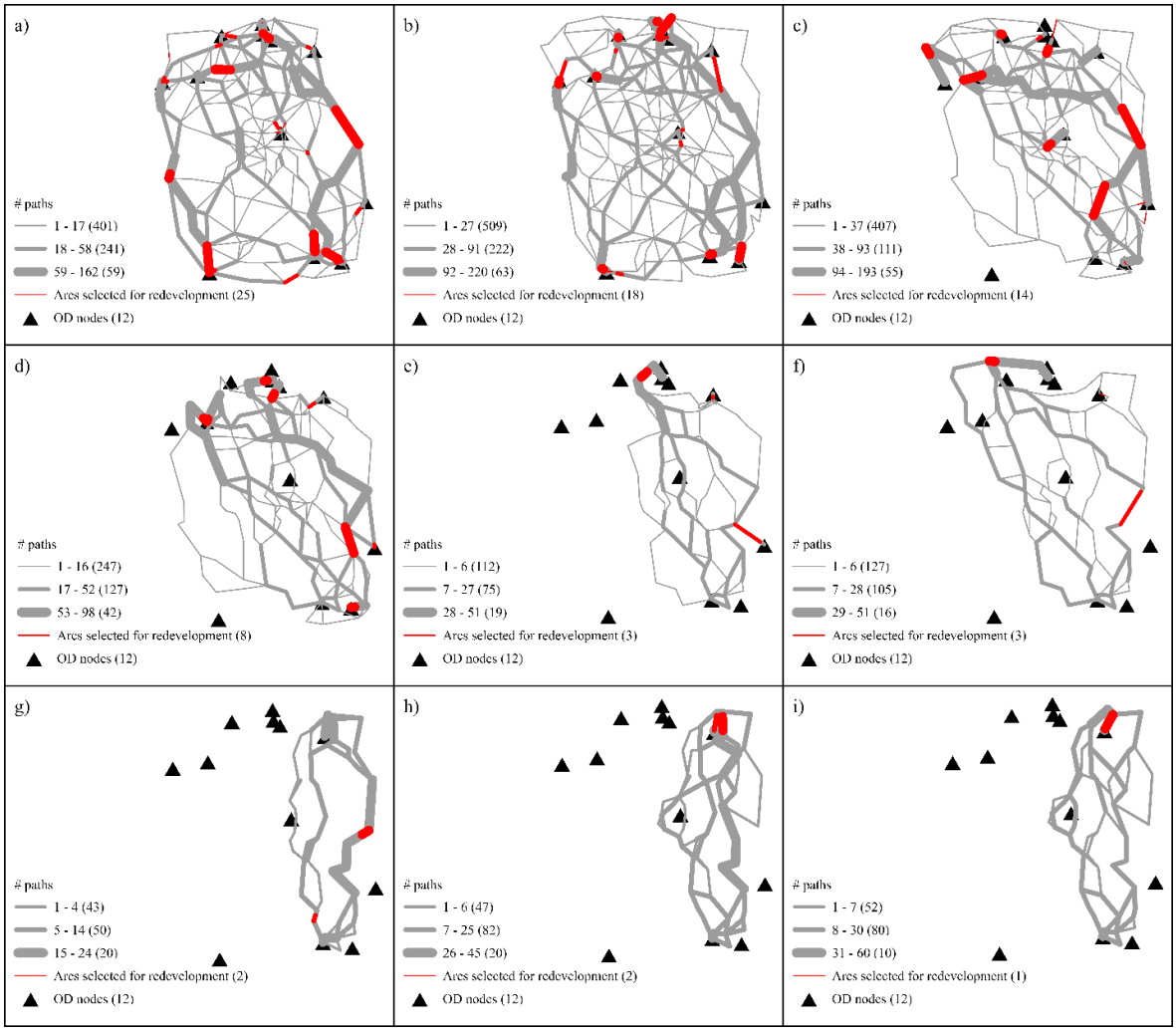

Figure 6-3 Habitat network connectivity degradation given $\tau_0 = 35$ and using supported efficient paths: a) $t = 0$, b) $t = 1$, c) $t = 2$, d) $t = 3$, e) $t = 4$, f) $t = 5$, g) $t = 6$, h) $t = 7$ and i) $t = 8$.

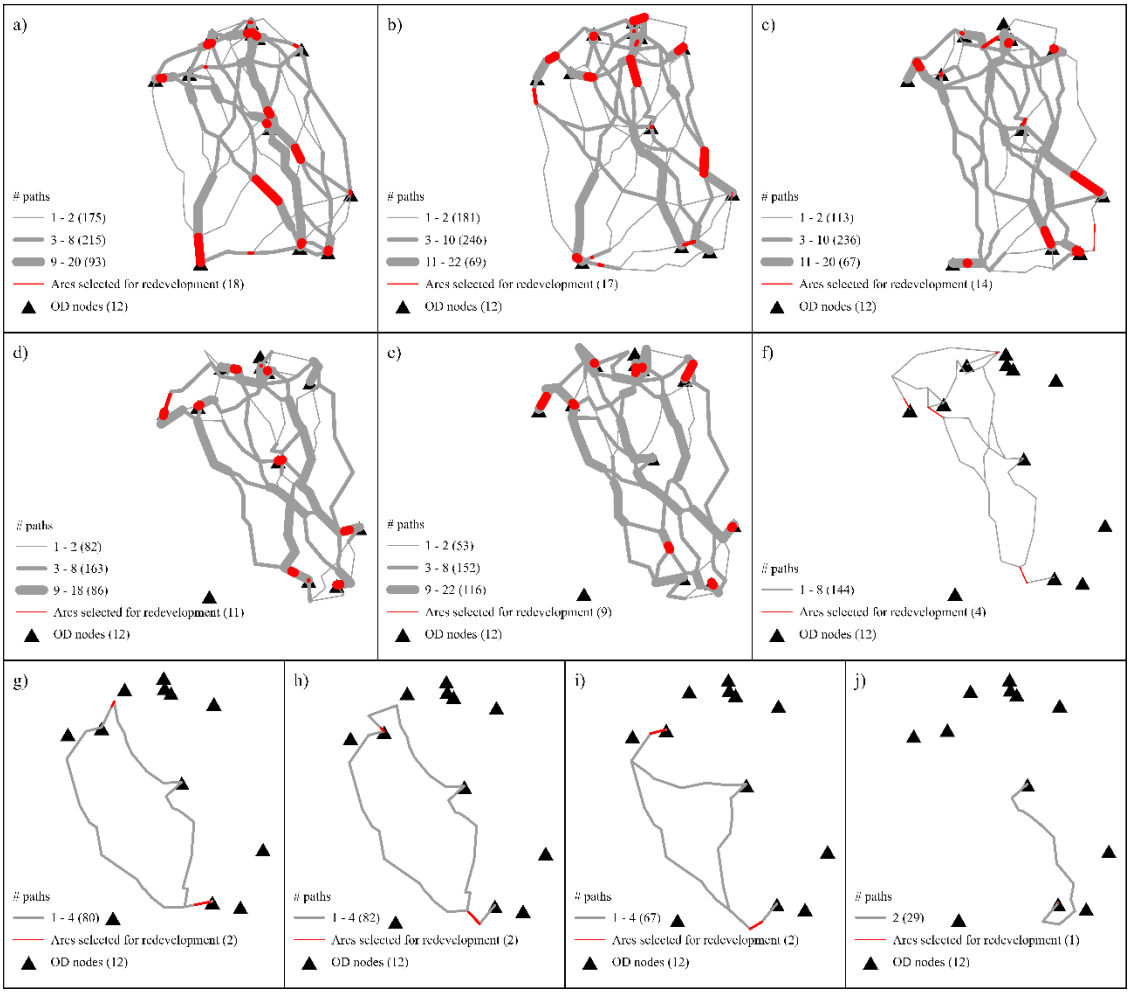

Figure 6-4 Habitat network connectivity degradation given $\tau_0 = 35$ and using the shortest path: a) $t = 0$, b) $t = 1$, c) $t = 2$, d) $t = 3$, e) $t = 4$, f) $t = 5$, g) $t = 6$, h) $t = 7$, i) $t = 8$ and j) $t = 9$.

6.4.2 Distribution of Path Objective Values

While θ_t, α_t and β_t are global network metrics for assessing connectivity, the objective values of paths identified in each period can be plotted for individual wetland pairs as a local network measure that provides direct insights into the change in movement cost under ongoing alteration to the landscape. As an example for one wetland pair, from Wetland 1 to Wetland 5, the objective values for traversal risk Φ_1 (Figure 6-5a), weighted distance Φ_2 (Figure 6-5b) and

elevation change Φ_3 (Figure 6-5c) are plotted. Given that distance is optimized when identifying the shortest path, the length of paths is also reported in Figure 6-5d to compare the length of shortest path to that of efficient paths found by MOHCP. The number of periods that connectivity exists between Wetlands 1 and 5 corresponds to the graphics presented earlier in Figure 6-2 to Figure 6-4. That is, Wetlands 1 and 5 are connected for eight periods when using all efficient paths (Figure 6-2h), nine periods when using supported efficient paths (Figure 6-3i) and five periods when using the shortest path (Figure 6-4e). In the initial period, both all efficient paths and supported efficient paths have the same lower bound for the three routing objectives, and monotonically increase in the next periods (Figure 6-5a, Figure 6-5b and Figure 6-5c). When using the shortest path, the path length monotonically increases over the five periods (Figure 6-5d). Given that the length of network arc is one of the terms in the second cost attribute when optimizing Φ_2, the weighted distance of the shortest path in Figure 6-5b and the length of the shortest path in Figure 6-5d exhibit similar trend over different periods.

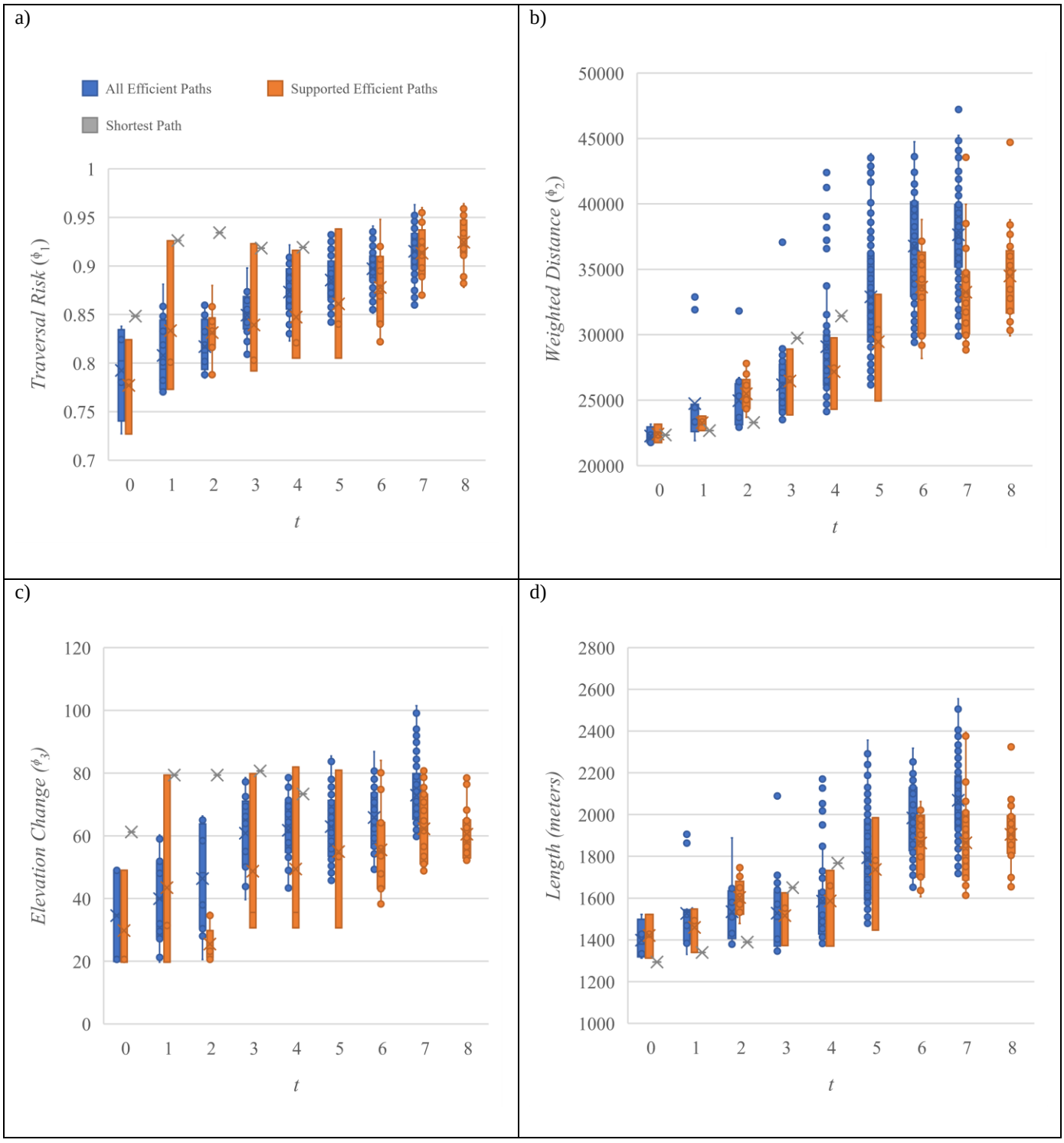

Figure 6-5 Box and Whisker diagram for path objective values: a) Φ_1, b) Φ_2, c) Φ_3 and d) length from Wetland 1 to Wetland 5 given $\tau_0 = 35$ and using three different set of paths.

CONCLUSION

Analyzing built and natural environments is a complex process which often involves consideration of many alternatives, objectives and constraints. Mathematical models and solution procedures can be applied to develop decision support systems and assess how resources can be best allocated to enhance some measures of system performance (e.g., safety, connectivity, etc.). In this dissertation, multi-objective optimization models are formalized to solve several real-world planning problems in networked systems.

7.1 Bike Routing Problem

A framework is proposed for evaluating urban bikeability given that a set of routing objectives may be considered in a range of ways by different bicyclists. Most studies have based measures of bikeability upon the characteristics of single objective and only one has considered the possibility of two objectives (Ehrgott et al. 2012). In an effort to better account for the wide range of criteria considered by bicyclists, three routing objectives are considered in the proposed framework. In particular, MCBPM proposed in Chapter 3 identifies a set of Pareto-optimal paths among origins/destinations. A label-correcting algorithm is then adapted to solve this model for the entire set of Pareto-optimal paths. Given that many OD pairs are often involved in urban transit systems, the developed approach could generate a large number of Pareto-optimal paths to characterize where and to what extent bikeable infrastructure is present. As such, a set of summary metrics for the identified paths are also provided to facilitate analysis of geographic variations in bikeability.

The developed framework is applied to a case study to demonstrate how it can be utilized in practice. This application involves the evaluation of 27,722 OD pairs, a non-trivial task. In light

of the large size of this transportation system, the extended label-correcting algorithm was able to efficiently identify all 329,931 Pareto-optimal paths among the OD pairs. The results indicate that paths involving fewer intersections and lower LTS stress are on average 1.01 miles longer than the shortest path. When limiting paths to those less than 2.0 miles, paths involving fewer intersections and lower LTS are only on average 0.31 miles longer than the shortest path. This level of deviation from the shortest path is within the range found to be acceptable to bicyclists in other studies (Shafizadeh and Niemeier 1997; Winters et al. 2010).

The developed framework could be used as a decision support tool to evaluate how bikeability and urban connectivity could be impacted given modification to the supporting infrastructure. In this application, movement possibilities between all OD pairs (or those within some distance threshold) are considered. However, depending on the nature of the analysis task, one might wish to focus on a more specific set of ODs and/or to incorporate other factors that could be related to bikeability. For example, demand for bicycle travel can vary greatly among OD pairs within a system depending on factors such as socio-demographic, built environment and temporal factors. Thus, if the goal was to evaluate bikeability relative to the demand for bicycle transport, the developed framework could be extended to weight the different path alternatives by the demand for bicycle travel between each OD pair. The proposed framework could also be applied to extend research relating actual observations of bike movement to bicyclists' preferences. For example, while Aultman-Hall, Hall, and Baetz (1997) compare bicyclists' routes with the shortest path, one might compare their routes with those optimizing an array of different routing objectives, such as those discussed in our study. Finally, given the criteria (or mix thereof) underlying bicyclist behavior could vary between different study sites, many opportunities for extension of this modeling framework to account for those criteria likely exist.

7.2 Placement of Information in Networks

A framework for siting facilities in a transportation system is developed to provide (and/or collect) information to network flows. In particular, the PFCP is structured in Chapter 4 to minimize the cost of siting a configuration of facilities to serve flows between network origins and destinations. Unlike many other flow capturing models, any number of paths supporting flows among OD pairs can be considered. Given that there is typically uncertainty as to the extent to which information will be received and/or collected from flows passing by sited facilities, probabilities of exposure are associated with candidate facilities. Probabilistic threshold constraints are then incorporated to ensure that the flows are sufficiently exposed to the facilities before they can be considered effectively served. While this type of threshold formulation can guarantee a base level of service for network flows, it does not place any value on exceeding thresholds should the ability to do so exist in light of alternative optima. As such, a biobjective formulation is explored by introducing a maximization objective to better evaluate the characteristics of the model structure. A NISE algorithm is applied to identify all supported efficient facility configurations for distributing information to flows in an interstate highway system. In order to explore sensitivity of the model to variations in the representation of the transportation system, distribution of flows, exposure probabilities, and coverage criteria, a range of modeling parameterizations were examined.

Information provision and collection in transportation systems can be resource intensive given the complexities of modern transportation infrastructure and the ways in which it is used. In our study, various configurations of paths supporting flows among OD pairs and assignments of flow to those paths were examined in order to reason about impacts to solution characteristics. Given the spatial and temporal dynamics of flows in transportation systems, future work is needed

to account for perturbations in flow when siting facilities for information collections/provision. Also, while managing the cost of siting facilities is an important consideration, other planning objectives often factor into the decision-making process. For instance, aside from general information provision, this study considered another planning criteria, that of providing information to facilitate the diversion of flows from upcoming portions of their paths that may be obstructed. In order to better leverage the capabilities of facility configurations over a broader range of purposes, future work is also needed as to how a wider range of planning criteria can be integrated in the modeling process.

7.3 Habitat Connectivity for Biodiversity Conservation

Assessing prospects for ecological corridor over a landscape involves consideration of a complex mixture of factors. Prior studies have focused on landscape connectivity and geographical aspects, finding corridors or paths that support movement of one or more species. Those studies have pointed to the need to better account for the multi-faceted nature of ecological corridor. A common approach in this respect is to construct a multi-objective least-cost path model to reason about prospects for ecological corridor over a landscape. A major realization of many studies is that while multi-objective least-cost paths do allow for the tradeoffs among unique combinations of movement criteria to be evaluated, sometimes even minor changes in how the criteria are combined can give rise to completely different solutions and interpretations of a landscape. One reason for this is that multi-objective least-cost path problems may indeed have a tremendous number of solutions that are best in some respect, known as Pareto-optimal or efficient solutions. There are two general categories of Pareto-optimal solutions, known as supported and unsupported efficient solutions. Most commonly used solution techniques for multi-objective least-cost path problems can identify the supported efficient solutions (or a portion thereof).

However, the number of supported efficient solutions can be very small relative to the number of unsupported efficient solutions. Unfortunately though, most applications of multi-objective least-cost path models only identify a very small proportion of the supported efficient solutions given the solution methodologies that are typically applied. As a result, the solutions that are used as a basis for analysis may only serve as a weak estimate of the set of movement possibilities that may actually exist.

To address these issues, Chapter 5 first provides an overview of the least-cost path problem in the context of ecological research, the distinction between supported and unsupported efficient solutions to least-cost path problems, and methods that can be used to identify each. Next, MOHCP accounting for a general set of objectives that are thought in some way to influence movement: a) minimizing risk, b) minimizing distance, and c) minimizing environmental change is formally described. Deriving solutions to a three objective model such as this can be very challenging and as such, two alternative methods for deriving efficient solutions to the model are detailed. The first solution method is MONISE algorithm for identifying all supported efficient solutions and associated non-dominated least-cost paths. While the MONISE approach can identify the supported efficient solutions, it cannot identify the unsupported efficient solutions. As such, a multi-criteria least-cost path labeling algorithm is extended to identify all efficient solutions (supported and unsupported) to the multi-objective least-cost path model.

The developed multi-objective least-cost path model is then applied to evaluate prospects for amphibian movement in a wetland system to demonstrate the approach. It was found that the MONISE approach can quickly and efficiently identify all of the supported efficient solutions to the multi-objective model. The supported efficient solutions on their own, provide only an estimate of the solutions in the efficient set. However, despite being a little more computationally

demanding, the multi-criteria labeling approach was able to identify *all* supported efficient solutions as well as *all* unsupported efficient solutions to the model. Of particular note is that 82% of the efficient solutions were in fact unsupported. Therefore, simply focusing on identification and analysis of supported efficient solutions (or small subset therein) could risk overlooking a significant proportion of viable and potentially important alternatives ecological corridor. Thus, analyst should be wary of interpretative problems that may arise when basing analysis on a limited sample of the efficient solutions to multi-objective least-cost path problems.

The interrelationship between habitat connectivity and landscape alteration is studied in Chapter 6. The proposed framework consists of two main network optimization components, CDP and MOHCP, and identifies the worst-case scenario of landscape change given a set of viable paths for species movement. Given that landscape condition is everchanging and development projects occur over time, it is essential to account for species adaption to the new environment at any given time over the planning horizon. To accomplish this goal, species navigation decisions are applied to a dynamic/changing habitat network that becomes updated after each landscape change scenario. For a fixed amount of resources for landscape development in each period, the worst-case scenario of landscape change found by CDP is associated with maximal connectivity loss to habitat system. The application of proposed framework reveals that the location of landscape changes has crucial impact on magnitude of habitat connectivity loss. Specifically, redevelopment of arcs traversed by many paths causes higher connectivity loss according to simultaneous visualization of paths and redeveloped arcs. In addition, proximity to wetlands seems to be another significant factor in locating redeveloped arcs with highest detrimental impact to habitat connectivity. This finding can be evidence for creating buffer zones around wetlands and use as conserved areas in support of biodiversity. Location and number of connected habitats as well as

those of paths over different periods indicate that some landscape change scenarios may initially have little impact on connectivity but coupled with future changes can be significant barrier to connectivity.

7.4 Future Work

This dissertation proposes solution procedures based on NISE, MONISE and labeling algorithm for several multi-objective network optimization problems. In future research, it would be of interest to solve these problems using other solution approaches (e.g., heuristics, other scalarization and labeling methods) and compare them based on computational time and complexity. Another research direction is to examine how network structure can be modified to reduce input size and computational tasks. The landscape network created for our applications in Chapters 5 and 6 was designed based on vector data model in geographic information system, however, one might be interested to investigate how the change in network representation of landscape (e.g., raster data model) may impact results. In this study, optimal paths connecting origin and destination pairs (Chapters 3 and 5), optimal locations for siting facilities to serve demand (Chapter 4) and optimal locations to disrupt movement (Chapter 6) are identified. There are many opportunities for future research to examine how and to what extent these optimal solutions align with actual observations of movement. Depending on study area and application type, the objectives in our proposed frameworks can be modified to account for other planning goals and criteria in future studies.

BIBLIOGRAPHY

Acevedo, Miguel A., Jorge A. Sefair, J. Cole Smith, Brian Reichert, and Robert J. Fletcher. 2015. "Conservation under Uncertainty: Optimal Network Protection Strategies for Worst-Case Disturbance Events." *Journal of Applied Ecology* 52 (6): 1588–97. https://doi.org/10.1111/1365-2664.12532.

Adriaensen, F., J. P. Chardon, G. De Blust, E. Swinnen, S. Villalba, H. Gulinck, and E. Matthysen. 2003. "The Application of 'least-Cost' Modelling as a Functional Landscape Model." *Landscape and Urban Planning* 64 (4): 233–47. https://doi.org/10.1016/S0169-2046(02)00242-6.

Akar, Gulsah, and Kelly J. Clifton. 2009. "Influence of Individual Perceptions and Bicycle Infrastructure on Decision to Bike." *Transportation Research Record*, no. 2140: 165–72. https://doi.org/10.3141/2140-18.

Anderson, M. D., and R. R. Souleyrette. 2002. "Pseudo-Dynamic Travel Model Application to Assess Traveler Information." *Transportation* 29 (3): 307–19. https://doi.org/10.1023/A:1015614208374.

Aultman-Hall, Lisa, Fred L. Hall, and Brian B. Baetz. 1997. "Analysis of Bicycle Commuter Routes Using Geographic Information Systems: Implications for Bicycle Planning." *Transportation Research Record*, no. 1578: 102–10. https://doi.org/10.3141/1578-13.

Baguette, Michel, and Hans Van Dyck. 2007. "Landscape Connectivity and Animal Behavior : Functional Grain as a Key Determinant for Dispersal." *Landscape Ecology* 22: 1117–29. https://doi.org/10.1007/s10980-007-9108-4.

Balachandran, M., and J.S. Gero. 1985. "The Noninferior Set Estimation (NISE) Method for Three Objective Problems." *Engineering Optimization* 9 (2): 77–88. https://doi.org/https://doi.org/10.1080/03052158508902504.

Basu, Debasis, and Bhargab Maitra. 2010. "Evaluation of VMS-Based Traffic Information Using Multiclass Dynamic Traffic Assignment Model: Experience in Kolkata." *Journal of Urban Planning and Development* 136 (1): 104–13. https://doi.org/10.1061/(ASCE)0733-9488(2010)136:1(104).

Beier, Paul, Daniel R. Majka, and Shawn L. Newell. 2009. "Uncertainty Analysis of Least-Cost Modeling for Designing Wildlife Linkages." *Ecological Applications* 19 (8): 2067–77.

https://doi.org/10.1890/08-1898.1.

Bellman, Richard. 1954. “The Theory of Dynamic Programming.” *Bulletin of the American Mathematical Society* 60 (6): 503–15.

Berman, Oded, Richard C. Larson, and Nikoletta Fouska. 1992. “Optimal Location of Discretionary Service Facilities.” *Transportation Science* 26 (3): 201–11. https://doi.org/10.1287/trsc.26.3.201.

Bérubé, Jean François, Michel Gendreau, and Jean Yves Potvin. 2009. “An Exact ε-Constraint Method for Bi-Objective Combinatorial Optimization Problems: Application to the Traveling Salesman Problem with Profits.” *European Journal of Operational Research* 194 (1): 39–50. https://doi.org/10.1016/j.ejor.2007.12.014.

Beven, K. J., and M. J. Kirkby. 1979. “A Physically Based, Variable Contributing Area Model of Basin Hydrology.” *Hydrological Sciences Bulletin* 24 (1): 43–69. https://doi.org/10.1080/02626667909491834.

Bowler, Diana E., and Tim G. Benton. 2005. “Causes and Consequences of Animal Dispersal Strategies: Relating Individual Behaviour to Spatial Dynamics.” *Biological Reviews of the Cambridge Philosophical Society* 80 (2): 205–25. https://doi.org/10.1017/S1464793104006645.

Boyles, Stephen D., and S. Travis Waller. 2011. “Optimal Information Location for Adaptive Routing.” *Networks and Spatial Economics* 11 (2): 233–54. https://doi.org/10.1007/s11067-009-9108-9.

Broach, Joseph, Jennifer Dill, and John Gliebe. 2012. “Where Do Cyclists Ride? A Route Choice Model Developed with Revealed Preference GPS Data.” *Transportation Research Part A: Policy and Practice* 46 (10): 1730–40. https://doi.org/10.1016/j.tra.2012.07.005.

Carlyle, W. Matthew, and R. Kevin Wood. 2005. “Near-Shortest and K-Shortest Simple Paths.” *Networks* 46 (2): 98–109. https://doi.org/10.1002/net.20077.

Carraway, R. L., and T. L. Morin. 1988. “Theory and Applications of Generalized Dynamic Programming: An Overview.” *Computers and Mathematics with Applications* 16 (10–11): 779–88. https://doi.org/10.1016/0898-1221(88)90188-5.

Caulfield, Brian, Elaine Brick, and Orla Thérèse McCarthy. 2012. “Determining Bicycle Infrastructure Preferences - A Case Study of Dublin.” *Transportation Research Part D: Transport and Environment* 17 (5): 413–17. https://doi.org/10.1016/j.trd.2012.04.001.

Chassein, André, and Marc Goerigk. 2016. “A Bicriteria Approach to Robust Optimization.” *Computers and Operations Research* 66: 181–89. https://doi.org/10.1016/j.cor.2015.08.007.

Chiu, Yi Chang, and Nathan Huynh. 2007. “Location Configuration Design for Dynamic Message Signs under Stochastic Incident and ATIS Scenarios.” *Transportation Research Part C: Emerging Technologies* 15 (1): 33–50. https://doi.org/10.1016/j.trc.2006.12.001.

Church, Richard L., Maria P. Scaparra, and Richard S. Middleton. 2004. “Identifying Critical Infrastructure: The Median and Covering Facility Interdiction Problems.” *Annals of the Association of American Geographers* 94 (3): 491–502. https://doi.org/10.1111/j.1467-8306.2004.00410.x.

Cohon, Jared L., Richard L. Church, and Daniel P. Sheer. 1979. “Generating Multi-objective Trade-offs: An Algorithm for Bicriterion Problems.” *Water Resources Research* 15 (5): 1001–10. https://doi.org/10.1029/WR015i005p01001.

Cosentino, Bradley J., Robert L. Schooley, and Christopher A. Phillips. 2011. “Connectivity of Agroecosystems: Dispersal Costs Can Vary among Crops.” *Landscape Ecology* 26 (3): 371–79. https://doi.org/10.1007/s10980-010-9563-1.

Dantzig, George B. 1957. “Discrete-Variable Extremum Problems.” *Operations Research* 5 (2): 266–77. https://doi.org/www.jstor.org/stable/167356.

Das, I., and J. Dennis. 1997. “A Closer Look at Drawbacks of Minimizing Weighted Sums of Objectives for Pareto Set Generation in Multicriteria Optimization Problems.” *Structural Optimization* 14: 63–69.

Diego-Rasilla, Francisco J., Rosa M. Luengo, and John B. Phillips. 2008. “Use of a Magnetic Compass for Nocturnal Homing Orientation in the Palmate Newt, Lissotriton Helveticus.” *Ethology* 114 (8): 808–15. https://doi.org/10.1111/j.1439-0310.2008.01532.x.

Dijkstra, E.W. 1959. “A Note on Two Problems in Connexion with Graphs.” *Numerische Mathematik* 1 (1): 269–71. https://doi.org/10.1007/BF01386390.

Edara, Praveen, and Timothy C Matisziw. 2015. “Traveler Behavior in Response to Network Disruptions.” In *Handbook of Transportation*, edited by Dusan Teodorovic, 177–87. New York: Routledge. https://doi.org/10.4324/9781315756684.ch12.

Ehrgott, M. 2008. “Multi-objective Optimization.” *AI Magazine*, 2008. https://doi.org/10.1007/978-0-387-76635-5_6.

Ehrgott, Matthias. 2006. “A Discussion of Scalarization Techniques for Multiple Objective

Integer Programming." *Annals of Operations Research* 147 (1): 343–60. https://doi.org/10.1007/s10479-006-0074-z.

Ehrgott, Matthias, Judith Y.T. Wang, Andrea Raith, and Chris Van Houtte. 2012. "A Bi-Objective Cyclist Route Choice Model." *Transportation Research Part A: Policy and Practice* 46 (4): 652–63. https://doi.org/10.1016/j.tra.2011.11.015.

Essen, Mariska van, Tom Thomas, Eric van Berkum, and Caspar Chorus. 2020. "Travelers' Compliance with Social Routing Advice: Evidence from SP and RP Experiments." *Transportation* 47 (3): 1047–70. https://doi.org/10.1007/s11116-018-9934-z.

Floyd, R.W. 1962. "Algorithm 97: Shortest Path." *Communications of the ACM* 5 (6): 345. https://doi.org/10.1145/367766.368168.

Galpern, Paul, Micheline Manseau, and Andrew Fall. 2011. "Patch-Based Graphs of Landscape Connectivity: A Guide to Construction, Analysis and Application for Conservation." *Biological Conservation* 144 (1): 44–55. https://doi.org/10.1016/j.biocon.2010.09.002.

Gamble, Lloyd R., Kevin McGarigal, and Bradley W. Compton. 2007. "Fidelity and Dispersal in the Pond-Breeding Amphibian, Ambystoma Opacum: Implications for Spatio-Temporal Population Dynamics and Conservation." *Biological Conservation* 139 (3–4): 247–57. https://doi.org/10.1016/j.biocon.2007.07.001.

Gentili, M., and P. B. Mirchandani. 2012. "Locating Sensors on Traffic Networks: Models, Challenges and Research Opportunities." *Transportation Research Part C: Emerging Technologies* 24: 227–55. https://doi.org/10.1016/j.trc.2012.01.004.

Gholamialam, A., and T.C. Matisziw. 2019. "Modeling Bikeability of Urban Systems." *Geographical Analysis* 51 (1): 73–89. https://doi.org/10.1111/gean.12159.

Giordano, Andrew R., Benjamin J. Ridenhour, and Andrew Storfer. 2007. "The Influence of Altitude and Topography on Genetic Structure in the Long-Toed Salamander (Ambystoma Macrodactulym)." *Molecular Ecology* 16 (8): 1625–37. https://doi.org/10.1111/j.1365-294X.2006.03223.x.

Grubesic, Tony H., and Timothy C. Matisziw. 2013. "A Typological Framework for Categorizing Infrastructure Vulnerability." *GeoJournal* 78 (2): 287–301. https://doi.org/10.1007/s10708-011-9411-0.

Guerriero, F., and R. Musmanno. 2001. "Label Correcting Methods to Solve Multicriteria Shortest Path Problems." *Journal of Optimization Theory and Applications* 111 (3): 589–

613. https://doi.org/10.1023/A:1012602011914.

Gurrutxaga, Mikel, Pedro J Lozano, and Gabriel D Barrio. 2010. “GIS-Based Approach for Incorporating the Connectivity of Ecological Networks into Regional Planning.” *Journal for Nature Conservation* 18 (4): 318–26. https://doi.org/10.1016/j.jnc.2010.01.005.

Gzara, Fatma, and Erhan Erkut. 2009. “A Lagrangian Relaxation Approach to Large-Scale Flow Interception Problems.” *European Journal of Operational Research* 198 (2): 405–11. https://doi.org/10.1016/j.ejor.2008.08.024.

Haight, Robert G., Charles S. ReVelle, and Stephanie A. Snyder. 2000. “An Integer Optimization Approach to a Probabilistic Reserve Site Selection Problem.” *Operations Research* 48 (5): 697–708. https://doi.org/10.1287/opre.48.5.697.12411.

Hamer, Andrew J. 2018. “Accessible Habitat and Wetland Structure Drive Occupancy Dynamics of a Threatened Amphibian across a Peri-Urban Landscape.” *Landscape and Urban Planning* 178 (March): 228–37. https://doi.org/10.1016/j.landurbplan.2018.06.008.

Harkey, David L. 1998. “The Bicycle Compatibility Index: A Level of Service Concept,” no. December 1998: 4.

Heard, Geoffrey W., Michael P. Scroggie, and Brian S. Malone. 2012. “Classical Metapopulation Theory as a Useful Paradigm for the Conservation of an Endangered Amphibian.” *Biological Conservation* 148 (1): 156–66. https://doi.org/10.1016/j.biocon.2012.01.018.

Henderson, Jeffrey M. 2004. “A Planning Model for Optimizing Locations of Changeable Message Signs.” University of Waterloo.

Hodgson, M. John. 1990. “A Flow-Capturing Location-Allocation Model.” *Geographical Analysis* 22 (3): 270–79. https://doi.org/10.1111/j.1538-4632.1990.tb00210.x.

Huber, Dennis L. 1980. “Alternative Methods in Corridor Routing.” The University of Tennessee, Knoxville.

Huynh, Nathan, Yi Chang Chiu, and Hani S. Mahmassani. 2003. “Finding Near-Optimal Locations for Variable Message Signs for Real-Time Network Traffic Management.” *Transportation Research Record* 1856 (1): 34–53. https://doi.org/10.3141/1856-05.

Ishibuchi, Hisao, Yuji Sakane, Noritaka Tsukamoto, and Yusuke Nojima. 2009. “Evolutionary Many-Objective Optimization by NSGA-II and MOEA/D with Large Populations.” *Conference Proceedings - IEEE International Conference on Systems, Man and*

Cybernetics 1 (October): 1758–63. https://doi.org/10.1109/ICSMC.2009.5346628.

Jiang, J., and X. Liu. 2018. "Multi-Objective Stackelberg Game Model for Water Supply Networks against Interdictions with Incomplete Information." *European Journal of Operational Research* 266 (3): 920–33. https://doi.org/10.1016/j.ejor.2017.10.034.

Jindahra, Pavitra, and Kasem Choocharukul. 2013. "Short-Run Route Diversion: An Empirical Investigation into Variable Message Sign Design and Policy Experiments." *IEEE Transactions on Intelligent Transportation Systems* 14 (1): 388–97. https://doi.org/10.1109/TITS.2012.2215854.

Jozefowiez, Nicolas, Frédéric Semet, and El Ghazali Talbi. 2008. "Multi-Objective Vehicle Routing Problems." *European Journal of Operational Research* 189 (2): 293–309. https://doi.org/10.1016/j.ejor.2007.05.055.

Khani, Alireza, and Stephen D. Boyles. 2014. "An Exact Algorithm for the Mean-Standard Deviation Shortest Path Problem." *Transportation Research Part B: Methodological* 81: 252–66. https://doi.org/10.1016/j.trb.2015.04.002.

Kuby, Michael, and Seow Lim. 2005. "The Flow-Refueling Location Problem for Alternative-Fuel Vehicles." *Socio-Economic Planning Sciences* 39 (2): 125–45. https://doi.org/10.1016/j.seps.2004.03.001.

Lam, W. H.K., and K. S. Chan. 2001. "A Model for Assessing the Effects of Dynamic Travel Time Information via Variable Message Signs." *Transportation* 28 (1): 79–99. https://doi.org/10.1023/A:1005235831457.

Landguth, E. L., B. K. Hand, J. Glassy, S. A. Cushman, and M. A. Sawaya. 2012. "UNICOR: A Species Connectivity and Corridor Network Simulator." *Ecography* 35 (1): 9–14. https://doi.org/10.1111/j.1600-0587.2011.07149.x.

Landis, Bruce W., Venkat R. Vattikuti, and Michael T. Brannick. 1997. "Real-Time Human Perceptions: Toward a Bicycle Level of Service." *Transportation Research Record*, no. 1578: 119–31. https://doi.org/10.3141/1578-15.

Laumanns, Marco, Lothar Thiele, and Eckart Zitzler. 2006. "An Efficient, Adaptive Parameter Variation Scheme for Metaheuristics Based on the Epsilon-Constraint Method." *European Journal of Operational Research* 169 (3): 932–42. https://doi.org/10.1016/j.ejor.2004.08.029.

Lei, Xiao, Siqian Shen, and Yongjia Song. 2018. "Stochastic Maximum Flow Interdiction

Problems under Heterogeneous Risk Preferences." *Computers and Operations Research* 90: 97–109. https://doi.org/10.1016/j.cor.2017.09.004.

Li, Meng, Xi Lin, Fang He, and Han Jiang. 2016. "Optimal Locations and Travel Time Display for Variable Message Signs." *Transportation Research Part C: Emerging Technologies* 69: 418–35. https://doi.org/10.1016/j.trc.2016.06.016.

Li, Qingwei, and Alex Savachkin. 2013. "A Heuristic Approach to the Design of Fortified Distribution Networks." *Transportation Research Part E: Logistics and Transportation Review* 50 (1): 138–48. https://doi.org/10.1016/j.tre.2012.10.004.

Losada, Chaya, M. Paola Scaparra, and Jesse R. O'Hanley. 2012. "Optimizing System Resilience: A Facility Protection Model with Recovery Time." *European Journal of Operational Research* 217 (3): 519–30. https://doi.org/10.1016/j.ejor.2011.09.044.

Lowe, Winsor H. 2009. "What Drives Long-Distance Dispersal? A Test of Theoretical Predictions." *Ecology* 90 (6): 1456–62. https://doi.org/10.1890/08-1903.1.

Lowe, Winsor H., Gene E. Likens, Mark A. McPeek, and Don C. Buso. 2006. "Linking Direct and Indirect Data on Dispersal: Isolation by Slope in a Headwater Stream Salamander." *Ecology* 87 (2): 334–39. https://doi.org/10.1890/05-0232.

Lowry, Michael B., Peter Furth, and Tracy Hadden-Loh. 2016. "Prioritizing New Bicycle Facilities to Improve Low-Stress Network Connectivity." *Transportation Research Part A: Policy and Practice* 86: 124–40. https://doi.org/10.1016/j.tra.2016.02.003.

Lowry, Michael, Daniel Callister, Maureen Gresham, and Brandon Moore. 2012. "Assessment of Communitywide Bikeability with Bicycle Level of Service." *Transportation Research Record*, no. 2314: 41–48. https://doi.org/10.3141/2314-06.

Lu, Zhaojun, Gang Qu, and Zhenglin Liu. 2019. "A Survey on Recent Advances in Vehicular Network Security, Trust, and Privacy." *IEEE Transactions on Intelligent Transportation Systems* 20 (2): 760–76. https://doi.org/10.1109/TITS.2018.2818888.

Marler, Timothy, and Jasbir Arora. 2010. "The Weighted Sum Method for Multi-Objective Optimization : New Insights." *Structural and Multidisciplinary Optimization* 41: 853–62. https://doi.org/10.1007/s00158-009-0460-7.

Marsh, David M., Bradley J. Cosentino, Kara S. Jones, Joseph J. Apodaca, Karen H. Beard, Jane Margaret Bell, Christine Bozarth, et al. 2017. "Effects of Roads and Land Use on Frog Distributions across Spatial Scales and Regions in the Eastern and Central United States."

Diversity and Distributions 23 (2): 158–70. https://doi.org/10.1111/ddi.12516.

Martins, EQV. 1984. "On a Multicriteria Shortest Path Model." *European Journal of Operational Research* 16 (2): 236–45. https://doi.org/10.1016/0377-2217(84)90077-8.

Matisziw, T.C. 2019. "Maximizing Expected Coverage of Flow and Opportunity for Diversion in Networked Systems." *Networks and Spatial Economics* 19 (1): 199–218.

Matisziw, T.C., M. Alam, K.M. Trauth, E.C. Inniss, R.D. Semlitsch, S. McIntosh, and J. Horton. 2015. "A Vector Approach for Modeling Landscape Corridors and Habitat Connectivity." *Environmental Modeling and Assessment* 20 (1): 1–16. https://doi.org/10.1007/s10666-014-9412-8.

Matisziw, T.C., and A.T. Murray. 2009. "Connectivity Change in Habitat Networks." *Landscape Ecology* 24: 89–100. https://doi.org/10.1007/s10980-008-9282-z.

Matisziw, Timothy C., Ashkan Gholamialam, and Kathleen M. Trauth. 2020. "Modeling Habitat Connectivity in Support of Multi-objective Species Movement: An Application to Amphibian Habitat Systems." *PLOS Computational Biology* 16 (12): e1008540. https://doi.org/10.1371/journal.pcbi.1008540.

Matisziw, Timothy C., Tony H. Grubesic, and Junyu Guo. 2012. "Robustness Elasticity in Complex Networks." *PLoS ONE* 7 (7). https://doi.org/10.1371/journal.pone.0039788.

Matisziw, Timothy C., and Alan T. Murray. 2006. "Promoting Species Persistence through Spatial Association Optimization in Nature Reserve Design." *Journal of Geographical Systems* 8 (3): 289–305. https://doi.org/10.1007/s10109-006-0020-2.

Matisziw, Timothy C., Alan T. Murray, and Tony H. Grubesic. 2007. "Bounding Network Interdiction Vulnerability through Cutset Identification." In *Critical Infrastructure: Reliability and Vulnerability*, edited by A.T. Murray and T.H. Grubesic, 243–56. Berlin: Springer-Verlag. https://doi.org/10.1007/978-3-540-68056-7_12.

Matos, Cátia, Silviu O. Petrovan, Philip M. Wheeler, and Alastair I. Ward. 2019. "Landscape Connectivity and Spatial Prioritization in an Urbanising World: A Network Analysis Approach for a Threatened Amphibian." *Biological Conservation* 237 (November 2018): 238–47. https://doi.org/10.1016/j.biocon.2019.06.035.

Medrano, F. Antonio, and Richard L. Church. 2014. "Corridor Location for Infrastructure Development: A Fast Bi-Objective Shortest Path Method for Approximating the Pareto Frontier." *International Regional Science Review* 37 (2): 129–48.

https://doi.org/10.1177/0160017613507772.

Mekuria, Maaza C., Peter G. Furth, and Hilary Nixon. 2012. “Loss-Stress Bicycling and Network Connectivity.” *Mineta Transportation Institute Report 11-19*, 68. http://transweb.sjsu.edu/PDFs/research/1005-low-stress-bicycling-network-connectivity.pdf.

Menghini, G., N. Carrasco, N. Schüssler, and K. W. Axhausen. 2010. “Route Choice of Cyclists in Zurich.” *Transportation Research Part A: Policy and Practice* 44 (9): 754–65. https://doi.org/10.1016/j.tra.2010.07.008.

Messac, Achille, and Christopher A Mattson. 2004. “Normal Constraint Method with Guarantee of Even Representation of Complete Pareto Frontier.” *AIAA Journal* 42 (10): 1–11. https://doi.org/10.2514/1.8977.

Mirchandani, Pitu, and Malgorzata Wiecek. 1993. “Routing with Nonlinear Multiattribute Cost Functions.” *Applied Mathematics and Computation* 54: 215–39.

MSDIS. 2019. “Missouri Spatial Data Information Service.” 2019. http://msdis.missouri.edu.

Nathan, Ran, Wayne M. Getz, Eloy Revilla, Marcel Holyoak, Ronen Kadmon, David Saltz, and Peter E. Smouse. 2008. “A Movement Ecology Paradigm for Unifying Organismal Movement Research.” *Proceedings of the National Academy of Sciences of the United States of America* 105 (49): 19052–59. https://doi.org/10.1073/pnas.0800375105.

Numminen, Elina, and Anna Liisa Laine. 2020. “The Spread of a Wild Plant Pathogen Is Driven by the Road Network.” *PLoS Computational Biology* 16 (3): 1–21. https://doi.org/10.1371/journal.pcbi.1007703.

Parks, Sean A., Kevin S. Mckelvey, and Michael K. Schwartz. 2012. “Effects of Weighting Schemes on the Identification of Wildlife Corridors Generated with Least-Cost Methods.” *Conservation Biology* 27 (1): 145–54. https://doi.org/10.1111/j.1523-1739.2012.01929.x.

Patrick, David, Calhoun Aram, and Hunter Malcoln. 2007. “Orientation of Juvenile Wood Frogs, Rana Sylvatica, Leaving Experimental Ponds.” *Journal of Herpetology* 41 (1): 158–63.

Pierre, Hansen. 1980. “Bicriterion Path Problems.” *Lecture Notes in Economics and Mathematical Systems* 177: 109–27.

Pinto, Naiara, and Timothy H. Keitt. 2009. “Beyond the Least-Cost Path: Evaluating Corridor Redundancy Using a Graph-Theoretic Approach.” *Landscape Ecology* 24 (2): 253–66. https://doi.org/10.1007/s10980-008-9303-y.

Pittman, Shannon E., Michael S. Osbourn, and Raymond D. Semlitsch. 2014. “Movement Ecology of Amphibians: A Missing Component for Understanding Population Declines.” *Biological Conservation* 169: 44–53. https://doi.org/10.1016/j.biocon.2013.10.020.

Pounds, J. Alan, and Martha L. Crump. 1994. “Amphibian Declines and Climate Disturbance: The Case of the Golden Toad and the Harlequin Frog.” *Conservation Biology* 8 (1): 72–85. https://doi.org/10.1046/j.1523-1739.1994.08010072.x.

Pounds, J. Alan, Michael P.L. Fogden, Jay M. Savage, and George C. Gorman. 1997. “Tests of Null Models for Amphibian Declines on a Tropical Mountain.” *Conservation Biology* 11 (6): 1307–22. https://doi.org/10.1046/j.1523-1739.1997.95485.x.

Raimundo, Marcos M., Paulo A.V. Ferreira, and Fernando J. Von Zuben. 2020. “An Extension of the Non-Inferior Set Estimation Algorithm for Many Objectives.” *European Journal of Operational Research* 1 (1): 53–66. https://doi.org/10.1016/J.EJOR.2019.11.017.

Rayfield, Bronwyn, Marie Josée Fortin, and Andrew Fall. 2010. “The Sensitivity of Least-Cost Habitat Graphs to Relative Cost Surface Values.” *Landscape Ecology* 25 (4): 519–32. https://doi.org/10.1007/s10980-009-9436-7.

Reinhardt, Line Blander, and David Pisinger. 2011. “Multi-Objective and Multi-Constrained Non-Additive Shortest Path Problems.” *Computers and Operations Research* 38 (3): 605–16. https://doi.org/10.1016/j.cor.2010.08.003.

ReVelle, Charles S., Justin C. Williams, and John J. Boland. 2002. “Counterpart Models in Facility Location Science and Reserve Selection Science.” *Environmental Modeling and Assessment* 7 (2): 71–80. https://doi.org/10.1023/A:1015641514293.

Ribeiro, John Wesley, Juliana Silveira dos Santos, Pavel Dodonov, Felipe Martello, Bernardo Brandão Niebuhr, and Milton Cezar Ribeiro. 2017. “LandScape Corridors (Lscorridors): A New Software Package for Modelling Ecological Corridors Based on Landscape Patterns and Species Requirements.” *Methods in Ecology and Evolution* 8 (11): 1425–32. https://doi.org/10.1111/2041-210X.12750.

Riemann, Raffaela, David Z.W. Wang, and Fritz Busch. 2015. “Optimal Location of Wireless Charging Facilities for Electric Vehicles: Flow Capturing Location Model with Stochastic User Equilibrium.” *Transportation Research Part C: Emerging Technologies* 58 (Part A): 1–12. https://doi.org/10.1016/j.trc.2015.06.022.

Romero, Fernando, Juan Gomez, Thais Rangel, Rafael Jurado-Piña, and José Manuel Vassallo.

2020. “The Influence of Variable Message Signs on En-Route Diversion between a Toll Highway and a Free Competing Alternative.” *Transportation* 47 (4): 1665–87. https://doi.org/10.1007/s11116-019-09976-8.

Ron, Santiago R., William E. Duellman, Luis A. Coloma, and Martín R. Bustamante. 2003. “Population Decline of the Jambato Toad Atelopus Ignescens (Anura: Bufonidae) in the Andes of Ecuador.” *Journal of Herpetology* 37 (1): 116–26. https://doi.org/10.1670/0022-1511(2003)037[0116:pdotjt]2.0.co;2.

Saura, Santiago, and Lucía Pascual-Hortal. 2007. “A New Habitat Availability Index to Integrate Connectivity in Landscape Conservation Planning: Comparison with Existing Indices and Application to a Case Study.” *Landscape and Urban Planning* 83 (2–3): 91–103. https://doi.org/10.1016/j.landurbplan.2007.03.005.

Sawyer, Sarah C., Clinton W. Epps, and Justin S. Brashares. 2011. “Placing Linkages among Fragmented Habitats: Do Least-Cost Models Reflect How Animals Use Landscapes?” *Journal of Applied Ecology* 48 (3): 668–78. https://doi.org/10.1111/j.1365-2664.2011.01970.x.

Scaparra, Maria P., Richard L. Church, and F. Antonio Medrano. 2014. “Corridor Location: The Multi-Gateway Shortest Path Model.” *Journal of Geographical Systems* 16 (3): 287–309. https://doi.org/10.1007/s10109-014-0197-8.

Scroggie, Michael P., Kathy Preece, Emily Nicholson, Michael A. McCarthy, Kirsten M. Parris, and Geoffrey W. Heard. 2019. “Optimizing Habitat Management for Amphibians: From Simple Models to Complex Decisions.” *Biological Conservation* 236 (November 2018): 60–69. https://doi.org/10.1016/j.biocon.2019.05.022.

Sefair, Jorge A., J. Cole Smith, Miguel A. Acevedo, and Robert J. Fletcher. 2017. “A Defender-Attacker Model and Algorithm for Maximizing Weighted Expected Hitting Time with Application to Conservation Planning.” *IISE Transactions* 49 (12): 1112–28. https://doi.org/10.1080/24725854.2017.1360533.

Semlitsch, Raymond D. 2008. “Differentiating Migration and Dispersal Processes for Pond-Breeding Amphibians.” *Journal of Wildlife Management* 72 (1): 260–67. https://doi.org/10.2193/2007-082.

Shafizadeh, Kevan, and Debbie Niemeier. 1997. “Bicycle Journey-to-Work: Travel Behavior Characteristics and Spatial Attributes.” *Transportation Research Record*, no. 1578: 84–90.

https://doi.org/10.3141/1578-11.

Shahabi, Mehrdad, Avinash Unnikrishnan, and Stephen D. Boyles. 2013. “An Outer Approximation Algorithm for the Robust Shortest Path Problem.” *Transportation Research Part E: Logistics and Transportation Review* 58: 52–66. https://doi.org/10.1016/j.tre.2013.07.002.

Shen, Siqian, J. Cole Smith, and Roshan Goli. 2012. “Exact Interdiction Models and Algorithms for Disconnecting Networks via Node Deletions.” *Discrete Optimization* 9 (3): 172–88. https://doi.org/10.1016/j.disopt.2012.07.001.

Shen, Zuo Jun Max, and Mark S. Daskin. 2005. “Trade-Offs between Customer Service and Cost in Integrated Supply Chain Design.” *Manufacturing and Service Operations Management* 7 (3): 188–207. https://doi.org/10.1287/msom.1050.0083.

Sherman, Cynthia K, and Martin L Morton. 1993. “Population Declines of Yosemite Toads in the Eastern Sierra Nevada of California.” *Journal of Herpetology* 27 (2): 186–98. https://doi.org/10.2307/1564935.

Shi, Ning, Shaorui Zhou, Fan Wang, Yi Tao, and Liming Liu. 2017. “The Multi-Criteria Constrained Shortest Path Problem.” *Transportation Research Part E: Logistics and Transportation Review* 101: 13–29. https://doi.org/10.1016/j.tre.2017.02.002.

Sinsch, U., N. Oromi, C. Miaud, J. Denton, and D. Sanuy. 2012. “Connectivity of Local Amphibian Populations: Modelling the Migratory Capacity of Radio-Tracked Natterjack Toads.” *Animal Conservation* 15 (4): 388–96. https://doi.org/10.1111/j.1469-1795.2012.00527.x.

Skriver, A J V, and K A Andersen. 2000. “A Label Correcting Approach for Solving Bicriterion Shortest-Path Problems” 27. https://doi.org/https://doi.org/10.1016/S0305-0548(99)00037-4.

Solanki, Rajendra, Perry Appino, and Jared Cohon. 1993. “Approximating the Noninferior Set in Multi-objective Linear Programming Problems.” *European Journal of Operational Research* 68 (3): 356–73. https://doi.org/10.1016/0377-2217(93)90192-P.

Starita, Stefano, and Maria Paola Scaparra. 2016. “Optimizing Dynamic Investment Decisions for Railway Systems Protection.” *European Journal of Operational Research* 248 (2): 543–57. https://doi.org/10.1016/j.ejor.2015.07.025.

Stuart, Simon N., Janice S. Chanson, Neil A. Cox, Bruce E. Young, Ana S.L. Rodrigues, Debra

L. Fischman, and Robert W. Waller. 2004. “Status and Trends of Amphibian Declines and Extinctions Worldwide.” *Science* 306 (5702): 1783–86. https://doi.org/10.1126/science.1103538.

Sutcliffe, Odette L., Vegar Bakkestuen, Gary Fry, and Odd E. Stabbetorp. 2003. “Modelling the Benefits of Farmland Restoration: Methodology and Application to Butterfly Movement.” *Landscape and Urban Planning* 63 (1): 15–31. https://doi.org/10.1016/S0169-2046(02)00153-6.

Tarapata, Zbigniew. 2007. “Selected Multicriteria Shortest Path Problems: An Analysis of Complexity, Models and Adaptation of Standard Algorithms.” *International Journal of Applied Mathematics and Computer Science* 17 (2): 269–87. https://doi.org/10.2478/v10006-007-0023-2.

Tischendorf, Lutz, and Lenore Fahrig. 2000. “On the Usage and Measurement of Landscape Connectivity.” *Oikos* 90 (1): 7–19. https://doi.org/10.1034/j.1600-0706.2000.900102.x.

Todd, Brian D., and Christopher T. Winne. 2006. “Ontogenetic and Interspecific Variation in Timing of Movement and Responses to Climatic Factors during Migrations by Pond-Breeding Amphibians.” *Canadian Journal of Zoology* 84 (5): 715–22. https://doi.org/10.1139/Z06-054.

Toi, Satoshi, Masaru Kiyota, Tetsuroh Nomura, Yoshitaka Kajita, Tetsunobu Yoshitake, and Hiroshi Tatsuni. 2005. “A Method for Planning of Road Sign System in Highway Using Straying Index.” *Journal of the Eastern Asia Society for Transportation Studies* 6: 981–96. https://doi.org/10.11175/easts.6.981.

Tong, Daoqin, and Alan T. Murray. 2012. “Spatial Optimization in Geography.” *Annals of the Association of American Geographers* 102 (6): 1290–1309. https://doi.org/10.1080/00045608.2012.685044.

Trombulak, Stephen C., and Christopher A. Frissell. 2000. “Review of Ecological Effects of Roads on Terrestrial and Aquatic Communities.” *Conservation Biology* 14 (1): 18–30. https://doi.org/10.1046/j.1523-1739.2000.99084.x.

Tsaggouris, George, and Christos Zaroliagis. 2009. “Multi-objective Optimization: Improved FPTAS for Shortest Paths and Non-Linear Objectives with Applications.” *Theory of Computing Systems* 45 (1): 162–86. https://doi.org/10.1007/s00224-007-9096-4.

Upchurch, Christopher, and Michael Kuby. 2010. “Comparing the P-Median and Flow-Refueling

Models for Locating Alternative-Fuel Stations." *Journal of Transport Geography* 18 (6): 750–58. https://doi.org/10.1016/j.jtrangeo.2010.06.015.

Urban, Dean, and Timothy Keitt. 2001. "Landscape Connectivity: A Graph-Theoritic Perspective." *Ecology* 82 (5): 1205–18. https://doi.org/https://doi.org/10.1890/0012-9658(2001)082[1205:LCAGTP]2.0.CO;2.

Wake, David B., and Vance T. Vredenburg. 2008. "Are We in the Midst of the Sixth Mass Extinction? A View from the World of Amphibians." *Proceedings of the National Academy of Sciences of the United States of America* 105 (1): 27–44. https://doi.org/10.17226/12501.

Walston, Leroy J., and Stephen J. Mullin. 2008. "Variation in Amount of Surrounding Forest Habitat Influences the Initial Orientation of Juvenile Amphibians Emigrating from Breeding Ponds." *Canadian Journal of Zoology* 86 (2): 141–46. https://doi.org/10.1139/Z07-117.

Wang, Fan, Xiaofan Lai, and Ning Shi. 2011. "A Multi-Objective Optimization for Green Supply Chain Network Design." *Decision Support Systems* 51 (2): 262–69. https://doi.org/10.1016/j.dss.2010.11.020.

Williams, Justin C. 1998. "Delineating Protected Wildlife Corridors with Multi-Objective Programming." *Environmental Modeling and Assessment* 3 (1–2): 77–86. https://doi.org/10.1023/A:1019006721277.

Winters, Meghan, Kay Teschke, Michael Grant, Eleanor M. Setton, and Michael Brauer. 2010. "How Far out of the Way Will We Travel? Built Environment Influences on Route Selection for Bicycle and Car Travel." *Transportation Research Record*, no. 2190: 1–10. https://doi.org/10.3141/2190-01.

Wu, Xiaolan, Alan T. Murray, and Ningchuan Xiao. 2011. "A Multi-objective Evolutionary Algorithm for Optimizing Spatial Contiguity in Reserve Network Design." *Landscape Ecology* 26 (3): 425–37. https://doi.org/10.1007/s10980-011-9571-9.

Yang, Hai. 1999. "Evaluating the Benefits of a Combined Route Guidance and Road Pricing System in a Traffic Network with Recurrent Congestion." *Transportation* 26 (3): 299–322. https://doi.org/10.1023/A:1005129309812.

Yang, Hai, Chao Yang, and Liping Gan. 2006. "Models and Algorithms for the Screen Line-Based Traffic-Counting Location Problems." *Computers and Operations Research* 33 (3): 836–58. https://doi.org/10.1016/j.cor.2004.08.011.

Yang, Yan, Liang Mao, and Sara S. Metcalf. 2019. "Diffusion of Hurricane Evacuation Behavior

through a Home-Workplace Social Network: A Spatially Explicit Agent-Based Simulation Model." *Computers, Environment and Urban Systems* 74 (December 2018): 13–22. https://doi.org/10.1016/j.compenvurbsys.2018.11.010.

Yim, Paul K.N., and William H.K. Lam. 1998. "Evaluation of Count Location Selection Methods for Estimation of O-d Matrices." *Journal of Transportation Engineering* 124 (4): 376–83. https://doi.org/10.1061/(asce)0733-947x(1998)124:4(376).

Zeller, Katherine A., Kevin McGarigal, and Andrew R. Whiteley. 2012. "Estimating Landscape Resistance to Movement: A Review." *Landscape Ecology* 27 (6): 777–97. https://doi.org/10.1007/s10980-012-9737-0.

Zhang, Guohui, Zhong Wang, Khali R. Persad, and C. Michael Walton. 2014. "Enhanced Traffic Information Dissemination to Facilitate Toll Road Utilization: A Nested Logit Model of a Stated Preference Survey in Texas." *Transportation* 41 (2): 231–49. https://doi.org/10.1007/s11116-013-9449-6.

Zhang, Junping, Fei Yue Wang, Kunfeng Wang, Wei Hua Lin, Xin Xu, and Cheng Chen. 2011. "Data-Driven Intelligent Transportation Systems: A Survey." *IEEE Transactions on Intelligent Transportation Systems* 12 (4): 1624–39. https://doi.org/10.1109/TITS.2011.2158001.

Zheng, Xinhu, Wei Chen, Pu Wang, Dayong Shen, Songhang Chen, Xiao Wang, Qingpeng Zhang, and Liuqing Yang. 2016. "Big Data for Social Transportation." *IEEE Transactions on Intelligent Transportation Systems* 17 (3): 620–30. https://doi.org/10.1109/TITS.2015.2480157.

VITA

Ashkan Gholamialam holds a Ph.D. in traffic and transportation engineering from MU, Columbia, U.S.A. He received his M.Sc. in transportation planning from University of Isfahan, Isfahan, and B.Sc. from Shahid Beheshti University, Abbaspour School of Engineering, Tehran, Iran. His research interests are transportation engineering, network design and optimization, sustainable and active transportation, spatial data analysis and GIS. The primary focus in his research is evaluation and optimization of transportation systems using mathematical and computational models. Prior to joining MU, he was working as adjunct instructor in Lorestan University, teaching traffic engineering courses to undergraduate students majoring in civil engineering. Before Lorestan University, he was involved in research projects funded by City of Isfahan DOT.